NASA Contractor Report 194880

Final Report on the Implementation and Evaluation of The New Wind Algorithm in NASA's 50 MHz Doppler Radar Wind Profiler

Prepared By:
Applied Meteorology Unit

NASA
National Aeronautics and
Space Administration

Office of Management

Scientific and Technical
Information Program

1993

Attributes and Acknowledgments:

Applied Meteorology Unit (AMU)

Gregory E. Taylor, primary author
John T. Manobianco
Robin S. Schumann
Mark M. Wheeler
Ann M. Yersavich

Table Of Contents

List of Illustrations

List of Illustrations
(Continued)

List of Illustrations
(Continued)

List of Tables

1.0 Introduction

1.1 Purpose of the Report

The purpose of this report is to document the AMU's implementation and evaluation of the wind algorithm developed by Marshall Space Flight Center (MSFC) on the Data Analysis Processor (DAP) of NASA's 50 MHz Doppler Radar Wind Profiler (DRWP). The report also includes a summary of the 50 MHz DRWP characteristics and performance and a proposed concept of operations for the DRWP.

1.2 Organization of the Report

The information presented within this report is subdivided into five major sections. Section 1, Introduction, contains a summary of the 50 MHz DRWP characteristics and performance, the objectives of the KSC certification of the DRWP, and a restatement of the AMU tasks associated with the implementation and evaluation of the new wind algorithm in the DRWP. Section 2, Proposed Concept of Operations, describes how the DRWP could be used to support day-of-launch activities and routine day-to-day forecasting. A description of the algorithm implementation including algorithm description, development approach, and software design, is contained in Section 3, Algorithm Implementation. Results from the AMU's meteorological evaluation of the DRWP are contained in Section 4, Meteorological Evaluation. Section 5, Summary and Recommendations, highlights key points from the implementation of the new wind algorithm and the meteorological evaluation and presents recommendations regarding operational use of the DRWP and suggestions for future work.

1.3 NASA's 50 MHz DRWP

Wind profiling radars depend upon the scattering of electromagnetic energy by minor variations in the index of refraction of the air. The index of refraction is a measure of the speed of propagation of electromagnetic energy through the atmosphere and, in the troposphere and stratosphere, depends primarily upon the temperature, pressure, and moisture content of the air. Small variations in these atmospheric parameters produce minor irregularities in the index of refraction that initiate scattering of electromagnetic radiation. As the transmitted electromagnetic pulse propagates through the atmosphere, part of the energy is scattered in all directions because of these refractive irregularities. A small portion of this scattered energy is returned to the radar antenna where it is received for analysis.

In the case of wind profiling radars, the transmitted signal is coherent so the "Doppler shift" of the returned signal can be determined. The Doppler shift is proportional to the velocity of the air parallel to the transmitted radar beam. By using a three beam configuration (Figure 1.1) with two of the beams tilted from the vertical axis, three different radial velocities can be estimated from the returned signals from the three radar beams. Then, assuming a homogeneous and slowly varying wind field, it is possible to estimate all three components of the wind velocity (e.g., east, north, and vertical wind components) by algebraic manipulation of the three radial velocities. Some wind

profiling radars use a five beam configuration with four beams tilted from the vertical axis.

NASA's 50 MHz DRWP was procured by MSFC and developed by Tycho, Inc. The system was installed adjacent to the Shuttle Landing Facility (SLF) at the Kennedy Space Center (KSC) in 1989 in a low power configuration (4 kilowatts). The system was completed in 1990 with the installation of the high power amplifier (250 kilowatts) that extended the vertical range of the system from about 12 kilometers to 18 kilometers. The basic operation of the DRWP is illustrated in Figure 1.2.
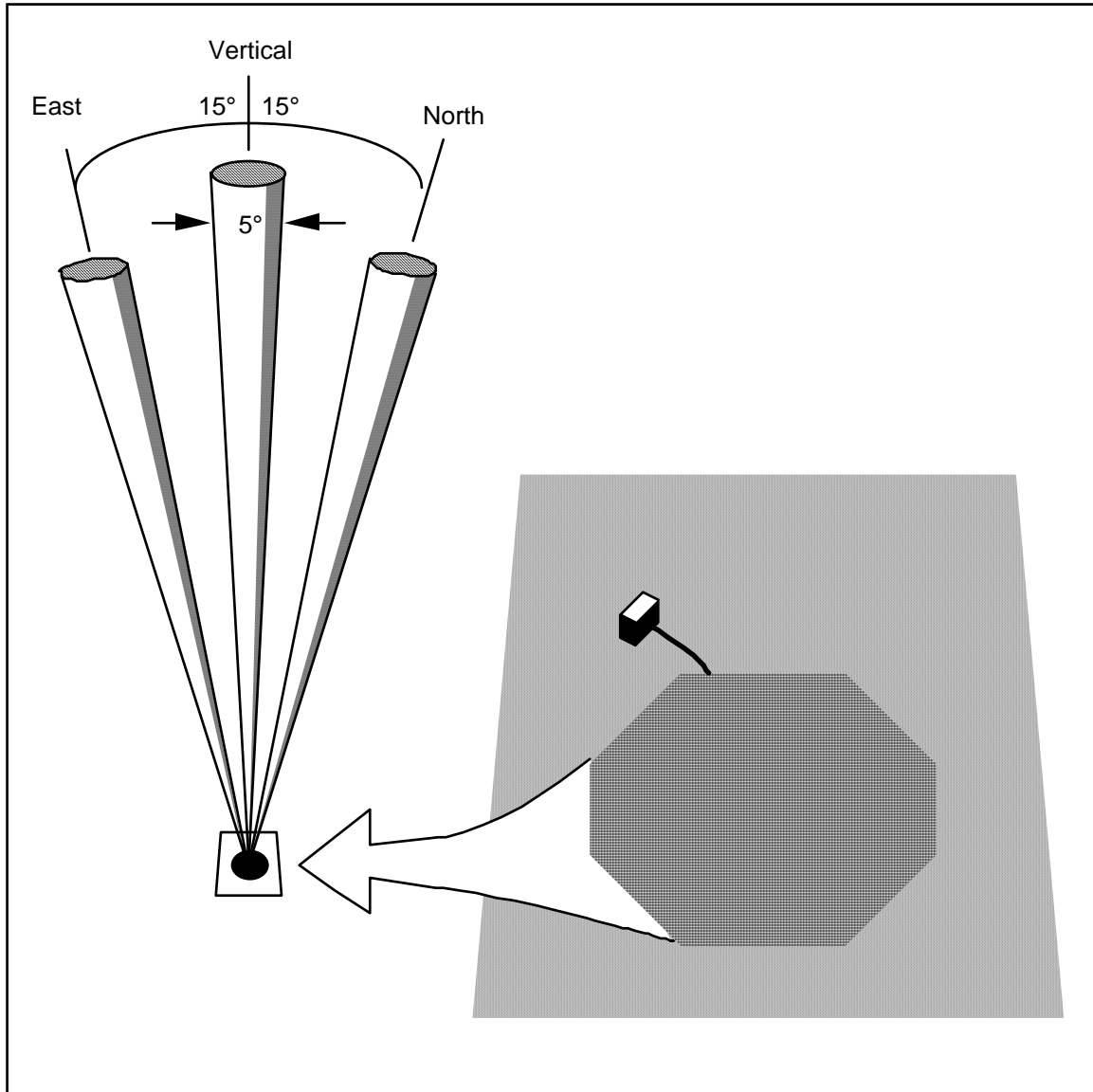
Figure 1.1.   Typical beam configuration for a three beam wind profiling radar. One vertical beam and two oblique beams tilted 15° from the zenith with azimuth directions of east and north.

On command from the Real-Time Processor (RTP) the antenna controller sets up the proper phasing for the antenna elements so that a predetermined beam pattern is produced. The RTP sends a transmit receive (T/R) pulse to set the T/R switch to the transmit mode. The RTP also sends a transmit pulse to the receiver/modulator which then produces a pulsed radio frequency (RF) signal. The RF signal is amplified by the transmitter and then sent to the antenna completing the transmit cycle. Note the receiver is disconnected during the transmit cycle to prevent overloading.

The system is then set to the receive mode by the RTP. The receiver is reconnected and the T/R switch sends the returned signal from the antenna to the receiver. The receiver amplifies the returned signal and extracts the in-phase and quadrature components and sends them to the RTP. The RTP performs the various processing steps necessary to derive the radial velocity, spectrum width, and other parameters from the data provided by the receiver.

The RTP sequences through one of these cycles for each beam position (east, north, and vertical) to produce the three dimensional velocity field. The spectral moments and the raw spectral data are sent from the RTP to the DAP. The DAP in turn reformats the data and computes the consensus averaged profile. The data are available for display on the user terminal and for distribution to other systems. The user terminal can also be used to control the operation of the DRWP by sending commands to the DAP and/or RTP.
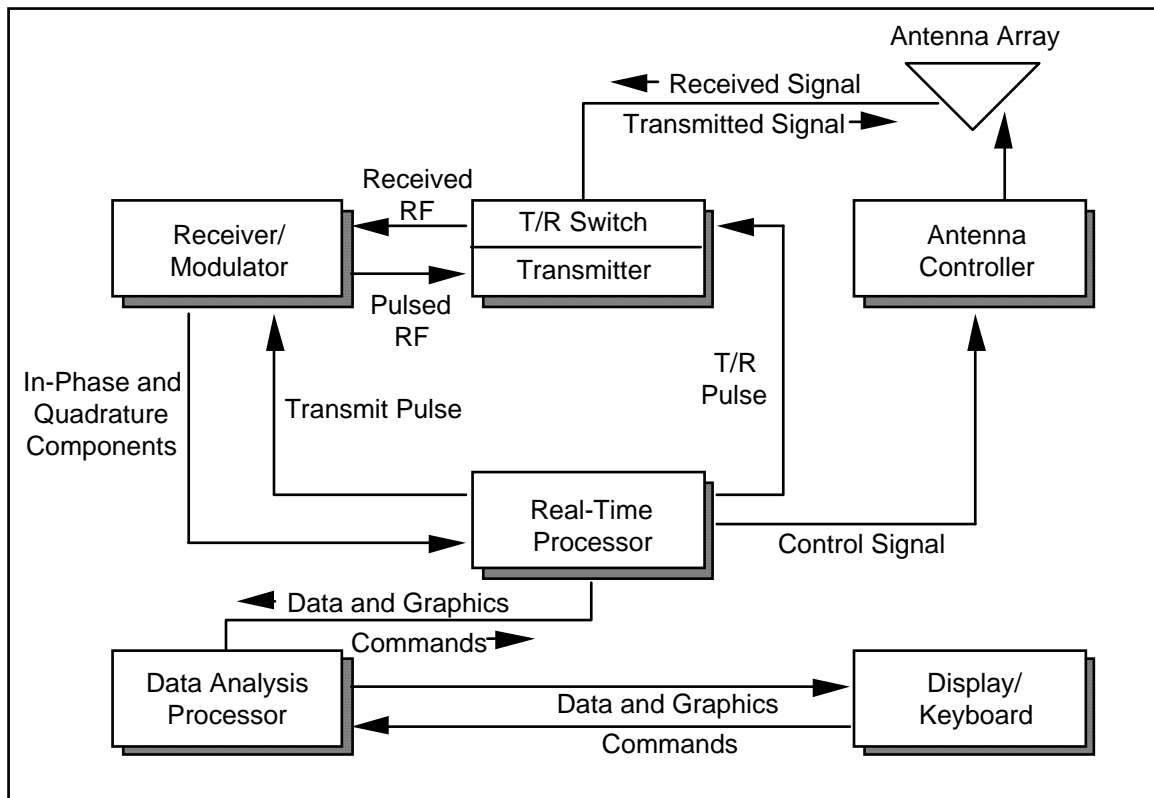
Figure 1.2.   Simplified block diagram for NASA's 50 MHz DRWP.

The NASA DRWP is a three beam system. The azimuth and elevation angles of the three beams are given in Table 1.1. The system has an operating frequency of 49.25 MHz and provides estimates of the horizontal wind components with an estimated accuracy of 1 to 2 m/s. In the current configuration, the system produces consensus averaged wind profiles with an update rate of 30 minutes and single-cycle profiles with an update rate of 3 minutes. The vertical range of the DRWP is nominally 2 km to 20 km with a resolution of 150 meters. The system is also capable of estimating winds in the stratosphere and mesosphere from 20 km to 90 km with a vertical resolution of 600 meters.

Table 1.1. Beam Configuration		
Beam	Azimuth Angle	Elevation Angle
Vertical	135°	90°
North	45°	75°
East	135°	75°

Since its installation in 1989, MSFC has been evaluating the accuracy, resolution, and reliability of the NASA DRWP. Although the system performed well, MSFC quickly identified problems with the single-cycle and consensus wind algorithms used by the DRWP.

The single-cycle technique provides wind profile updates every 3 minutes, but is susceptible to transient and side lobe signals which result in numerous erroneous wind estimates. The consensus technique sacrifices time resolution to mitigate the transient signal problem. The result is a technique that minimizes the effect of transient signals (i.e., fewer erroneous wind estimates) but is still susceptible to side lobes while only providing wind profile updates every 30 minutes.

1.4   MSFC New Wind Algorithm

To improve the quality and time resolution of the DRWP wind profiles, MSFC developed a new wind algorithm to replace the single-cycle and consensus techniques within the DRWP. The new wind algorithm uses a first guess velocity profile, a temporal median filter, and an interactive quality control procedure to mitigate the effects of transient and side lobe signals while still providing wind profile updates every 5 minutes.

MSFC's experience with the new wind algorithm has been quite favorable. After initialization with a reasonable first guess velocity, the technique is usually able to correctly identify the meteorological signal even when transient and/or side lobe signals are present. However, there are certain situations that are difficult for the technique to handle. The new algorithm has difficulty producing an accurate wind estimate when the meteorological signal is weak (most any technique would) or when the meteorological

signal tracks through a relatively large side lobe return. In the latter case, the technique occasionally "locks on" to the side lobe and uses the side lobe signal to estimate the wind velocity. When this situation develops, the operator will have to intervene and edit the first guess velocity file by replacing the erroneous wind value with a more realistic value. In subsequent profile updates, the technique will correctly identify the meteorological signal.

Using spectral data archived at the DRWP, MSFC developed wind profiles utilizing the new wind algorithm and compared those profiles to time proximate jimsphere profiles. The data used in this analysis spans the time frame from October 1990 to March 1992 and includes 239 jimsphere/DRWP profile pairs. Key results from these analyses are presented in Table 1.2.

Table 1.2. Jimsphere / DRWP Comparison (239 Pairs)*	
Mean Component Difference	<0.15 m/s
Average RMS Difference	1.8 m/s

*Data provided by MSFC in a briefing to NASA management in September 1992.

The small mean component difference (Table 1.2) indicates there is no bias between the jimsphere and DRWP wind estimates. Furthermore, the average root mean square (RMS) difference (Table 1.2) is not large considering the fact that the two instruments are not sampling the same volume of air. In fact, the RMS differences are correlated with the distance separation between the jimsphere balloon and the radar beam. Over distances from 20 to 100 kilometers, the RMS velocity differences between the DRWP data and jimsphere data exhibit a significant correlation with distance separation to the 1/3 power. This is important since results from other data analyses indicate similar correlations with sensor separation (e.g., Gage, 1979).

Although the MSFC analysis indicates the DRWP and the jimsphere provide similar wind information, these comparisons cannot be used to determine the precision of the DRWP because of the temporal and spatial sampling differences between the two instruments.

In addition to the analyses performed by MSFC, an assessment of the dynamic load on the Shuttle produced by the atmospheric winds (i.e., loads assessment) was performed by Rockwell using approximately 90 jimsphere/DRWP profile pairs supplied by MSFC. This preliminary assessment shows very little difference between the DRWP and jimsphere measured winds. Although a number of the DRWP profiles utilized in this preliminary assessment were produced by the single-cycle wind algorithm, over half of

the DRWP profiles used in this analysis were produced by the new MSFC wind algorithm.

1.5   NASA/KSC DRWP Certification

Because of the favorable preliminary evaluations and the expected value of the instrument to day-of-launch activities and daily weather forecasting, NASA/KSC is conducting a certification of the Doppler Radar Wind Profiler. The certification will validate the engineering performance of all system components, acquire or develop all documentation and appropriate spares to maintain the system, ensure the maintenance philosophy will satisfy user requirements[1], and verify the quality of the meteorological data output from the system.

These four tasks have been categorized into three major components: hardware validation, software validation, and meteorological validation. Engineering performance, documentation, spares and maintenance constitute the hardware validation being conducted by NASA/KSC Instrumentation and Measurements Branch personnel. The software validation, which includes testing existing profiler software and new/modified software associated with the MSFC wind algorithm, is being performed by AMU and NASA/KSC Instrumentation and Measurements Branch personnel. The verification of the quality of the meteorological data comprises the meteorological validation component of the certification effort and is being conducted by MSFC, Rockwell, and AMU personnel. Key components of this task include verifying that the resolution, accuracy, and reliability of the DRWP will satisfy user requirements. In essence, this means verifying that the meteorological data produced by the system could potentially be used for persistence calculations in support of launch activities, as well as routine day-to-day weather forecasting activities.

1.6   AMU Tasking

In association with the KSC certification effort, the AMU has been tasked to implement and evaluate the new wind algorithm developed by MSFC. The subtasks that comprise this task are:

- Implement the new wind algorithm developed by MSFC on the DRWP hardware.

- Test the new algorithm and software. This will include meteorological validation and evaluation of system function in relation to operational requirements.

- Provide software documentation for the AMU effort to include:
    Software Requirements Specification

---

[1] At this time only NASA organizations have submitted requirements for DRWP data. However, other organizations (e.g., Range Weather Operations, the Expendable Launch Vehicle community) are encouraged to submit their requirements for DRWP data. As new requirements for DRWP data are documented, the maintenance procedures will be modified accordingly, if funding is available.

Software User's Manual
Software Maintenance Manual
Software Test Descriptions and Results

- Provide training to both operations and maintenance personnel.

- Prepare a final meteorological validation report quantitatively describing overall system meteorological performance.

2.0 Data Analysis Processor Capabilities

The configuration of the DRWP after implementation of the new wind algorithm is completed is illustrated in Figure 2.1. The configuration is based on the algorithmic processing being performed on the DAP of the DRWP and the interactive quality control of the processed wind profile being performed by an operator using a VT 340 terminal located at the DRWP site or at a remote location such as the balloon facility.

Implementation of the new wind algorithm will not inhibit or remove any current processing on the DAP. It will enhance the capability of the system by adding the new algorithm's code and required user interface and display routines. The system will still produce the current single-cycle and 30 minute consensus wind profiles but will also produce a wind profile using the new wind algorithm. Profiles from the new wind algorithm will be available every cycle (approximately every three-to-five minutes).

Using the terminal at the DRWP site or a remote terminal at another location, the operator will have the ability to review wind profiles from both techniques (i.e., the consensus wind profiles from the current processing algorithms and the wind profile from MSFC's new wind algorithm), interactively quality control (QC) the new wind algorithm profile, and modify the first guess wind profile. The operator will also have the ability to select between manual and automatic distribution of new wind algorithm profiles to the Meteorological Interactive Data Display System (MIDDS).

The display used for interactive QC of the new wind algorithm profile is patterned after the MSFC QC display. The QC display features the velocity profile for each beam plotted over a color enhanced depiction of the intensity of the spectral data for each beam, respectively. The display includes data from the three most recent wind profiles and allows the operator to review the velocity data in light of the spectral data. Based on this display, the operator can determine if the velocity profile correctly tracks the atmospheric signal in the spectral data and then correct the first guess velocity file when it does not.

In the manual mode, which would be used for day-of-launch support, wind profiles from the new algorithm will not be distributed to the user community until an operator reviews the data and elects to output the wind profile. Updated wind profiles could be distributed at least as frequently as every 15 minutes in the manual mode.

In the automatic mode, which could be used to support daily weather forecasting, the wind profiles will be automatically distributed to MIDDS. The update rate in the automatic mode will be approximately three-to-five minutes depending upon the cycle time of the radar. Manual quality control would not be required. However, even in the automatic mode the operator can, at any time, review the new algorithm wind profile and manually edit the first guess velocity file which will in turn correct subsequent profiles.
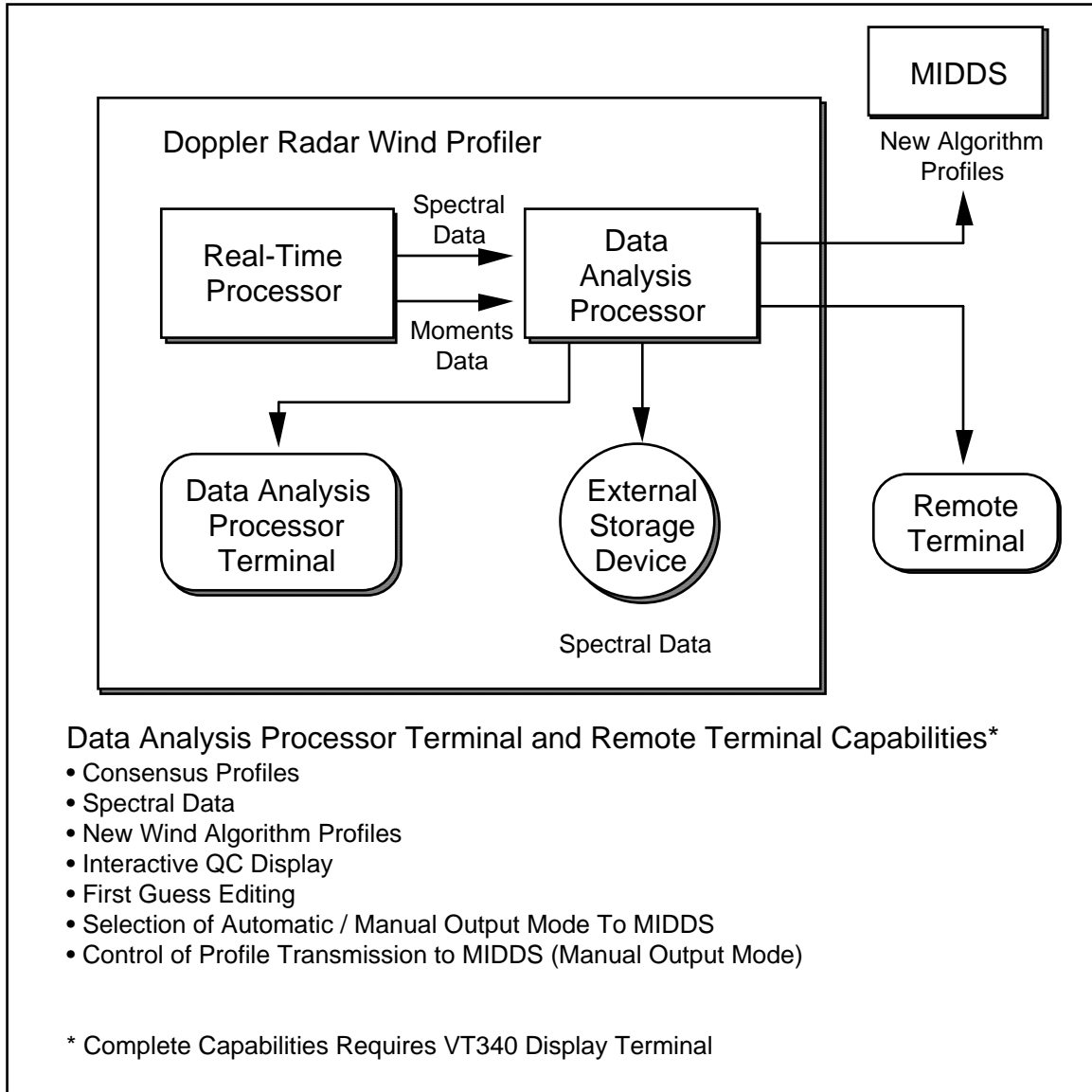
Figure 2.1.   Configuration of NASA's 50 MHz DRWP after implementation of the
                MSFC wind algorithm.

3.0 Algorithm Implementation

3.1   Algorithm Description

This section of the report contains a description of the MSFC wind algorithm and is intended to provide a basic understanding of the algorithmic processing and interactive quality control functionality of the MSFC wind algorithm. It is not, however, a mathematically and scientifically thorough description. The complete description of the specifications of the MSFC wind algorithm as implemented within the DRWP is contained within the *Software Requirements Specification for the New Wind Algorithm in NASA's 50 MHz Doppler Radar Wind Profiler* (Schumann et al., 1993).

The data processing in the MSFC wind algorithm (Figure 3.1) can be organized into four major components. Descriptions of the four components are presented in the following paragraphs.
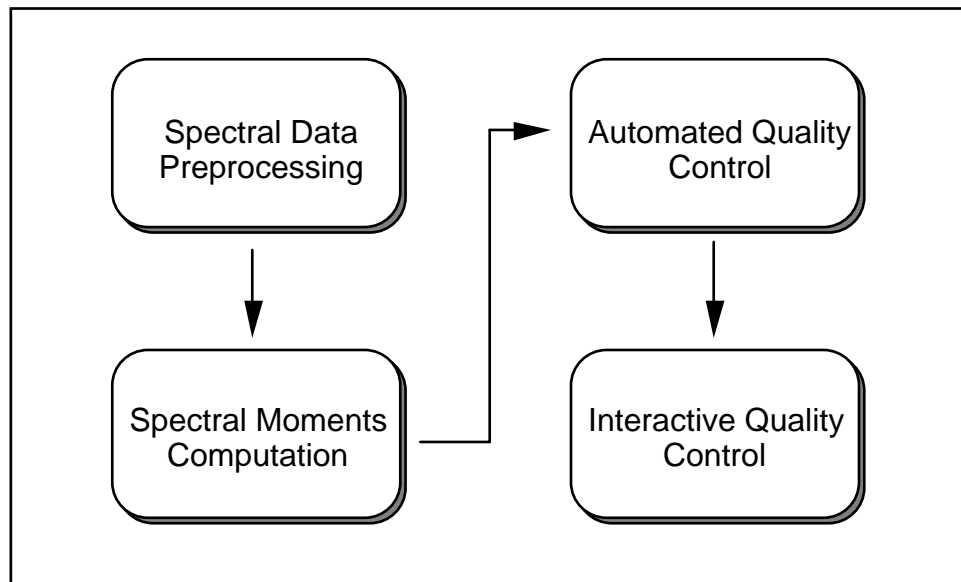
Figure 3.1.   Data processing in the MSFC wind algorithm.

3.3.1   Spectral Data Preprocessing

The Spectral Data Preprocessing component contains two functions, a temporal median filter and a running mean filter. The temporal median filter is a major feature of the MSFC wind algorithm and is used to remove transient signals from the spectral estimates. The temporal median filter can operate in either a three point or five point mode. The three point temporal median filter will select the median spectral estimate from a set of three estimates from the same range gate from the same frequency bin produced from returns from three different time periods. The five point median filter will function similarly but use five different spectral estimates. The default setting for the temporal filter for each beam is:

- North beam: Three point median filter.

- East beam: Three point median filter.

- Vertical beam: Median filter is off.

The running mean filter can be used to smooth the spectral estimates. Since the filter is a five point running mean, its most significant impact will be upon the amplitude of narrow bandwidth features. The filter computes a mean spectral estimate for each frequency bin by averaging the original spectral estimate from the given frequency bin and the spectral estimates within $\pm$ two frequency bins of the given frequency bin. For the ends of the spectrum where the running mean cannot be computed, the original estimate is not modified by this filter. The default setting for the running mean filter for each beam is:

- North beam: Running mean filter is off.

- East beam: Running mean filter is off.

- Vertical beam: Running mean filter is on.

3.1.2 Spectral Moments Computation

The Spectral Moments Computation function includes ground clutter removal and noise power and spectral moments calculations. The ground clutter removal technique is a logarithmic interpolation of the spectral estimates around the zero Doppler shift. The number of interpolated spectral estimates is a user configurable item. The default setting for the number of interpolated spectral estimates is three. The formula used for the logarithmic interpolation is contained in the Software Requirements Specification.

The noise power for each range gate is computed according to the Hildebrand and Sekhon method (Hildebrand and Sekhon, 1974). This objective automated technique is based on the fact that the standard deviation of the spectral densities is equal to the mean spectral density for white Gaussian noise. This technique is also used in the RTP of the DRWP.

This implementation of the Hildebrand and Sekhon method for noise power computation includes the capability of excluding a set number of spectral estimates around the zero Doppler shift from the calculations. The number of spectral estimates excluded from the noise power calculations is a user configurable item. The default setting for the number of spectral estimates around the zero Doppler shift excluded from the noise power calculations is three.

There are four algorithms used to compute the spectral moments - one for the lower range gates of the oblique beams, one for the upper range gates of the oblique beams, one for the mid range gate of the oblique beams, and one for all range gates of the vertical beam. Four different algorithms are used because different first guess velocity procedures and different smoothing procedures are used among the different beams and range gates to estimate the spectral moments. The range gate which separates the lower and upper range gate is identified as the mid range gate and is a user configurable item. The default setting for the mid gate is gate seven. The formulas used to compute the

signal power, the average Doppler shift, and the spectral width are presented in the Software Requirements Specification.

The key to the computation of the spectral moments is deciding which spectral estimates are used in the spectral moments integrations. There are three unique components of the MSFC wind algorithm which significantly influence this decision, the first guess velocity, the first guess velocity window width, and the integration window width. The procedure for determining which spectral estimates are used in the spectral moments integrations is presented in the following paragraphs.

First, the maximum spectral estimate, M, is found within the first guess window. The first guess window is defined by the range from the first guess velocity minus one-half the first guess window width to the first guess velocity plus one-half the first guess window width (Figure 3.2). By default, the first guess velocity is the antecedent velocity produced by the MSFC wind algorithm. If no first guess velocity is available, then the first guess window width is set equal to the entire spectrum which is equivalent to the current single-cycle technique. The first guess window widths are user configurable items and the recommended settings are presented in Section 5.1 of this document.
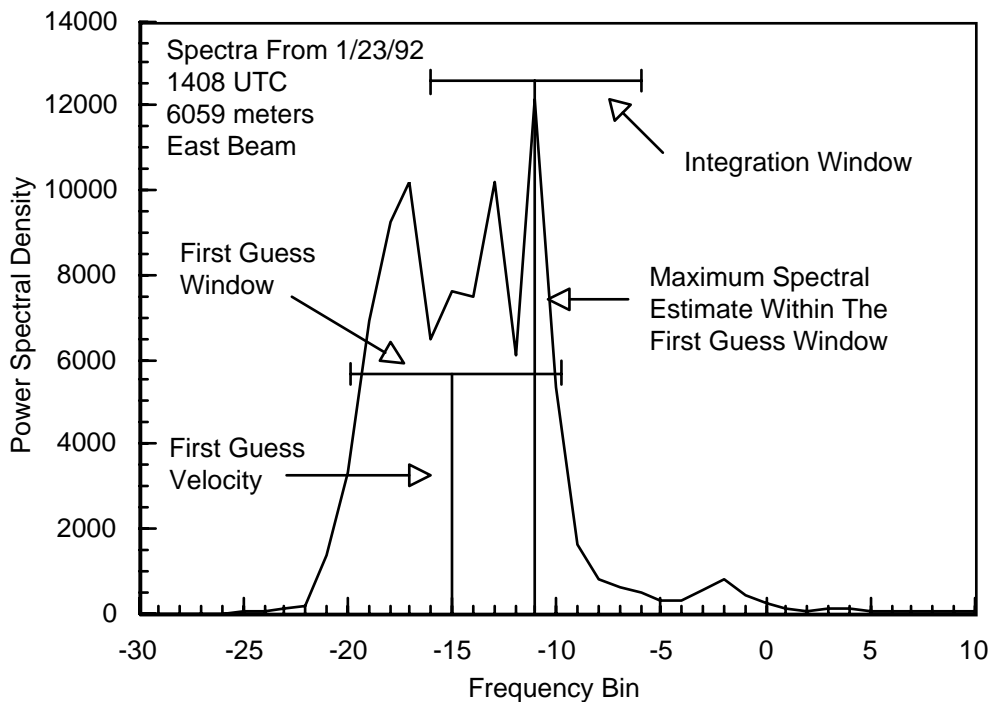
Figure 3.2.   Example of how the first guess velocity, the first guess window width, and the integration window width are used to compute the spectral moments.

After the maximum spectral estimate is found, the first and last spectral estimates to be used in the spectral moments computations are determined by comparing the test signal, T, to the spectral estimates within the integration window. The test signal is given by

$$T \quad = \quad B * (M - N)$$

where   B = the cut off percent and

N = the noise power.

The cut off percent is a user configurable item with a default value of 0.01. The integration window is defined by the range from the maximum spectral estimate frequency bin minus one-half the integration window width to the maximum spectral estimate frequency bin plus one-half the integration window width. The integration window widths are user configurable items. The recommended settings are presented in Section 5.1 of this document.

The first spectral estimate is the first frequency bin number within the integration window which satisfies the following criteria. For a given frequency bin number i,

$$(S_i - N) \quad > \quad T \quad \text{and} \quad (S_j - N) \quad > \quad T \text{ for all } j \text{ where } i < j < k$$

where S = the spectral estimate and

k = the frequency bin number of the maximum spectral estimate within the integration window.

The last spectral estimate is the last frequency bin number within the integration window which satisfies the following criteria. For a given frequency bin number i,

$$(S_i - N) \quad > \quad T \quad \text{and} \quad (S_j - N) \quad > \quad T \text{ for all } j \text{ where } k < j < i.$$

Figure 3.3 illustrates the relationship among the test signal, T, the maximum spectral estimate within the first guess window less the noise, M - N, the integration window width, and the spectral estimates used in the spectral moments computations.
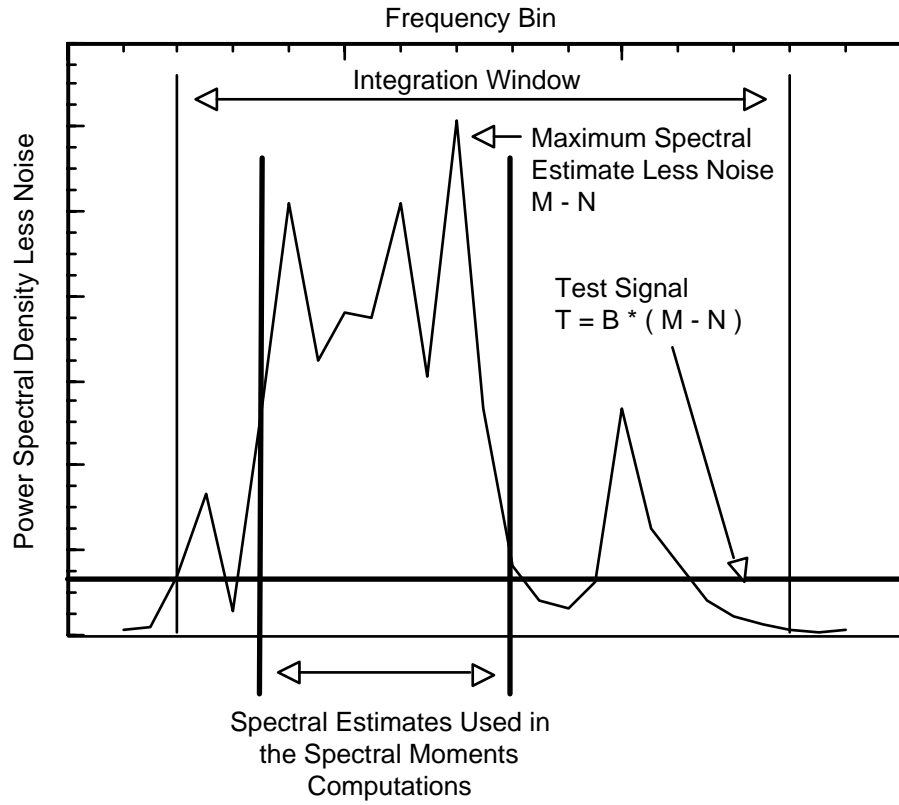
Figure 3.3. Example of the relationship among the test signal, T, the maximum spectral estimate within the first guess window less the noise, M - N, the integration window width, and the spectral estimates used in the spectral moments computations.

Given the above procedure for determining the first and last spectral estimates used in the spectral moments integrations, Figures 3.4, 3.5, and 3.6 define the procedures to be used to compute the spectral moments for the oblique beams' lower, mid, and upper range gates, respectively. For the oblique beams, the spectral moments for the mid gate are computed first. This is followed by computation of the spectral moments for the upper gates and then the lower gates. Figure 3.7 defines the procedures to be used to compute the spectral moments for the vertical beam.

Procedure For Computing Spectral Moments For Lower Gates Of Oblique Beams

Start Processing For Next Range Gate → Compute Noise Power → Compute Moments (FG Vel. = Vel. From Gate Above)

Is S/N > Critical Value? — Yes → Set Vel. = Avg Doppler Shift / Set FG Prop. Counter = 0

Is S/N > Critical Value? — No → Smooth Spectra (Running Mean - Frequency) → Compute Noise Power → Compute Moments (FG Vel. = Vel. From Gate Above)

FG = First Guess
Prop. = Propagation
Vel. = Velocity

Is S/N > Critical Value? — Yes → Set Vel. = Avg Doppler Shift / Set FG Prop. Counter = 0

Is S/N > Critical Value? — No → Set Vel. = First Guess Velocity / Increment FG Prop. Counter

Figure 3.4.   Procedure for computing the spectral moments for the lower gates of the oblique beams.

Procedure For Computing Spectral Moments For Mid Gate Of Oblique Beams

Start Processing For Next Range Gate → Compute Noise Power → Compute Moments (FG Vel. = FG Vel. From File)

Is S/N > Critical Value? — Yes → Set Vel. = Avg Doppler Shift / Set FG Prop. Counter = 0

Is S/N > Critical Value? — No → Smooth Spectra (Running Mean - Frequency) → Compute Noise Power → Compute Moments (FG Vel. = FG Vel. From File)

Is S/N > Critical Value? — Yes → Set Vel. = Avg Doppler Shift / Set FG Prop. Counter = 0

Is S/N > Critical Value? — No → Set Vel. = First Guess Velocity / Increment FG Prop. Counter

FG = First Guess
Prop. = Propagation
Vel. = Velocity

Figure 3.5.   Procedure for computing the spectral moments for the mid gate of the oblique beams.

16

**Procedure For Computing Spectral Moments
For Upper Gates Of Oblique Beams**

Start Processing For Next Range Gate

Compute Noise Power

Compute Moments (FG Vel. = FG Vel. From File)

Set Vel. = Avg Doppler Shift

Set FG Prop. Counter = 0

Is S/N > Critical Value?

Yes

No

Compute Moments (FG Vel. = Vel. From Gate Below)

Set Vel. = Avg Doppler Shift

Set FG Prop. Counter = 0

Is S/N > Critical Value?

Yes

No

Smooth Spectra (Running Mean - Frequency)

FG = First Guess
Prop. = Propagation
Vel. = Velocity

Compute Moments (FG Vel. = FG Vel. From File)

Compute Noise Power

Set Vel. = Avg Doppler Shift

Set FG Prop. Counter = 0

Is S/N > Critical Value?

Yes

No

Set Vel. = First Guess Velocity

Increment FG Prop. Counter

Figure 3.6. Procedure for computing the spectral moments for the upper gates of the oblique beams.

17

Figure 3.7.   Procedure for computing the spectral moments for all of the range
                gates of the vertical beam.

3.1.3 Automated Quality Control

The Automated Quality Control function contains two components, the vertical shear
quality control and the first guess propagation quality control. The vertical shear
control procedure examines the vertical shear in the horizontal velocities derived from
the oblique beams' radial velocities. The purpose of the procedure is to detect and
remove excessive vertical shears which result from a horizontal wind component at a
single level being highly disparate from its neighbors (i.e., the horizontal wind
components just above and below the given level). The procedure, which is applied to
both horizontal wind components, examines the vertical shear in the horizontal wind
component, ΔV, given by

$$\Delta V_k \quad = \quad |V_k - V_{k-1}|$$

where V = the horizontal wind component for one
                      of the oblique beams and

k = the range gate.

18

If ΔV_k and ΔV_{k+1} both exceed critical shear values and $| \Delta V_{k+1} - \Delta V_k |$ exceeds the critical differential shear value, then the horizontal wind component at range gate k, V_k, is highly disparate from its neighbors and is replaced by

$$V_k = (V_{k+1} + V_{k-1}) / 2.$$

In addition to replacing the horizontal wind component, the first guess propagation count for that beam is incremented by one. The critical shear and differential shear values are contained within the Software Requirements Specification.

The second component of the automated quality control function is the first guess propagation quality control. The purpose of this procedure is to limit the number of times the first guess velocity is successively propagated at a given level. If the first guess velocity for range gate k has been propagated more than five times successively for either or both oblique beams, then the radial velocities, V1 and V2, for both oblique beams at range gate k are replaced by

$$V1_k = (V1_{k-2} + V1_{k-1} + V1_k + V1_{k+1} + V1_{k+2}) / 5$$

$$\text{for } k = 2 \text{ to max gate - 2}$$

$$V1_k = V1_2 \qquad \text{for } k = 0 \text{ or } 1$$

$$V1_k = V1_{\text{max gate -2}} \qquad \text{for } k = \text{max gate or max gate - 1.}$$

$$V2_k = (V2_{k-2} + V2_{k-1} + V2_k + V2_{k+1} + V2_{k+2}) / 5$$

$$\text{for} \quad k = 2 \text{ to max gate - 2}$$

$$V2_k = V2_2 \qquad \text{for } k = 0 \text{ or } 1$$

$$V2_k = V2_{\text{max gate -2}} \qquad \text{for } k = \text{max gate or max gate - 1.}$$

Users of the data can tell if the profile has been smoothed by examining the first guess propagation count for the two oblique beams. At a given level, if the first guess propagation count exceeds four for either or both oblique beams, then the radial wind components for that level have been smoothed.

3.1.4 Interactive Quality Control

The final major component of the MSFC wind algorithm is the interactive quality control. This technique allows a user to review the DRWP wind profile in conjunction with the spectral estimates to determine if the wind algorithm is tracking the meteorological signal at all levels. If the user decides the wind algorithm is not, then the user may edit the first guess velocity profile and replace the erroneous wind estimates

with more realistic values. This modified first guess velocity profile will then be a key controlling factor in the estimation of the subsequent wind profile.

The interactive quality control display contains the velocity data and the spectral estimates for each beam from the three most recent wind profiles produced by the MSFC wind algorithm. Thus, the data from nine beams are displayed concurrently. Displaying information from the three most recent wind profiles provides the user with a record of the recent performance of the profiler and the MSFC wind algorithm.

The key aspects of the quality control display are illustrated in Figures 3.8 and 3.9. For each beam, the spectral estimate for each frequency bin within each range gate is displayed in a color-coded fashion. For each range gate, the relatively larger spectral estimates are represented by lighter colors (e.g., white) while the relatively smaller spectral estimates are represented by darker colors (e.g., blue). Four colors are used to represent the relative magnitudes of the spectral estimates. For this display, the horizontal axis represents the frequency bins and the vertical axis represents the range gates (height).
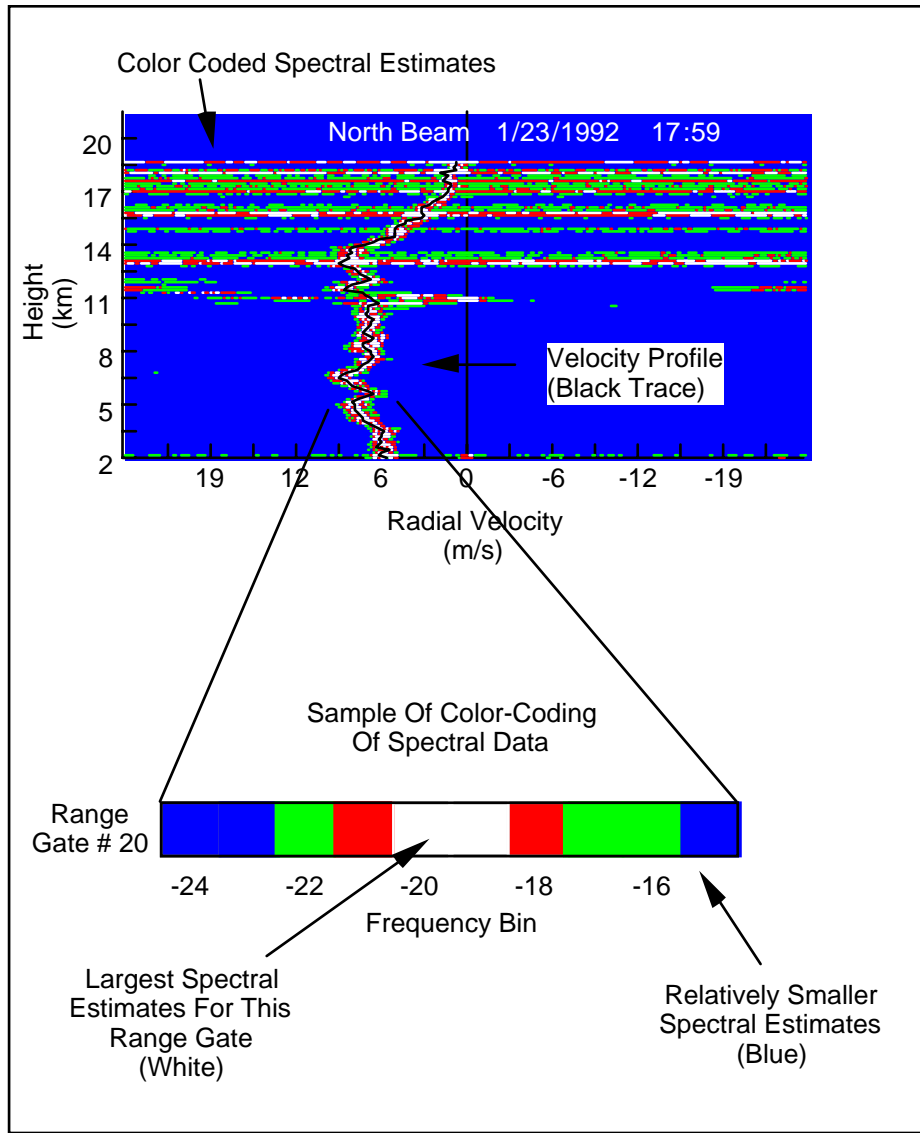
Figure 3.8.   Sample spectral estimates/velocity profile plot for the interactive quality control display.

In addition to the spectral estimates, this display also contains an x-y plot of the velocity profile with height (range gate) for that beam. This line graph overlays the color-coded spectral data.

The interactive quality control display also contains x-y plots of the signal-to-noise ratios for the north and east beams for the three most recent wind profiles produced by the MSFC wind algorithm (Figure 3.9). These graphs help the user assess the quality of the DRWP wind estimates.
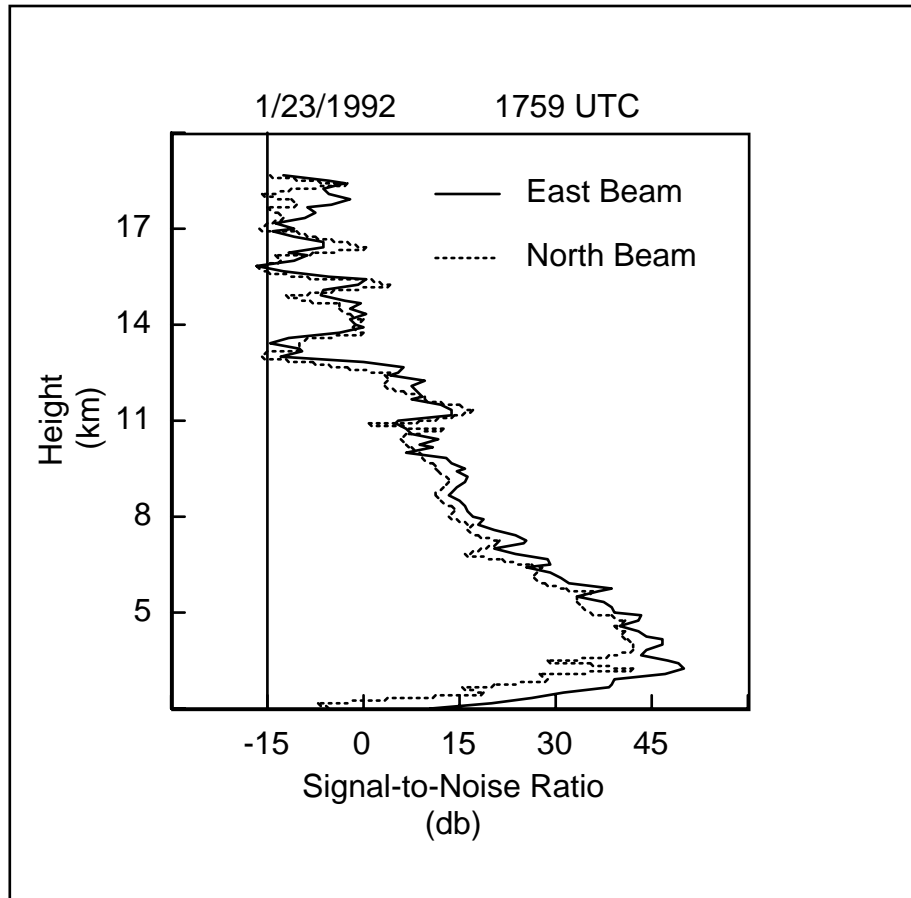
Figure 3.9.   Sample signal-to-noise ratio plot for the interactive quality control display.

3.2   Development Approach

The approach used by the AMU to implement the MSFC wind algorithm into the DRWP is illustrated in Figure 3.10.   The approach is typical of many software development programs with one exception.   Most structured software development methodologies require the development of the software documentation in parallel with the design and development of the code.   The AMU approach is more efficient since documentation does not have to be continually updated through out the development process.

Although all of the components of the development process must be executed properly to ensure a successful program, there are three components of this effort that were particularly important to the implementation of the MSFC wind algorithm. First is the emulation of the Post Data Handler (PDH) on ENSCO's MicroVAX computer. This enabled AMU personnel to use ENSCO's computer to analyze the PDH software and code and test the software for the new wind algorithm. This greatly reduced the number of conflicts between software development and research, testing, or operations use of the DRWP. Consequently, the labor and the time span required to implement the new wind algorithm was reduced.

The second component key to the implementation of the new wind technique was the optimization of the algorithms used within the technique and the associated quality control displays. The PDH is hosted on a MicroVAX II computer which is, by today's standards, a very slow processor. Consequently, the code for the new wind algorithm had to be efficient to meet the performance requirements.
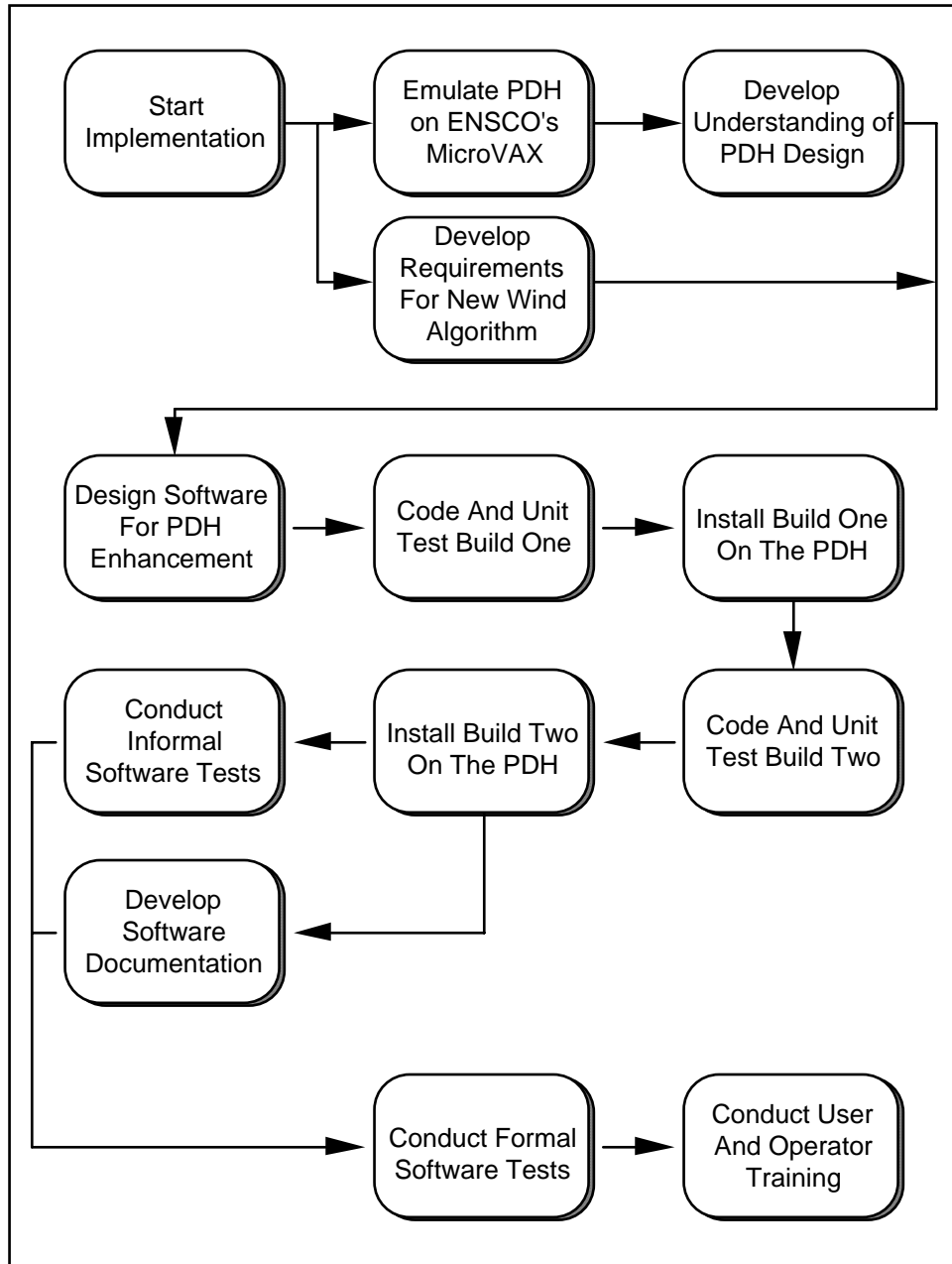
Figure 3.10.   New wind algorithm development approach.

The code used to compute the basic spectral moments was optimized by replacing the sort algorithms used by the MSFC code with more efficient algorithms and by improving

the procedure for accessing data from arrays. These modifications resulted in an 83% reduction in the processing time required to compute the spectral moments.

The MSFC code for the quality control display requires the computation of 86,000 base 10 logarithms and then maps 86,000 data points to the screen for each wind profile. A MicroVAX II computer connected via a serial communications line to a VT340 terminal could not support these processing demands and meet the performance requirements described in the Software Requirements Specification.

The optimization of the quality control display code preserves the salient features of the MSFC quality control display and yet significantly reduces (i.e., by approximately 90%) the processing time required to produce the display. The optimized code contains no base 10 logarithm calls and reduces the number of data points mapped to the screen from 86,000 to an average of less than 10,000.

The third key component of the implementation of the new wind algorithm was the Build One / Build Two strategy. This aspect of the implementation focused on developing and testing critical components of the new software as early as possible within the development cycle. This facilitated testing and, where necessary, modifying design concepts at a point in time where changes could be implemented without significant impact to schedule or cost.

The critical items included in Build One were the modification of the spectral archive process, the computation of the wind profile, and the quality control display. The remaining items assigned to Build Two were the user control of the new wind algorithm processing, the output of the wind profile to MIDDS, and the wind speed and direction display.

3.3   Software Design

This section of the report presents top-level design information for the enhanced PDH of the DRWP. It contains only information regarding the design of the new wind algorithm and other key components of the enhanced PDH. The reader should consult the *Program Maintenance Manual for the NASA 50 MHz Wind Profiler System* (Tycho, 1990) and the *Software User's Manual for the NASA 50 MHz Wind Profiler System* (Tycho, 1990) for additional information regarding the PDH.

The code for the new wind algorithm and the modification to existing PDH software was written in the C programming language under the Virtual Memory System (VMS) operating system. The Graphical Kernel System (GKS) was used for the graphical displays, and Curses was used for the menu systems. These are the same languages and systems used for the development of the existing PDH software.

The enhanced PDH ingests raw spectral estimates and single-cycle spectral moments data, computes consensus averaged and new algorithm wind profiles, provides a user interface to monitor and control the products produced by the PDH, outputs wind profiles to MIDDS, and has the capability of archiving/retrieving spectral data. This functionality has been allocated to one of five software components - the User Interface Function, the

Consensus Averaging Function, the Spectral Data Ingest Function, the MIDDS Output Function, or the New Wind Algorithm Function (Figure 3.11). The functionality and input and outputs of each component will be described in the following paragraphs.

```
┌─────────────────────────────────────────────────────────┐
│                                                         │
│                   Post Data Handler                     │
│                                                         │
│    ┌──────────────┐  ┌──────────────┐  ┌──────────────┐ │
│    │User Interface│  │  Consensus   │  │ Spectral Data│ │
│    │  Function    │  │Averaging Func.│  │Ingest Function│ │
│    └──────────────┘  └──────────────┘  └──────────────┘ │
│                                                         │
│          ┌──────────────┐    ┌──────────────┐           │
│          │ MIDDS Output │    │  New Wind    │           │
│          │  Function    │    │Algorithm Func.│           │
│          └──────────────┘    └──────────────┘           │
│                                                         │
└─────────────────────────────────────────────────────────┘
```
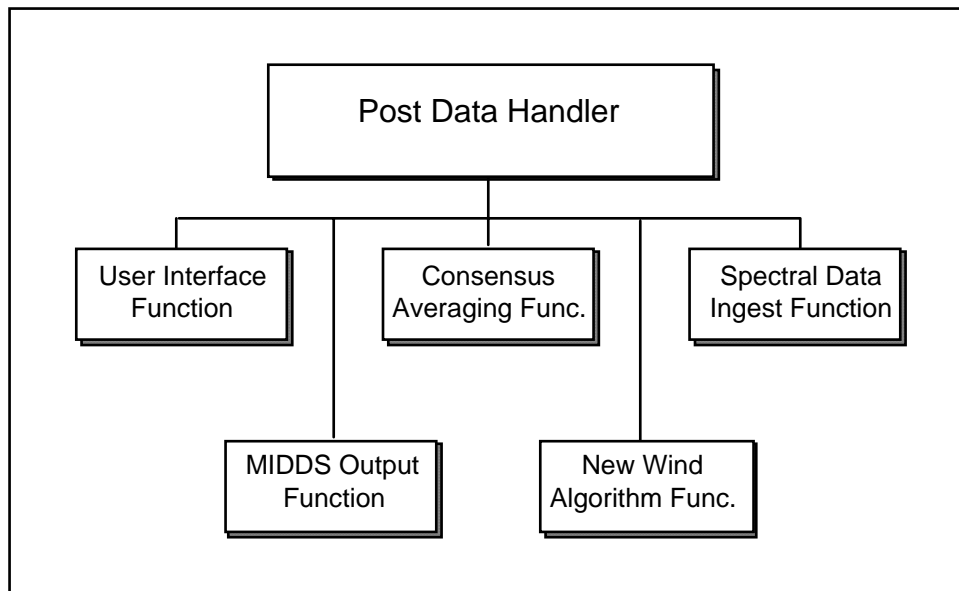
Figure 3.11.   Post Data Handler software components.

To support the PDH functionality, the enhanced PDH has four external interfaces (Figure 3.12). The PDH has an external interface with the RTP of the DRWP to ingest raw spectral estimates and single-cycle spectral moments data. The PDH has an external interface with MIDDS to export either consensus averaged or MSFC wind profiles. The PDH has an external interface with the user display terminal to export graphics commands for the display of menu systems and wind profile data. This external interface is also used to ingest keyboard entries from the user to control the graphics products displayed on the terminal and to control the operation of the PDH. The PDH has an external interface with an external storage device (i.e., 9 track tape drive) to archive and retrieve spectral data.

The User Interface Function performs all of the processing for the graphic displays on the User Display Terminal. The user displays associated with the MSFC wind profiles include:

- Spectral estimates / velocity profile quality control display.

- Wind speed versus height and wind direction versus height display.

The User Interface Function also provides the user with the capability to:

- Edit the first guess velocity profile.

- Edit the process parameter file.

- Select whether the output to MIDDS is automatic or manual.

- Select whether lower range profile (e.g., 2 km to 20 km) or upper range profile (e.g., 20 km to 90 km) is used in the new algorithm wind profile displays.

- Turn on/off the output of spectral estimates to the external storage device.

This is not a complete list of the all of the capabilities of the user interface. Only those capabilities associated with the implementation of the new wind algorithm have been included.
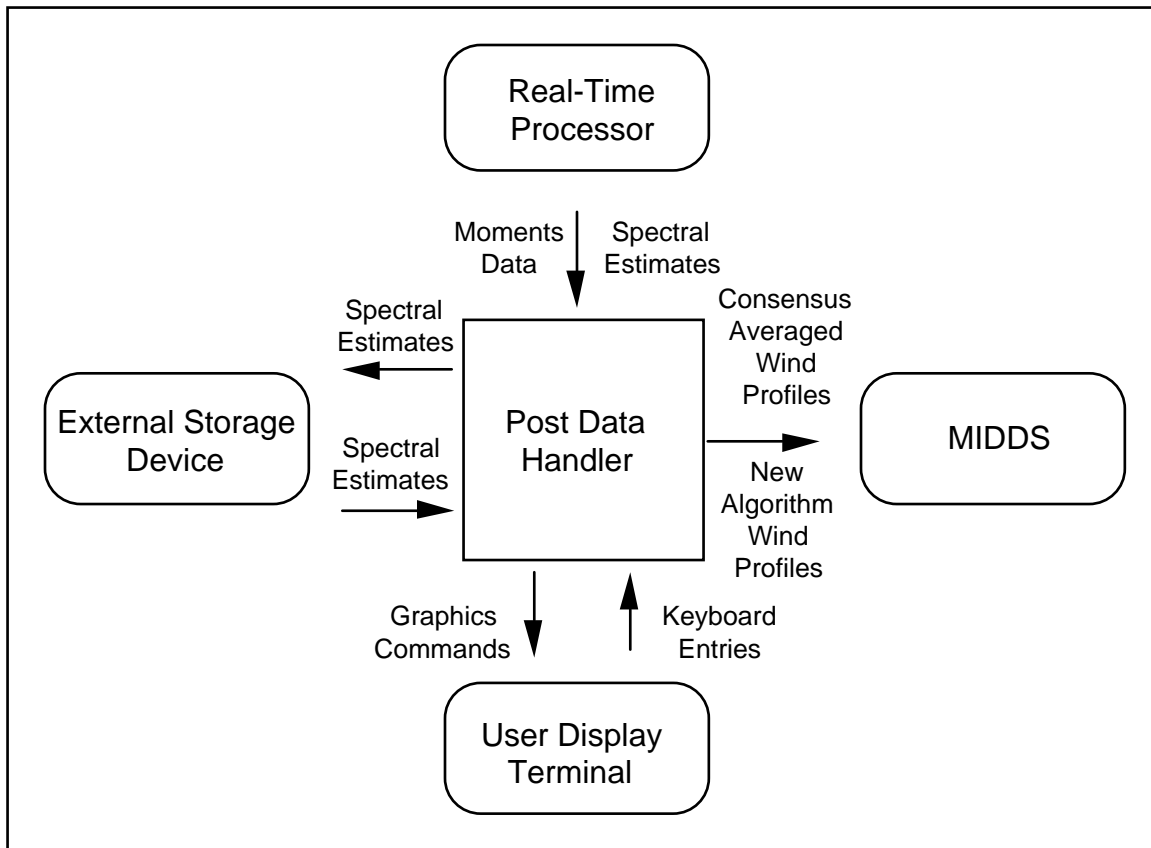
Figure 3.12. External interfaces of the Post Data Handler. The control and data flows between the User Interface Function and other components of the DRWP are illustrated in Figure 3.13. Data input into the User Interface Function include:

- Wind profiles from the single-cycle, consensus, and new algorithm wind profiles disk files.

- Filtered spectral estimates from global memory.

- First guess velocity profiles from the first guess data files.

- Wind algorithm parameter values from the new wind algorithm parameters file.
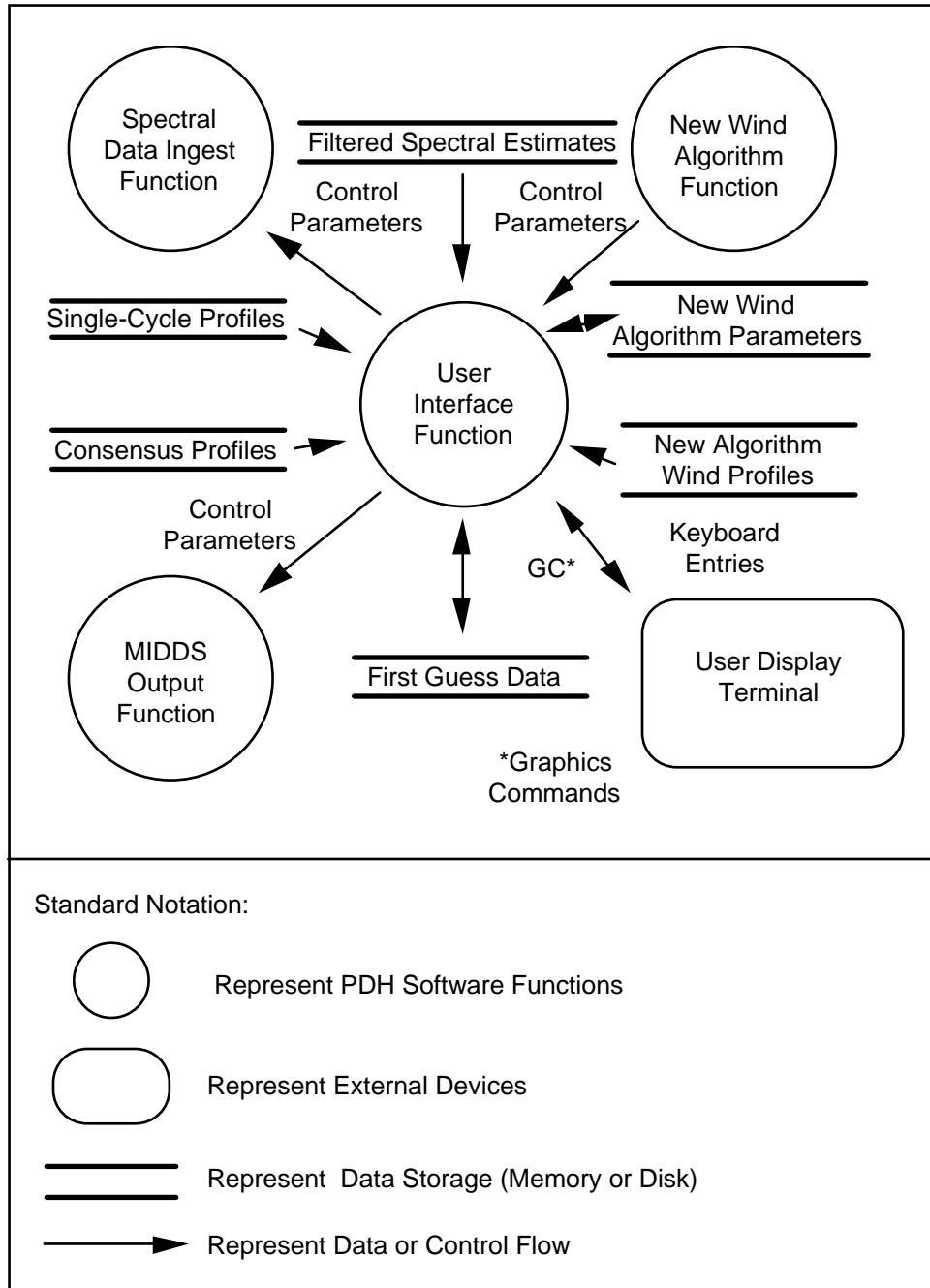
Figure 3.13.   Data/control flow diagram for the User Interface Function.

Data output from the User Interface Function include:

- Modified first guess velocity profiles to the first guess data file.

27

- Modified wind algorithm parameter values to the new wind algorithm parameters file.

Controls output from the User Interface Function include:

- Control parameter to the MIDDS Output Function directing the MIDDS Output Function to transmit another new algorithm wind profile to MIDDS (manual mode only).

- Control parameter to the Spectral Data Ingest Function that turns on/off the archiving of spectral estimates.

- Graphics commands to the User Display Terminal for the wind profile displays and the menu systems.

Controls input to the User Interface Function include:

- Control parameter from the New Wind Algorithm Function indicating that a new wind profile has been written to disk.

- User keyboard entries from the User Display Terminal.

The primary function of the Consensus Averaging Function component is the computation of the consensus averaged wind profiles from the single-cycle wind profiles. A complete description of the consensus averaging algorithm is contained within the Tycho documentation. The Consensus Averaging Function also writes the single-cycle and consensus averaged wind profiles to disk files.

The control and data flows between the Consensus Averaging Function and other components of the DRWP are illustrated in Figure 3.14. As evidenced by the figure, the Consensus Averaging Function operates independently of the other PDH components.
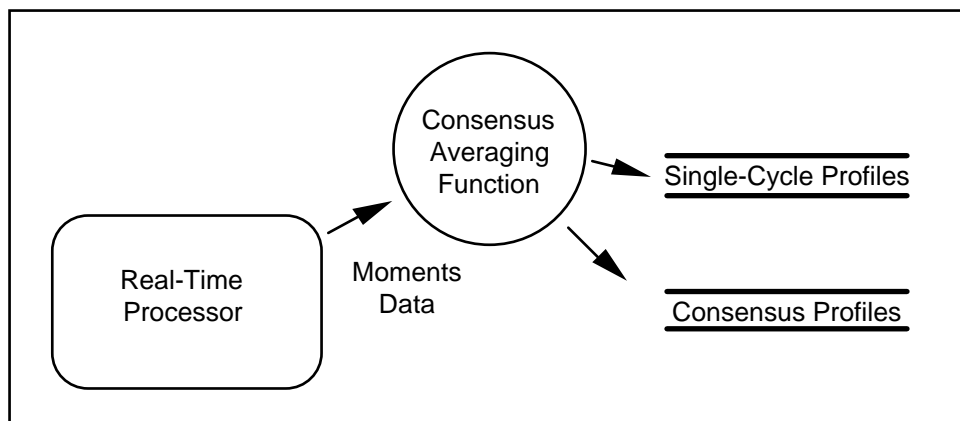
Figure 3.14. Data/control flow diagram for the Consensus Averaging Function.

Data input into the Consensus Averaging Function include:

28

- Single-cycle spectral moments from the RTP.

Data output from the Consensus Averaging Function include:

- Single-cycle wind profiles to the single-cycle profile disk files.

- Consensus averaged wind profiles to the consensus profile disk files.

The MIDDS Output Function is responsible for transmitting the consensus averaged or new algorithm wind profiles to MIDDS. The format of the new algorithm wind profile is described in the Software Requirements Specification. The type of wind profiles (e.g., consensus averaged or new algorithm) transmitted to the MIDDS is determined by the MicroVAX system manager. The default configuration of the system will output new algorithm profiles to the MIDDS. It will require action by the MicroVAX system manager, not the operator, to change the configuration of the system such that consensus averaged profiles would be transmitted to the MIDDS.

The control and data flows between the MIDDS Output Function and other components of the DRWP are illustrated in Figure 3.15. As evidenced by the figure, the only other PDH software components with a direct interface with the MIDDS Output Function are the User Interface Function and the New Wind Algorithm Function.
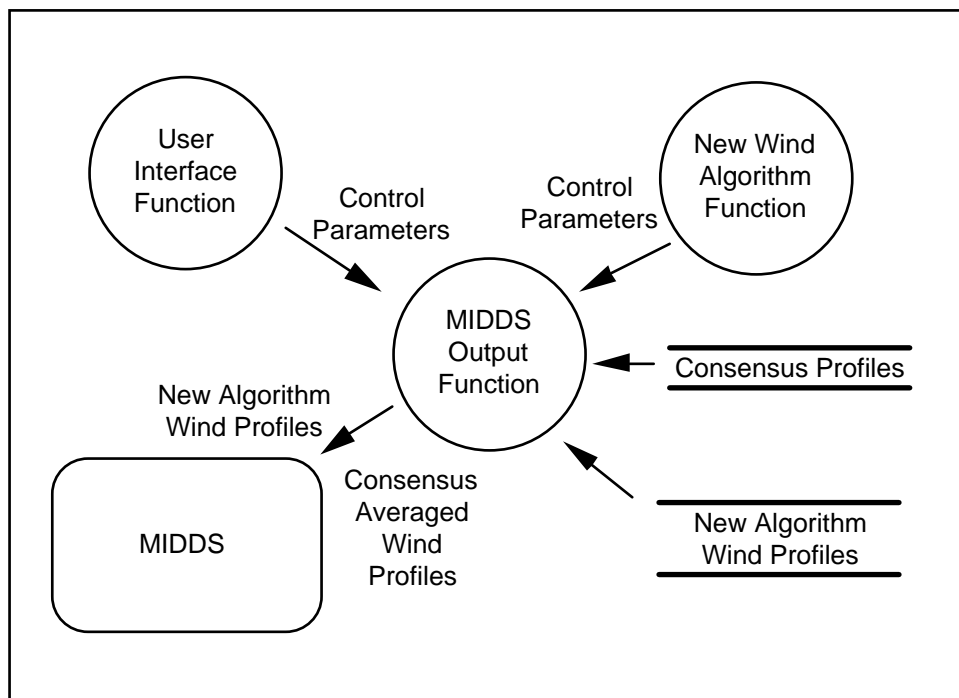
Figure 3.15.   Data/control flow diagram for the MIDDS Output Function.

Data input into the MIDDS Output Function include:

- Wind profiles from the consensus and new algorithm wind profiles disk files.

Data output from the MIDDS Output Function include:

- Wind profiles from the consensus and new algorithm wind profiles disk files.

Controls input to the MIDDS Output Function include:

- Control parameter from the User Interface Function directing the MIDDS Output Function to transmit the new wind algorithm profile to MIDDS (manual mode only).

- Control parameter from the New Wind Algorithm Function directing the MIDDS Output Function to transmit the new wind algorithm profile to MIDDS (automatic mode only).

The New Wind Algorithm Function is responsible for all of the processing required to produce new algorithm wind profiles from the raw spectral data. The functionality of this component includes:

- Ability to smooth the spectral estimates with a running mean filter.

- Ability to smooth the spectral estimates with temporal median filter.

- Ability to compute the noise power of the spectral estimates by the Hildebrand and Sekhon method (Hildebrand and Sekhon, 1974).

- Ability to compute the average Doppler shift, the spectrum width, and the signal power according to the new wind algorithm.

- Ability to automatically perform a vertical wind shear quality control procedure.

- Ability to automatically perform a first guess velocity propagation quality control procedure for the oblique beams.

- Ability to output the following products for each range gate with every wind profile update:

  - Horizontal wind speed,
  - Horizontal wind direction,
  - Vertical wind speed,
  - Vertical wind shear,
  - North beam signal power,
  - East beam signal power,
  - Vertical beam signal power,
  - North beam noise power,
  - East beam noise power,
  - Vertical beam noise power,
  - North beam spectral width,

- East beam spectral width,
- Vertical beam spectral width,
- Number of successive first guess velocity propagations for the east beam, and
- Number of successive first guess velocity propagations for the north beam.

The New Wind Algorithm Function will write to disk the new algorithm wind profiles in accordance with the on-line storage format. The specification for this format is contained in the Software Requirements Specification.

The data flows between the New Wind Algorithm Function and other components of the DRWP are illustrated in Figure 3.16. As evidenced by the figure, the New Wind Algorithm Function interfaces with three other PDH software components. These interfaces perform the function of notifying the software components receiving the message that new data are available for further processing.
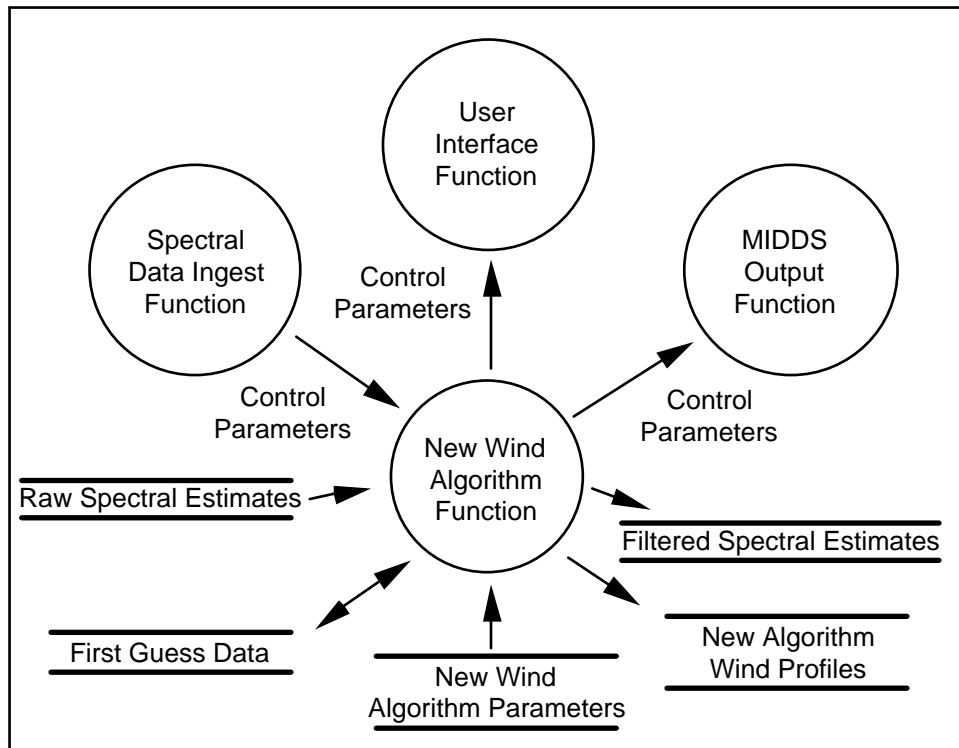
Figure 3.16.   Data/control flow diagram for the New Wind Algorithm Function.

Data input into the New Wind Algorithm Function include:

- Raw spectral estimates from global memory.

- First guess velocity profile from the first guess velocity disk file.

- New algorithm processing parameters from the new wind algorithm parameter disk file.

31

Data output from the New Wind Algorithm Function include:

- Wind profiles to the new algorithm wind profiles disk files.

- Filtered spectral estimates to global memory.

- First guess velocity profile to the first guess velocity disk file.

Controls input to the New Wind Algorithm Function include:

- Control parameter from the Spectral Data Ingest Function indicating that new spectral estimates have been placed in global memory and are available for processing.

Controls output from the New Wind Algorithm Function include:

- Control parameter to the User Interface Function indicating new filtered spectral estimates have been placed in global memory and a new wind profile has been written to disk.

- Control parameter to the MIDDS Output Function directing the MIDDS Output Function to transmit the new algorithm wind profile to MIDDS (automatic mode only).

The Spectral Data Ingest Function ingests the raw spectral estimates from the RTP, decodes the spectral estimates, and then stores the estimates in global memory (Figure 3.17). The Spectral Data Ingest Function also has the capability to output the raw spectral estimates to the external storage device and retrieve spectral estimates from the external storage device.

Data input into the Spectral Data Ingest Function include:

- Spectral estimates from the RTP.

- Spectral estimates from the External Storage Device.

Data output from the Spectral Data Ingest Function include:

- Spectral estimates to global memory.

Controls input to the Spectral Data Ingest Function include:

- Control parameter from the User Interface Function that turns on/off the archiving of spectral estimates.

Controls output from the Spectral Data Ingest Function include:

- Control parameter to the New Wind Algorithm Function indicating that new spectral estimates have been placed in global memory and are available for processing.
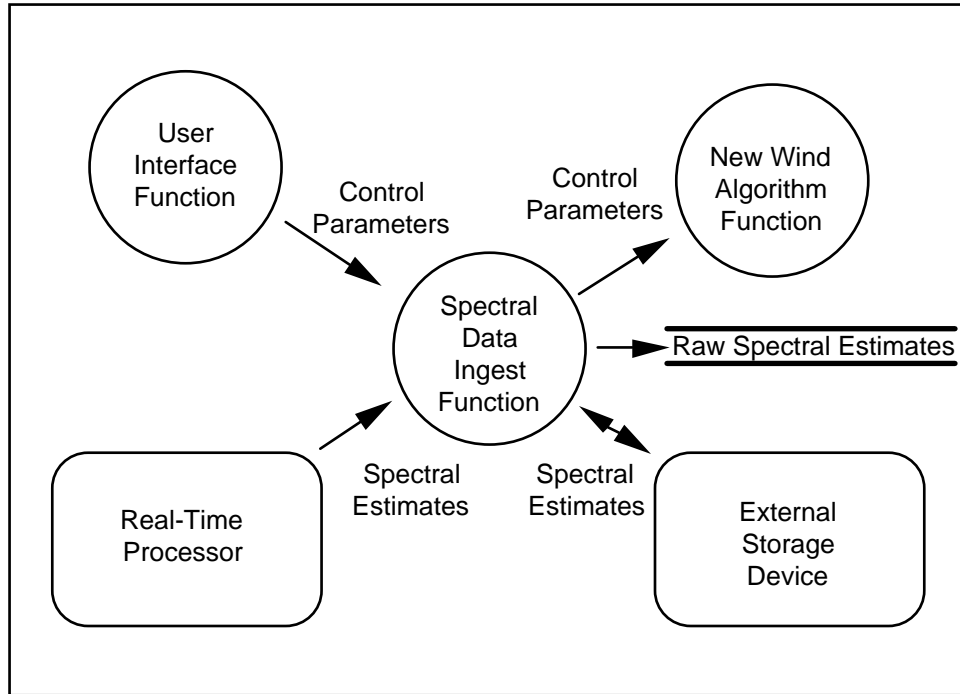
Figure 3.17.   Data/control flow diagram for the Spectral Data Ingest Function.

4.0 Meteorological Evaluation

The meteorological evaluation of the MSFC wind algorithm is comprised of three major components,

- A comparison of jimsphere wind profiles and time proximate DRWP wind profiles produced by the MSFC wind algorithm (Section 4.1),

- A comparison of consensus averaged DRWP wind profiles and time proximate DRWP wind profiles produced by the MSFC wind algorithm (Section 4.1), and

- A comparison of DRWP wind profiles produced by the MSFC wind algorithm using different parameter configurations (Section 4.2).

Since the jimsphere is the current accepted standard for tropospheric wind measurements at KSC/CCAFS, it is important to have a thorough understanding of the relative performance and advantages and disadvantages of the jimsphere and DRWP systems. Consequently, a comparison of jimsphere and DRWP profiles was deemed appropriate. Although this analysis does not provide an absolute measure of the quality of the data from the DRWP, it does provide a relative measure of performance of the DRWP and information regarding the advantages and disadvantages of the DRWP.

In addition to the jimsphere/MSFC wind algorithm profile comparisons, the wind profiles produced by the MSFC wind algorithm were compared to time proximate consensus averaged DRWP wind profiles. This analysis provides a quantitative measure of the differences in performance between the two methods of profile estimation and the advantages and disadvantages of the two methods.

The MSFC wind algorithm contains a number of user configurable parameters which influence the performance of the wind profile estimation technique. Consequently, as part of the meteorological evaluation, the performance of a number of different configurations of these parameters were examined to determine an optimum configuration for the MSFC wind algorithm.

The data used for these analyses includes 16 hours of profiler data from three different time periods. The data set contains:
- 5 hours of profiler data from 12 September 1991.
- 5.5 hours of profiler data from 23 January 1992.
- 5.5 hours of profiler data from 20 February 1992.

For each of the three time periods, the initial first guess velocity used in the MSFC wind algorithm was based on a time proximate jimsphere profile. For each case, the jimsphere profile proved to be an effective first guess velocity profile and it was not necessary to modify the first guess velocity profile at any time within the 5 or 5.5 hour analysis period.

There were no significant weather events which would contaminate the profiler data at or near the Shuttle Landing Facility (SLF) during the analysis periods from 12 September 1991 and 20 February 1992. However, there were two significant weather events at the SLF during the data analysis period from 23 January 1992. A rain shower was reported at the SLF from 1650 UTC to 1700 UTC and a thunderstorm was in the vicinity from 1812 to 1830 UTC. Examination of the data from 23 January 1992 indicates the profiler data were not adversely affected by the rain shower, but were significantly affected by the thunderstorm. Examples of spectral data contaminated by lightning and the resulting impacts upon consensus and MSFC wind algorithm profiles are presented in Section 4.1.11.

Using the 16 hours of profiler data, wind profiles were produced using five different configurations of the key user configurable parameters of the MSFC wind algorithm (Table 4.1). For each configuration, 256 wind profiles were produced for a total of 1280 wind profiles. A subset of these wind profiles have been inter-compared to determine the optimum configuration of the MSFC wind algorithm parameters for operational use. In addition to the inter-comparisons, the MSFC wind algorithm profiles have been compared to 34 time proximate consensus averaged DRWP wind profiles and 11 time proximate jimsphere profiles. In order to compare the DRWP and jimsphere profiles, the jimsphere data were interpolated to the DRWP profile reporting levels.

Table 4.1. DRWP Configurations			
Configuration Number	First Guess Window Width (Frequency Bin #)	Integration Window Width (Frequency Bin #)	Minimum SNR (dB)
DRWP #1	6	10	-15
DRWP #2	6	20	-15
DRWP #3	12	10	-15
DRWP #4	6	10	-8
DRWP #5	12	20	-8

4.1 Comparison of Jimsphere, Consensus Averaged DRWP, and MSFC Wind Algorithm DRWP Profiles

The following paragraphs present the results of the comparisons of jimsphere, consensus averaged DRWP, and MSFC wind algorithm DRWP profiles. Although comparisons have been performed and analyzed for all five DRWP configurations, only the results of the comparisons using DRWP configuration #3 (Table 4.1) are presented in this report.

Limiting the comparison results in the report to those from DRWP configuration #3 provides quantitative information about the merits and limitations of the MSFC wind

algorithm without burdening the reader with redundant information. Furthermore, no significant information is omitted from the report because:

- The results using DRWP configurations #1 and #2 are very similar to the results using configuration #3, and

- The results from DRWP configurations #4 and #5 indicate configurations #4 and #5 are not as effective as configurations #1, #2, and #3.

To supplement the analysis and understanding of the horizontal wind profiles presented in this section, the corresponding SNR profiles from DRWP configuration #3 are presented in Appendix A.

4.1.1 First Wind Profile Comparison From 12 September 1991

The first set of time proximate jimsphere, consensus averaged DRWP, and MSFC wind algorithm DRWP profiles from 12 September 1991 is presented in Figures 4.1 and 4.2. The large scale features present in the three profiles are very similar; however, the small scale features exhibit differences, particularly in the east beam velocities. The differences in the small scale features are not surprising in light of the spatial and temporal differences in data collection between the jimsphere and the DRWP. The sampling period of the DRWP is three to five minutes and the volume of air sampled is almost directly above the antenna field. In contrast, the jimsphere sampling period is of the order of 45 minutes and the balloon travels downwind as it rises. Thus, in addition to a relatively long sampling period, the jimsphere is likely to be sampling air many kilometers downwind from the release site at higher altitudes.

The relatively large east beam velocity shear zones between 13 km and 16 km are described similarly by all three profiles. The same is true of the relatively large north beam velocity shear zone from 13 km to 15 km. One major difference among the profiles occurs in the east beam velocities between 5 km and 7 km where the velocities are near zero. Velocities near zero are a known problem for the DRWP. A second major difference among the profiles occurs in the east beam velocities between 8 km and 12 km. Examination of a series of MSFC wind algorithm DRWP profiles from 1846 UTC to 2015 UTC indicates temporal changes in the east beam velocities as large as 4 m/s within this 90 minute period in the 8 km to 12 km region. Consequently, the east beam velocity difference in the 8 km to 12 km range between the jimsphere and DRWP profiles is probably due to the sampling differences between the two systems.

The degree of correlation between the jimsphere profiles and the MSFC wind algorithm DRWP profiles was quantified by cross spectrum analysis. One of the products of cross spectrum analysis is the coherency spectrum which measures the correlation between the two signals (e.g., profiles) at each wavelength (Jenkins and Watts, 1968). The square of the coherency can vary between 0 and 1 and is analogous to the square of the correlation coefficient, except the coherency is a function of wavelength. As the square of the coherency approaches 1 for a given wavelength, then the two signals are highly linearly correlated at the given wavelength. Conversely, as the

36

square of the coherency approaches 0 for a given wavelength, then the two signals are not linearly correlated at the given wavelength.

The data in Figure 4.3 indicate both components of the jimsphere and MSFC wind algorithm DRWP profiles are highly coherent (i.e., coherency squared values of ~ 0.7 or greater) to wavelengths as short as 1400 meters (i.e., wave number $4.5 \infty 10^{-3}$ m^{-1} where wave number equals 2π / wavelength). At shorter wavelengths, the coherence of the north beam velocities remains relatively high whereas the coherence of the east beam velocities is generally less. This is expected since the small scale features exhibited greater differences in the east beam velocities than the north beam velocities (Figures 4.1 and 4.2).
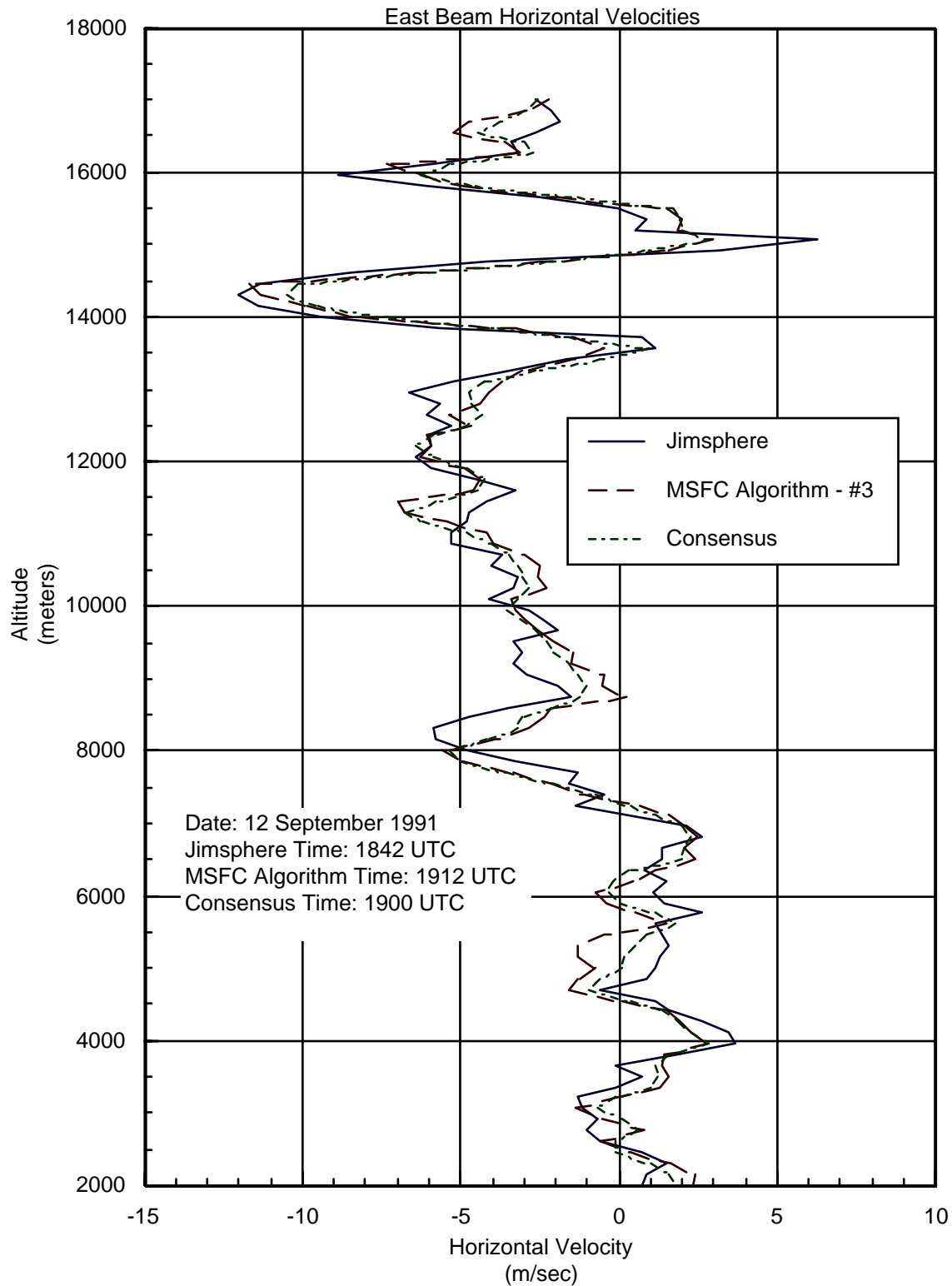
Figure 4.1.   East beam velocities for 12 September 1991. Profile time stamps are:
Jimsphere 1842 UTC, Consensus 1900 UTC, and MSFC wind
algorithm 1912 UTC.
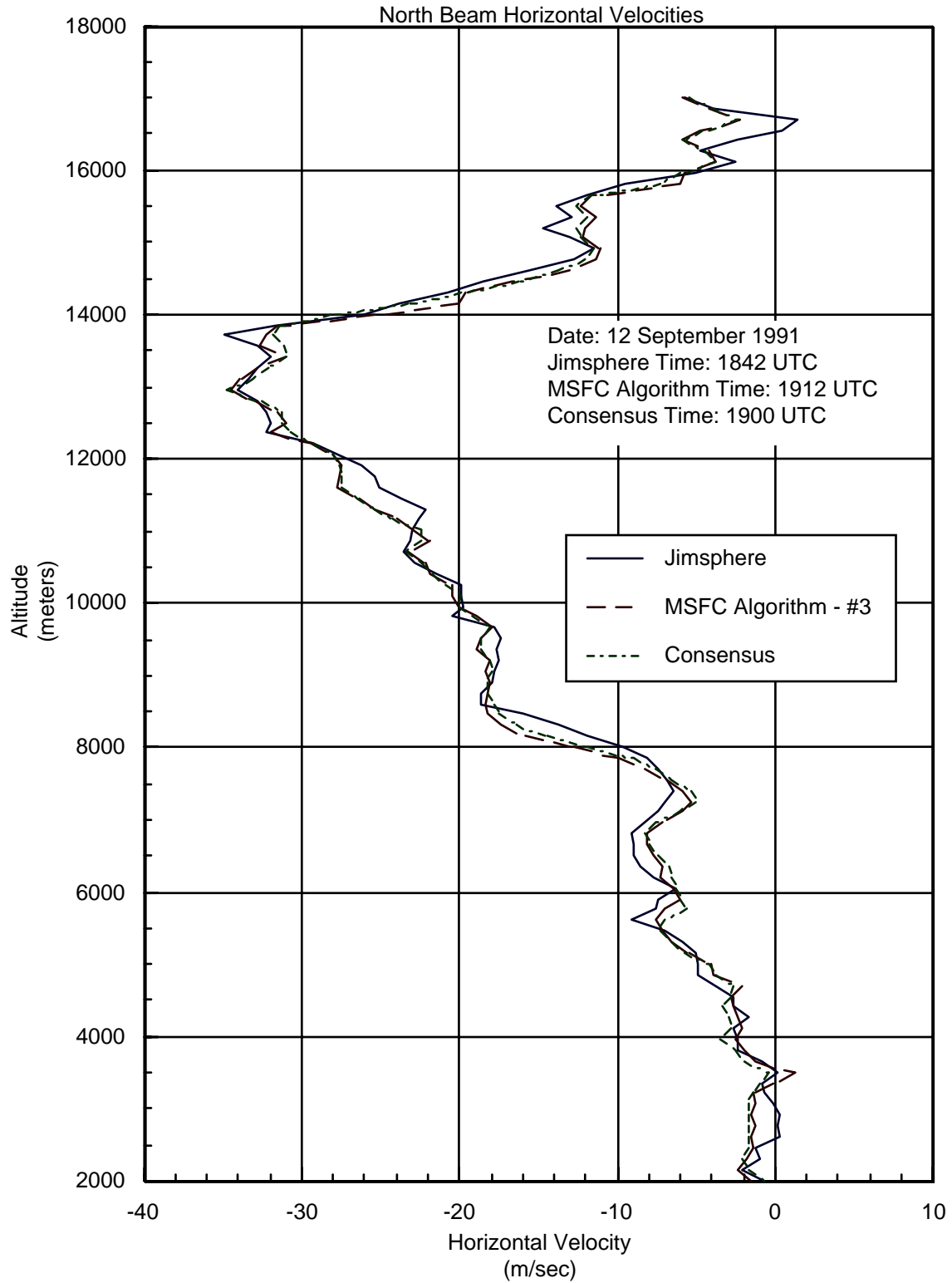
Figure 4.2.   North beam velocities for 12 September 1991. Profile time stamps are: Jimsphere 1842 UTC, Consensus 1900 UTC, and MSFC wind algorithm 1912 UTC.

Date: 12 September 1991
Jimsphere Time: 1842 UTC
DRWP Time: 1912 UTC
DRWP Configuration #3
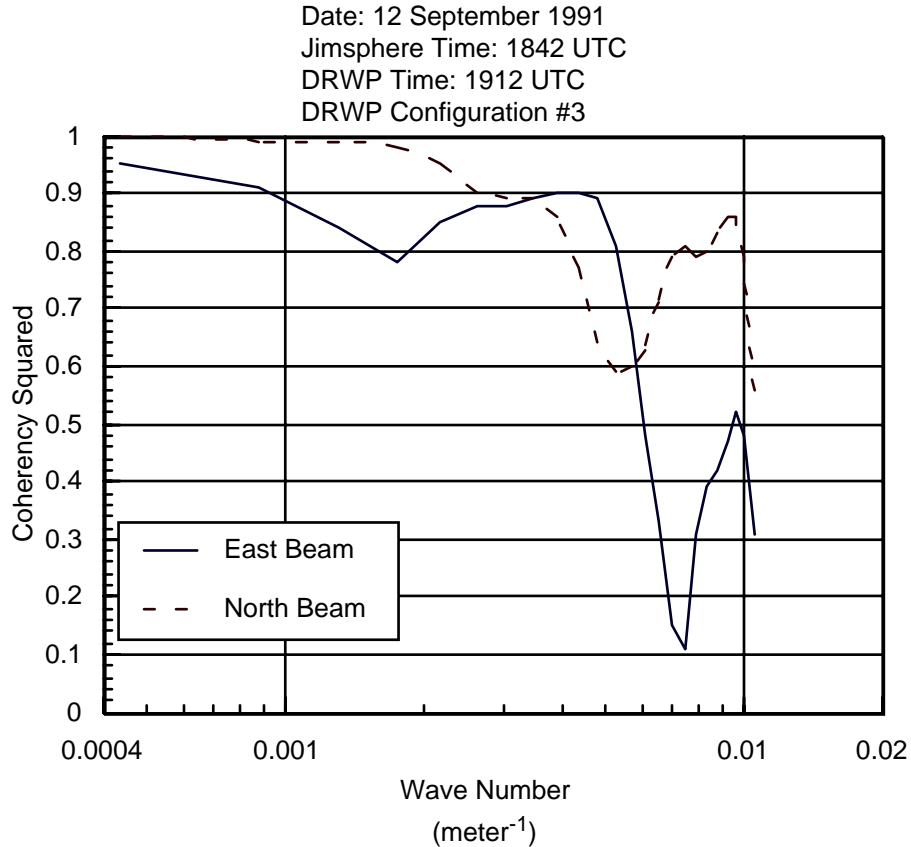
Figure 4.3.   Coherency analysis of jimsphere and MSFC wind algorithm DRWP
profiles for 12 September 1991. Profile times are: Jimsphere 1842
UTC and MSFC wind algorithm 1912 UTC.

4.1.2   Second Wind Profile Comparison From 12 September 1991

The second set of time proximate jimsphere, consensus averaged DRWP, and MSFC
wind algorithm DRWP profiles from 12 September 1991 is presented in Figures 4.4 and
4.5. The large scale features present in the three profiles are very similar; however, the
small scale features exhibit considerable differences particularly between the two DRWP
profiles and the jimsphere profile.

The relatively large east beam velocity shear zones between 6 km and 9 km and
between 14 km and 15 km are described similarly by all three profiles. The same is true
of the relatively large north beam velocity shear zone from 13 km to 15 km. The major
difference among the profiles occurs in the east beam velocities between 9 km and 14
km. Examination of a series of MSFC wind algorithm DRWP profiles from 2030 UTC to
2231 UTC indicates temporal changes in the east beam velocities ranging from 2 m/s to 5
m/s within this 2 hour period in the 9 km to 14 km region. Consequently, a large
component of the east beam velocity differences in the 9 km to 14 km range between the
jimsphere and DRWP profiles is probably due to the sampling differences between the
two systems.

40

The degree of correlation between the jimsphere profile and the MSFC wind algorithm DRWP profile was quantified by cross spectrum analysis (Figure 4.6). The data in Figure 4.6 indicate both components of the two profiles are highly coherent to
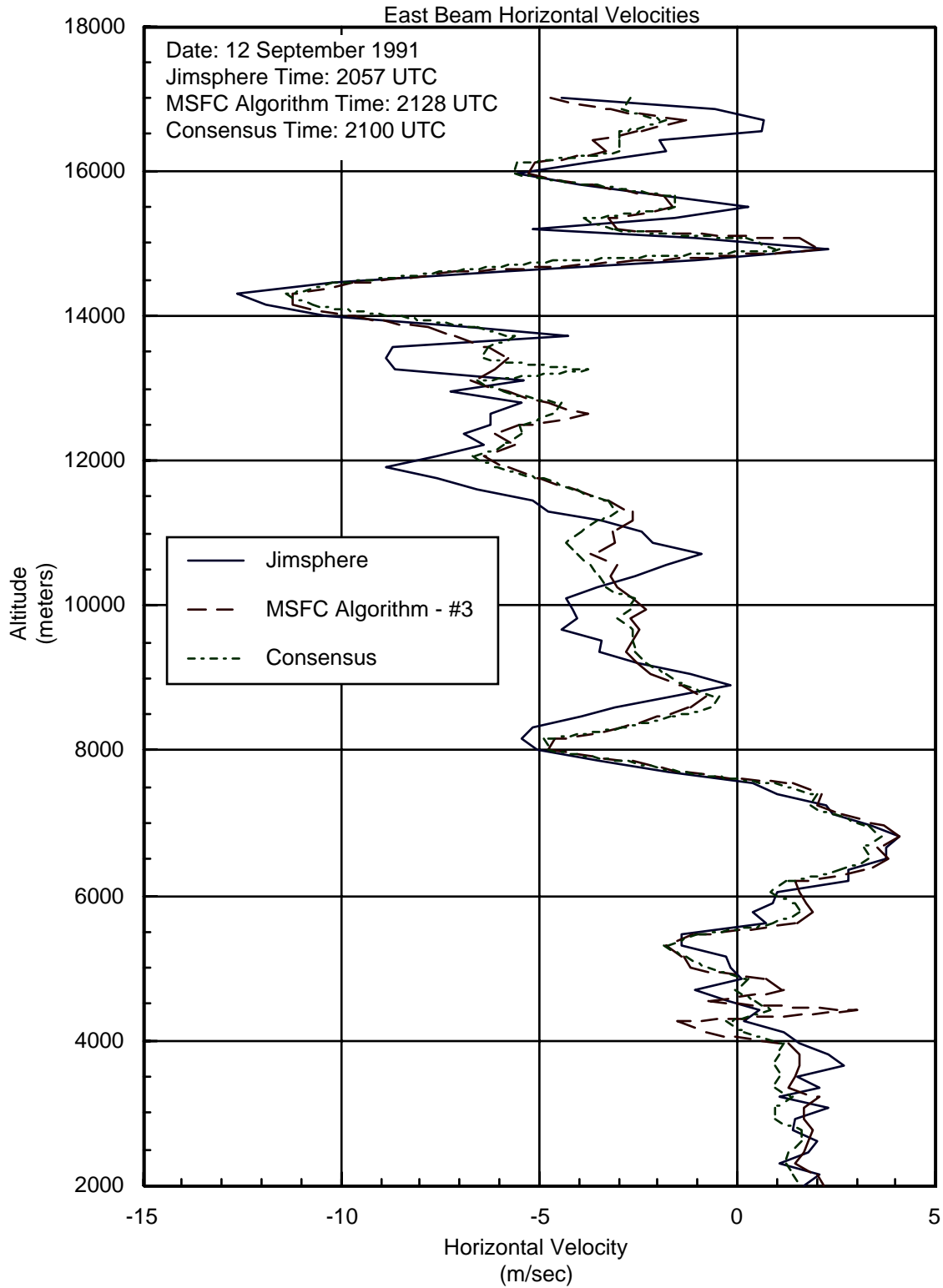
Figure 4.4.   East beam velocities for 12 September 1991. Profile time stamps are: Jimsphere 2057 UTC, Consensus 2100 UTC, and MSFC wind algorithm 2128 UTC.

North Beam Horizontal Velocities

Date: 12 September 1991
Jimsphere Time: 2057 UTC
MSFC Algorithm Time: 2128 UTC
Consensus Time: 2100 UTC

Jimsphere
MSFC Algorithm - #3
Consensus

Altitude (meters)

Horizontal Velocity
(m/sec)
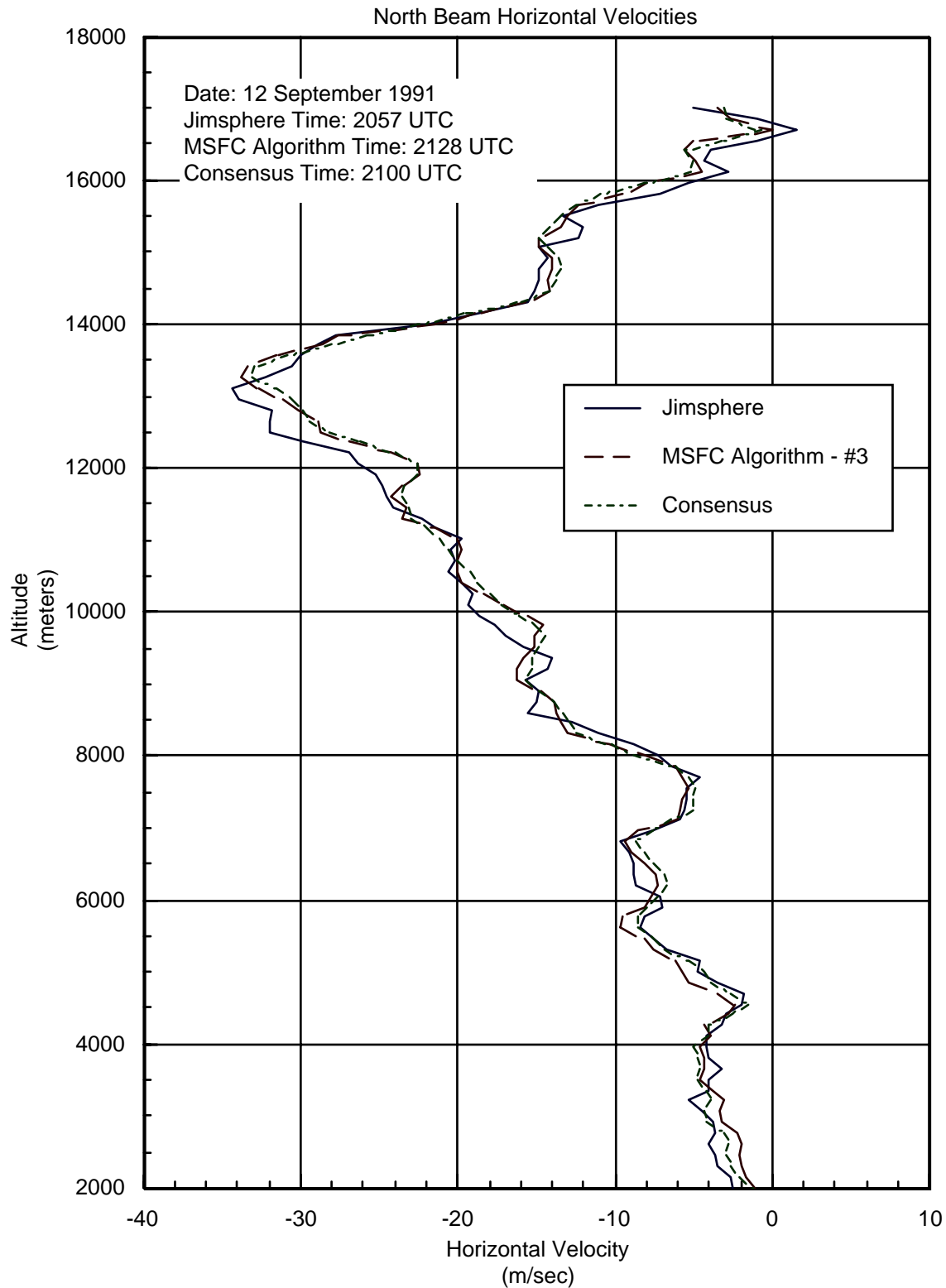
Figure 4.5.   North beam velocities for 12 September 1991. Profile time stamps are: Jimsphere 2057 UTC, Consensus 2100 UTC, and MSFC wind algorithm 2128 UTC.

Date: 12 September 1991
Jimsphere Time: 2057 UTC
DRWP Time: 2128 UTC
DRWP Configuration #3
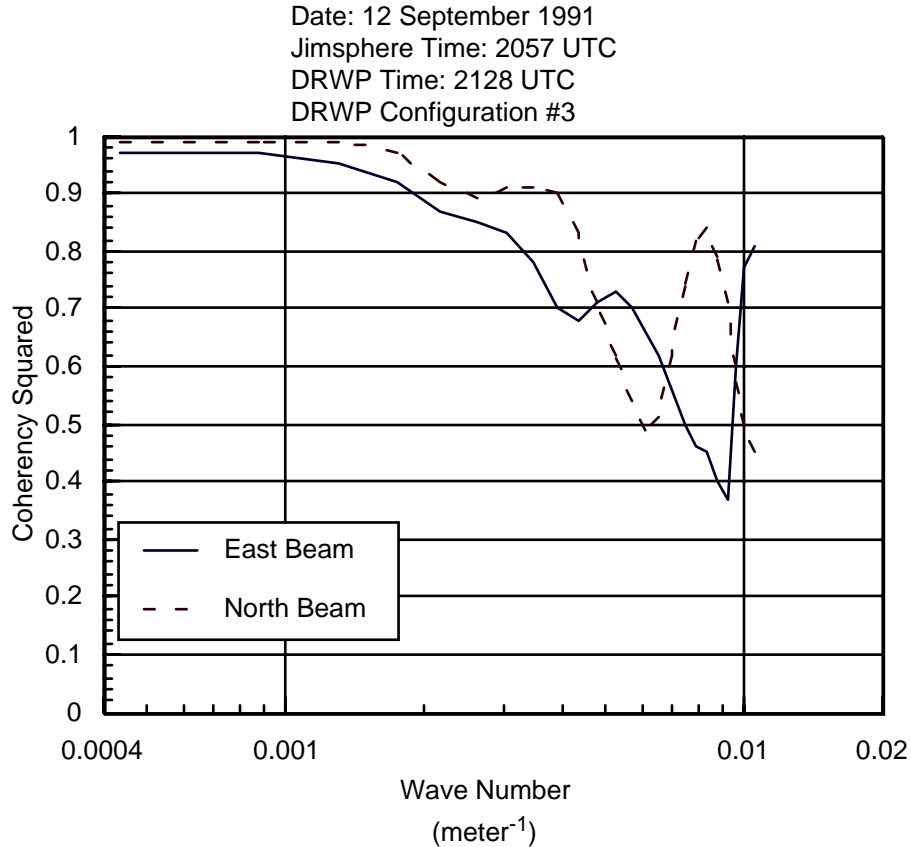
Figure 4.6.   Coherency analysis of jimsphere and MSFC wind algorithm DRWP
profiles for 12 September 1991. Profile times are: Jimsphere 2057
UTC and MSFC wind algorithm 2128 UTC.

wavelengths as short as 1200 meters (i.e., wave number $5 \infty 10^{-3}$ m^{-1}). At shorter
wavelengths, the coherence of both components is generally less. This is not surprising
in light of the temporal and spatial differences in data collection between the jimsphere
and the DRWP.

4.1.3 Third Wind Profile Comparison From 12 September 1991

The third set of time proximate jimsphere, consensus averaged DRWP, and MSFC
wind algorithm DRWP profiles from 12 September 1991 is presented in Figures 4.7 and
4.8. The large scale features present in the three profiles are very similar for the north
beam velocities; however, in contrast to the other two time periods, even the larger scale
features in the east beam velocities exhibit noticeable differences between the two
DRWP profiles and the jimsphere profile. In particular is the rather consistent difference
in the east beam velocities between the two DRWP profiles and the jimsphere profile
from approximately 11 km to 14 km. Examination of a series of MSFC wind algorithm
DRWP profiles from 2300 UTC to 2358 UTC indicates temporal changes in the east
beam velocities generally ranged from 2 m/s to 3 m/s within this one hour period in the
11 km to 14 km region. However, the magnitudes of the east beam velocities of the
jimsphere profile exceeded by at least 2 m/s the magnitudes of all of the DRWP profiles
from 2300 UTC to 2358 UTC for many of the levels within the 11 km to 14 km region.

44

Consequently, a large component of the east beam velocity differences in the 11 km to 14
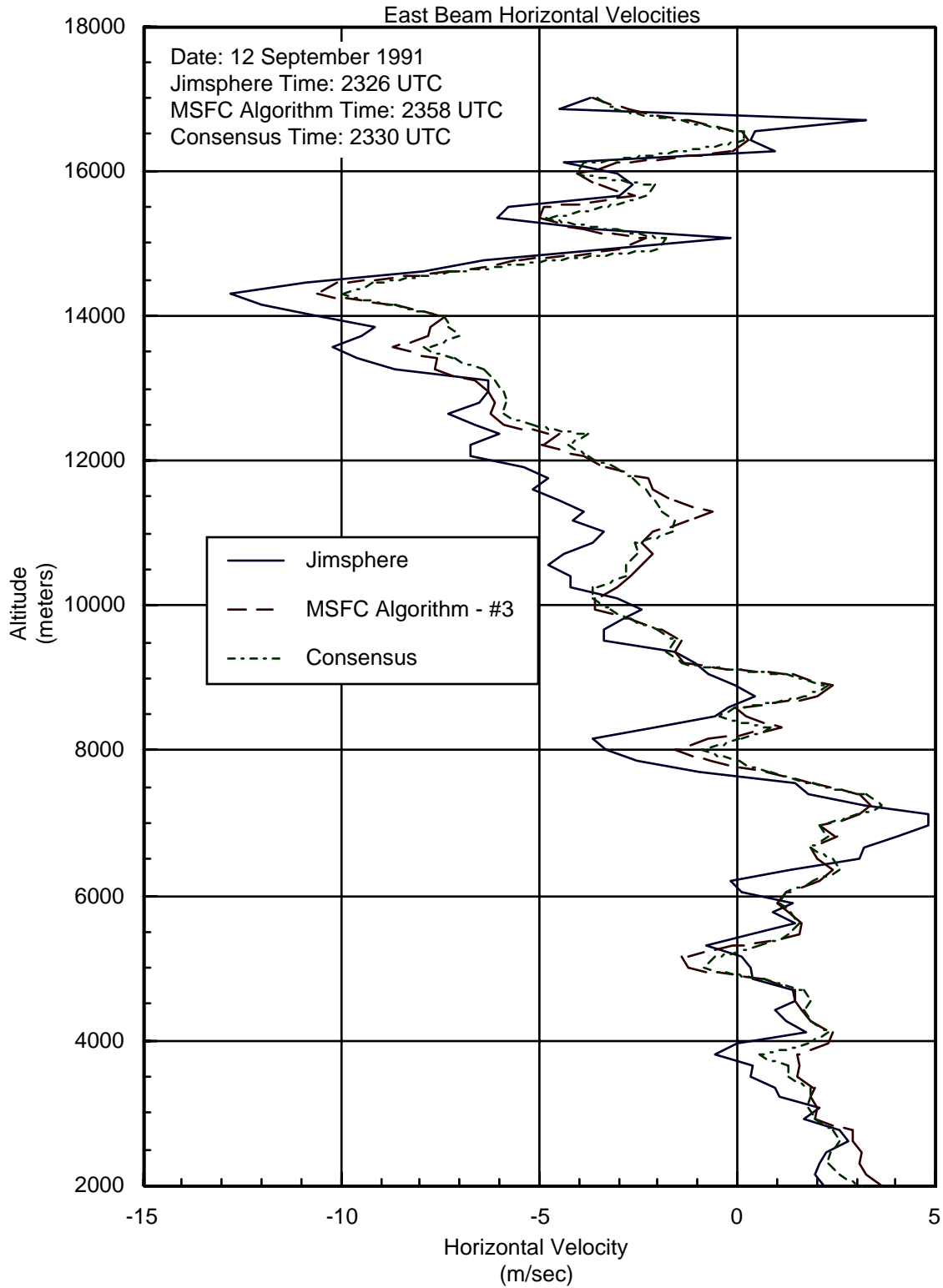
Figure 4.7.   East beam velocities for 12 September 1991. Profile time stamps are: Jimsphere 2326 UTC, Consensus 2330 UTC, and MSFC wind algorithm 2358 UTC.
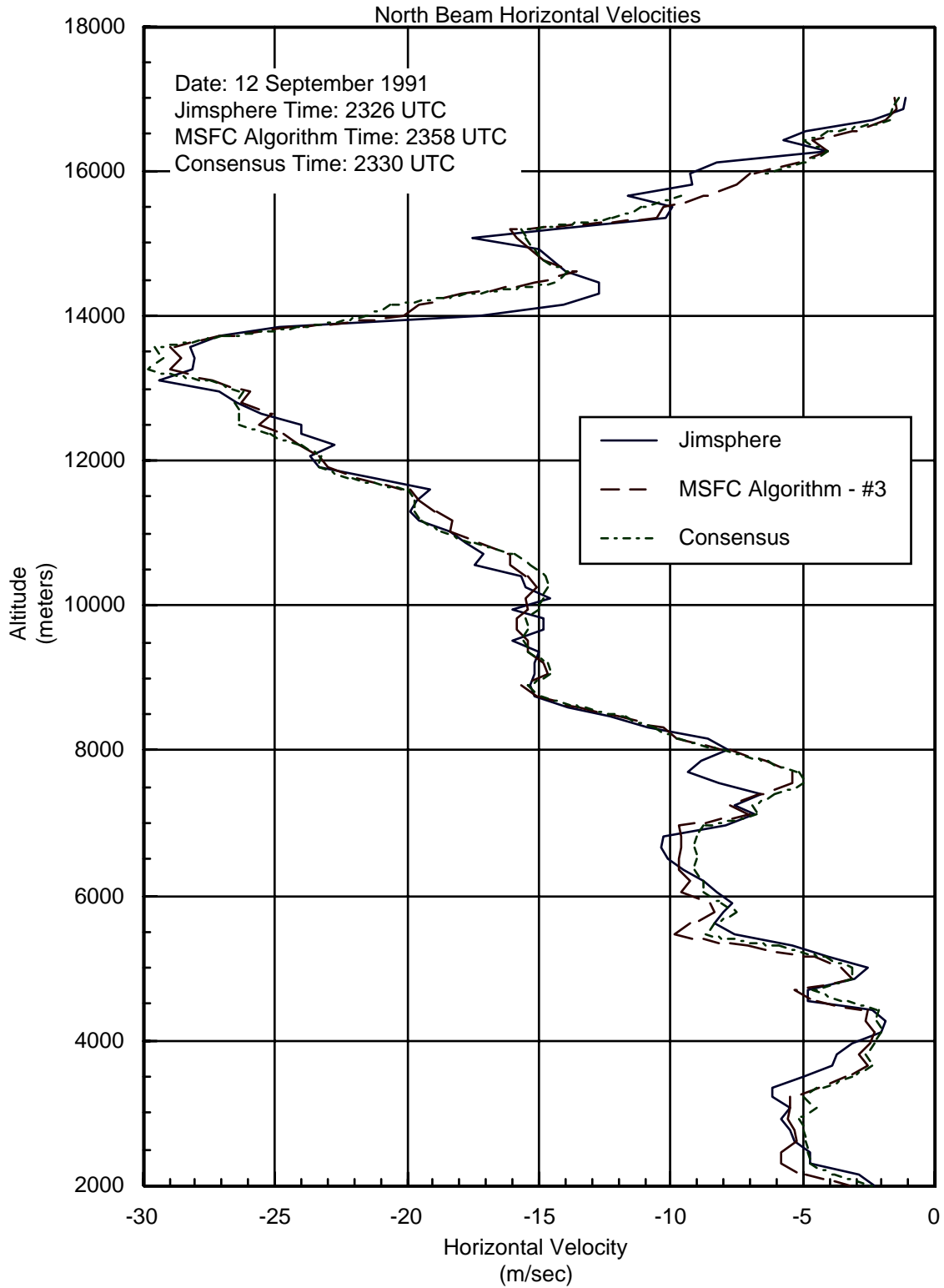
Figure 4.8. North beam velocities for 12 September 1991. Profile time stamps are: Jimsphere 2326 UTC, Consensus 2330 UTC, and MSFC wind algorithm 2358 UTC.

km range between the jimsphere and DRWP profiles is probably due to the combination of inherent system error and spatial separation of the jimsphere balloon and the DRWP.

The data in Figure 4.9 indicate the north beam component of the two profiles are highly coherent to wavelengths as short as 1200 meters. In contrast to the other two time periods, the coherence of the east beam components is less than 0.7 for wavelengths as long as 2500 meters (i.e., wave number $2.5 \infty 10^{-3}$ m^{-1}) indicating less correlation at these wavelengths. This result correlates well with the observations stated in the previous paragraph regarding the differences in the east beam velocities. At wavelengths near 1200 meters, (i.e., wave number $5 \infty 10^{-3}$ m^{-1}), both components of the two profiles are highly coherent. At shorter wavelengths, the coherence of both components is generally less indicating less linear correlation between the profiles at the shorter wavelengths.

Date: 12 September 1991
Jimsphere Time: 2326 UTC
DRWP Time: 2358 UTC
DRWP Configuration #3
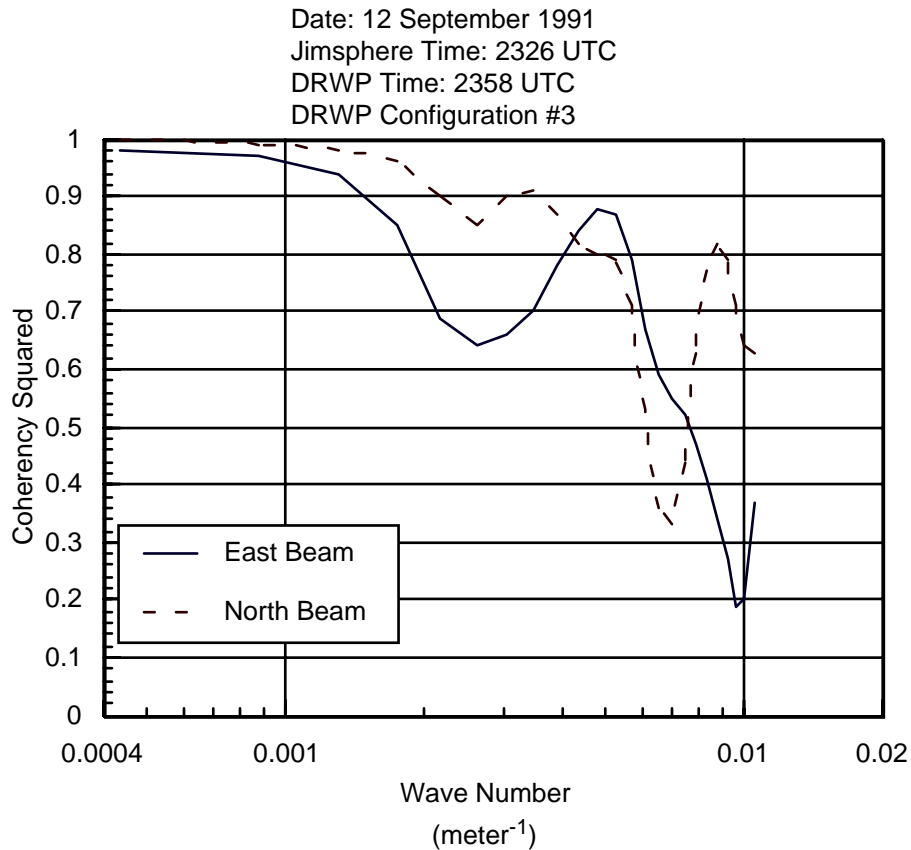
Figure 4.9.   Coherency analysis of jimsphere and MSFC wind algorithm DRWP profiles for 12 September 1991. Profile times are: Jimsphere 2326 UTC and MSFC wind algorithm 2358 UTC.

4.1.4   Jimsphere / MSFC Wind Algorithm RMS Velocity Differences From 12 September 1991

The RMS velocity differences between the MSFC wind algorithm DRWP profiles and the jimsphere profiles for 12 September 1991 are contained in Table 4.2. When evaluating the magnitude of the RMS velocity differences, it is important to note the

temporal and spatial differences in data collection between the jimsphere and the DRWP described in Section 4.1.2. Because of the sampling differences between the two systems, RMS velocity differences between two jimsphere profiles separated by 50 minutes were computed to provide a reference measure to facilitate evaluation of the RMS velocity differences between the MSFC wind algorithm DRWP profiles and the jimsphere profiles.

RMS velocity differences between two jimsphere profiles from 12 September 1991 separated by 50 minutes are approximately 1.7 m/s, which is very similar to the magnitude of the RMS velocity differences between the MSFC wind algorithm DRWP profiles and the jimsphere profiles (see Table 4.2). Consequently, the magnitude of the RMS velocity differences between the MSFC wind algorithm DRWP profiles and the jimsphere profiles appear reasonable and suggest the two systems are providing similar quality data.

Table 4.2. Jimsphere And MSFC Wind Algorithm DRWP Velocity Comparisons For 12 September 1991			
Jimsphere Profile Time (UTC)	MSFC Algorithm Profile Time* (UTC)	RMS Differences East Beam (m/s)	RMS Differences North Beam (m/s)
1842	1912	1.47	1.56
2009	2038	1.79	1.56
2057	2128	1.42	1.54
2147	2217	1.78	1.89
2326	2358	1.60	1.39

* The MSFC wind algorithm DRWP profiles were generated using configuration #3.

4.1.5 Consensus / MSFC Wind Algorithm RMS Velocity Differences From 12 September 1991

The RMS velocity differences between the MSFC wind algorithm DRWP profiles and the consensus averaged DRWP profiles for 12 September 1991 are contained in Table 4.3. The RMS differences in Table 4.3, which are typically on the order of .75 m/s, are less than the RMS velocity differences between two MSFC wind algorithm DRWP profiles from 12 September 1991 separated by 30 minutes which are approximately 1.3 m/s. This indicates the profiles produced by the MSFC wind algorithm are comparable to the consensus averaged wind profiles. In this particular case, the main advantage of the MSFC wind algorithm is the time resolution. The update rate of the consensus averaged profiles is 30 minutes. Conversely, the update rate of the MSFC wind algorithm is 3 minutes.

Table 4.3. Consensus Averaged And MSFC Wind Algorithm DRWP Velocity Comparisons For 12 September 1991			
Consensus Profile Time (UTC)	MSFC Algorithm Profile Time* (UTC)	RMS Differences East Beam (m/s)	RMS Differences North Beam (m/s)
1900	1915	0.79	0.57
1930	1946	0.87	0.71
2000	2015	0.87	0.71
2030	2044	0.80	0.80
2100	2116	0.70	0.63
2130	2145	0.72	0.85
2200	2214	0.76	0.76
2230	2246	0.72	0.59
2300	2314	0.91	0.81
2300	2346	0.51	0.40

* The MSFC wind algorithm DRWP profiles were generated using configuration #3.

4.1.6   First Wind Profile Comparison From 23 January 1992

The first set of time proximate jimsphere, consensus averaged DRWP, and MSFC wind algorithm DRWP profiles from 23 January 1992 is presented in Figures 4.10 and 4.11. The large scale features present in the three profiles are very similar; however, the small scale features represented by the three profiles exhibit notable differences.

In this particular case, all three profiles describe the shear zones in the east beam component from 10 km to 15 km similarly. However, there are some differences in magnitudes among the profiles particularly near 12.5 km. The most significant difference in the east beam profiles occurs between 6 km and 8 km. In this region, the magnitude of the consensus average profile is noticeably less than the jimsphere profile or the MSFC wind algorithm DRWP profile. Examination of a series of MSFC wind algorithm DRWP profiles from 1314 UTC to 1509 UTC indicates decreases in the east beam velocities as large as 8 m/s within this period in the 6 km to 8 km region. Consequently, the differences in the east beam velocities between the consensus profile and the MSFC wind algorithm profile are due to the temporal changes in the east beam component.

All three profiles describe the shear zones in the north beam component between 11 km and 12.5 km similarly. However, the consensus average profile exhibits less shear in the north beam component from 8 km to 11 km than either the jimsphere profile or the MSFC wind algorithm DRWP profile. Examination of a series of MSFC wind algorithm

DRWP profiles from 1314 UTC to 1509 UTC indicates increases in the north beam component of 10 m/s within this period near 8.5 km and increases in the north beam component ranging from 2 m/s to 3m/s within this period from 9 km to 11 km. These temporal changes in the north beam component reduce the strength of the vertical shear in the north beam component in the 8 km to 11 km region and account for the north beam component differences between the consensus profile and the MSFC wind algorithm

East Beam Horizontal Velocities

Date: 23 January 1992
Jimsphere Time: 1400 UTC
MSFC Algorithm Time: 1408 UTC
Consensus Time: 1400 UTC

Jimsphere
MSFC Algorithm - #3
Consensus

Altitude (meters)

Horizontal Velocity
(m/sec)
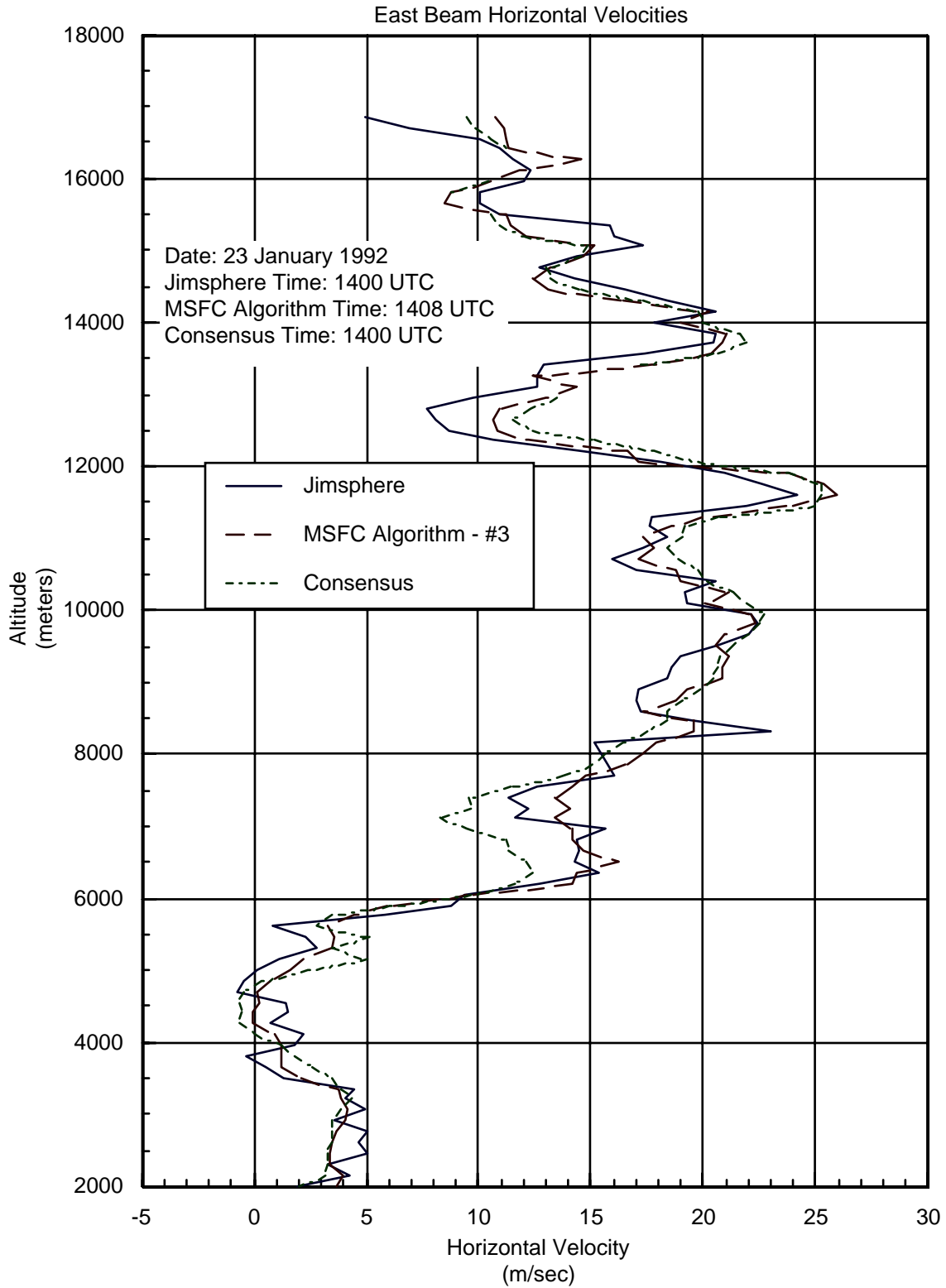
Figure 4.10. East beam velocities for 23 January 1992. Profile time stamps are: Jimsphere 1400 UTC, Consensus 1400 UTC, and MSFC wind algorithm 1408 UTC.
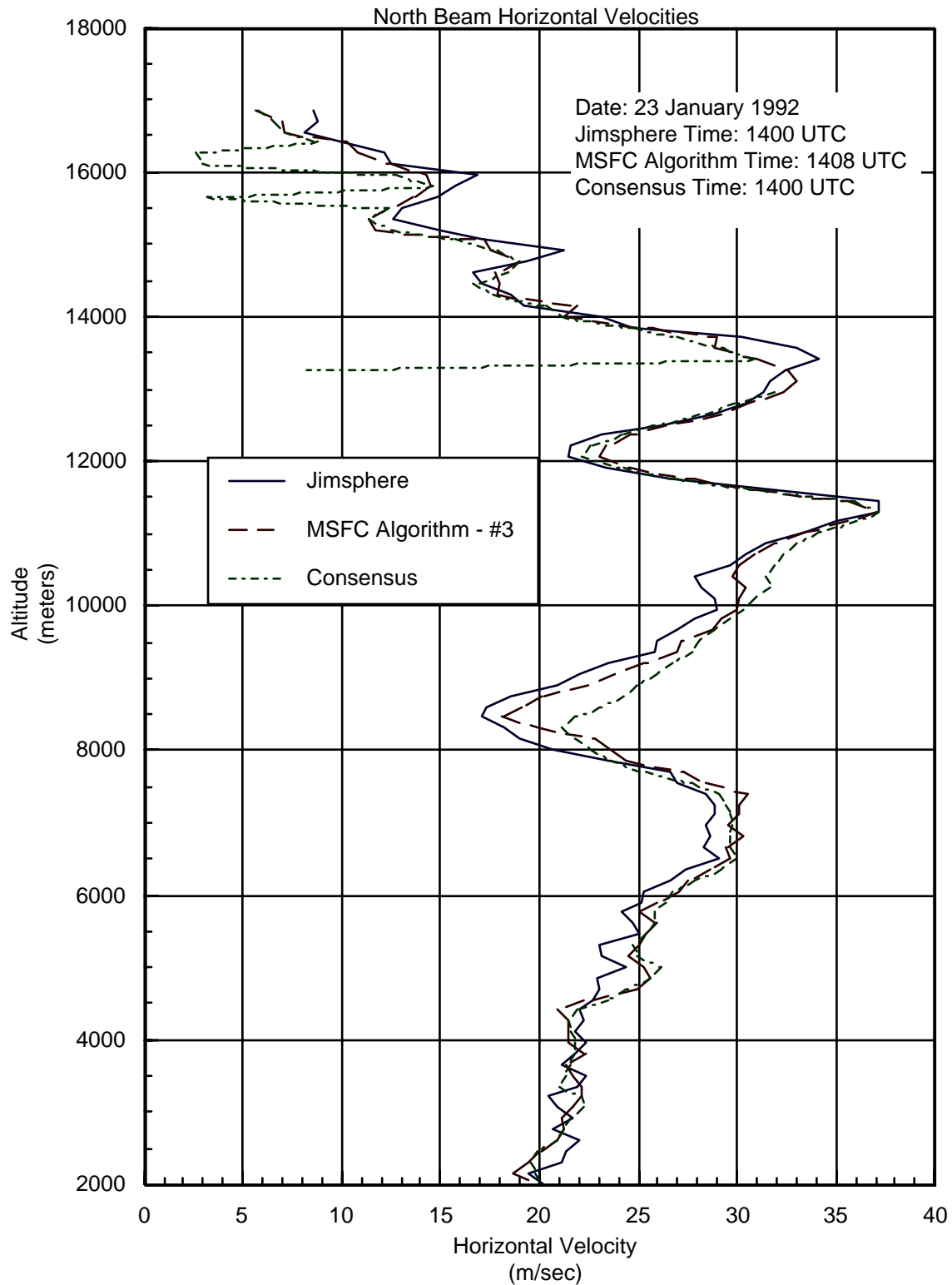
Figure 4.11. North beam velocities for 23 January 1992. Profile time stamps are: Jimsphere 1400 UTC, Consensus 1400 UTC, and MSFC wind algorithm 1408 UTC.

profile. In addition, the consensus averaging technique produced an erroneous wind estimates in the north beam component near 13 km and three erroneous wind estimates in the north beam component near 16 km.

The coherence data in Figure 4.12 indicate both components of the two profiles are highly coherent to wavelengths as short as 1100 meters (i.e., wave number $6 \infty 10^{-3}$ m^{-1}). Again, at shorter wavelengths, the coherence of both components is generally less; this is expected in light of the data collection differences between the jimsphere and the DRWP.

Date: 23 January 1992
Jimsphere Time: 1400 UTC
DRWP Time: 1408 UTC
DRWP Configuration #3
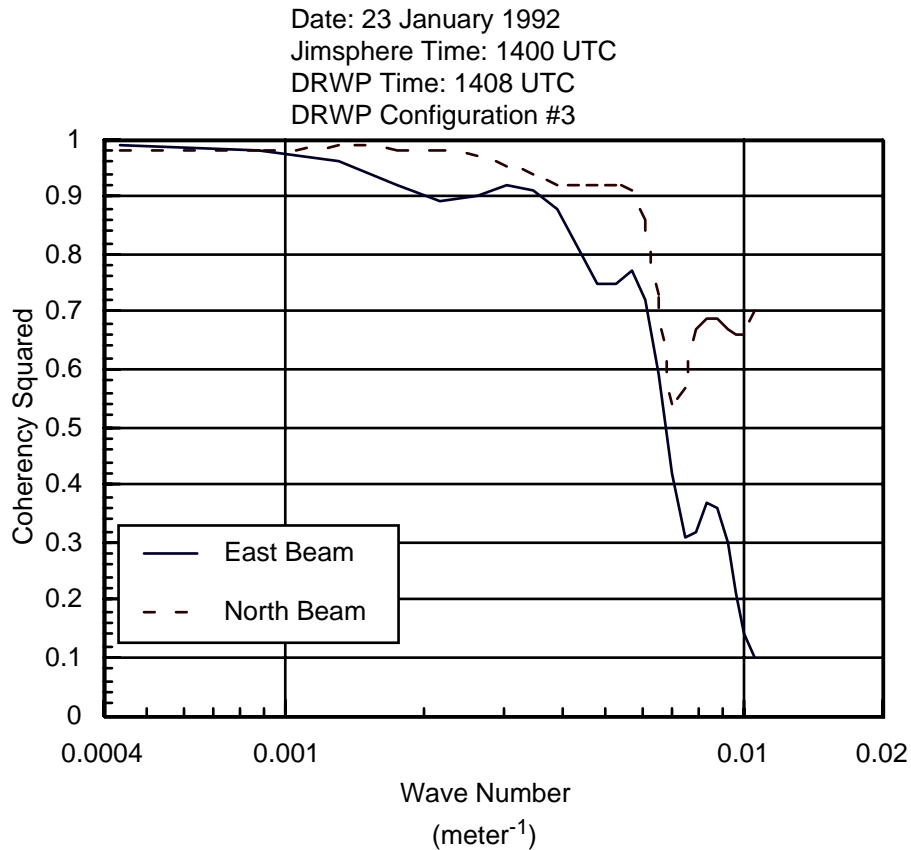
Figure 4.12. Coherency analysis of jimsphere and MSFC wind algorithm DRWP profiles for 23 January 1992. Profile times are: Jimsphere 1400 UTC and MSFC wind algorithm 1408 UTC.

4.1.7 Second Wind Profile Comparison From 23 January 1992

The second set of time proximate jimsphere, consensus averaged DRWP, and MSFC wind algorithm DRWP profiles from 23 January 1992 is presented in Figures 4.13 and 4.14. The large scale features present in the three profiles are very similar; however, the small scale features represented by the three profiles exhibit notable differences.

In this particular case, all three profiles describe the shear zones in the north beam component between 10 km and 15 km similarly. This is also true of the shear zone in the east beam component from 12 km to 14 km. However, the consensus average profile exhibits considerably less shear in the east beam component from 8 km to 12 km than

54

either the jimsphere profile or the MSFC wind algorithm DRWP profile. Examination of
a series of MSFC wind algorithm DRWP profiles from 1428 UTC to 1628 UTC indicates
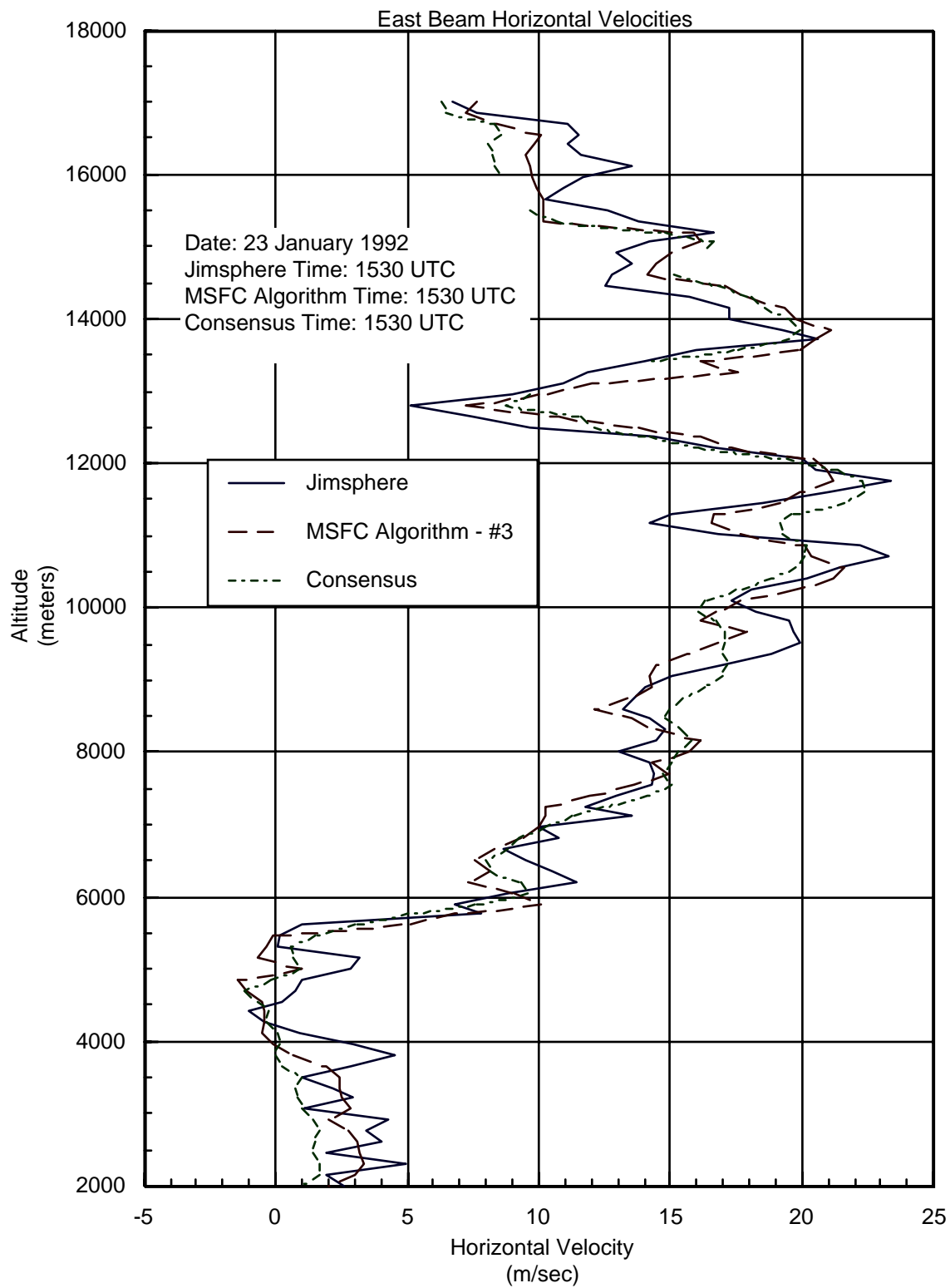
Figure 4.13.   East beam velocities for 23 January 1992. Profile time stamps are: Jimsphere 1530 UTC, Consensus 1530 UTC, and MSFC wind algorithm 1530 UTC.
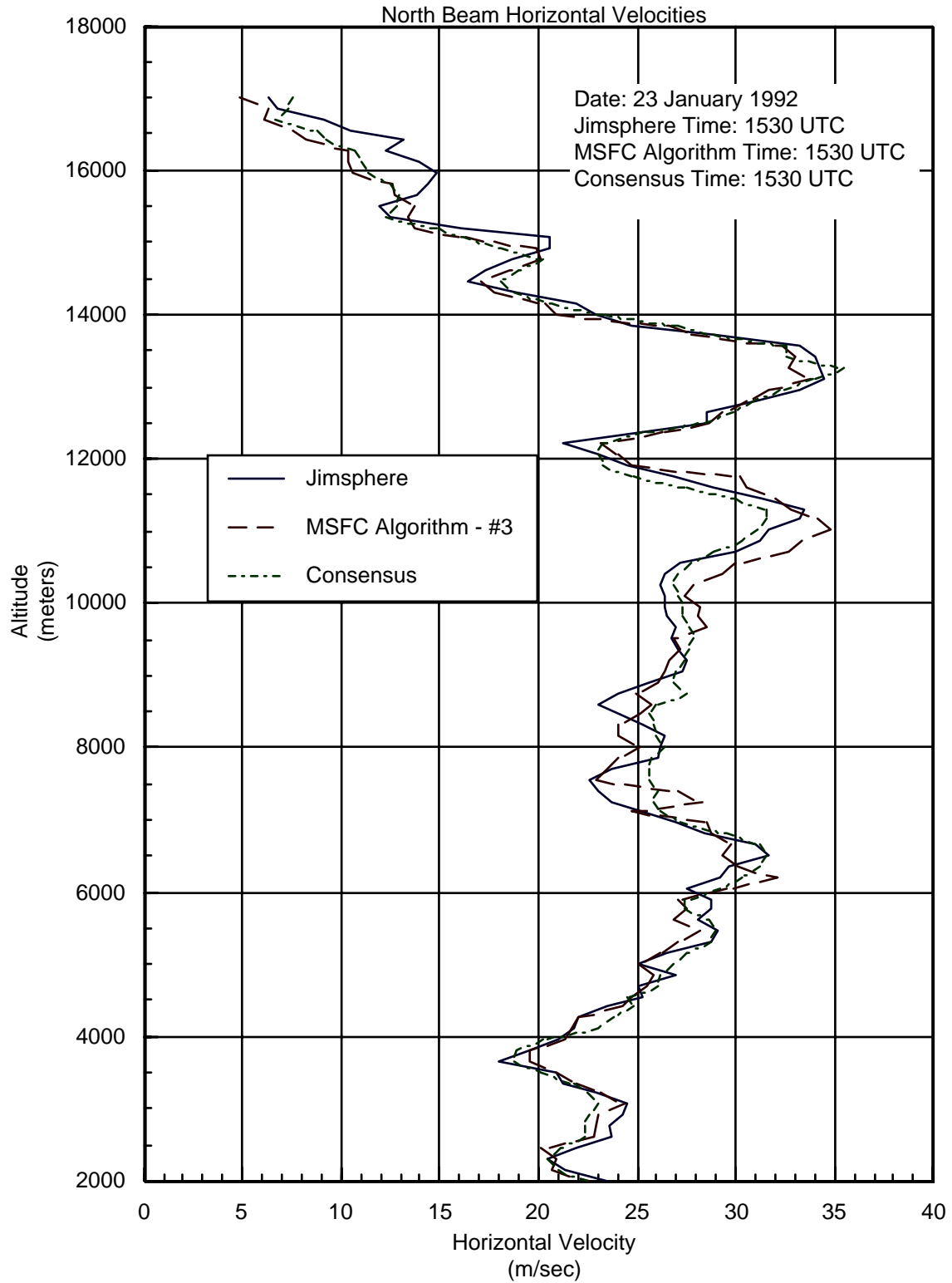
Figure 4.14.   North beam velocities for 23 January 1992. Profile time stamps are: Jimsphere 1530 UTC, Consensus 1530 UTC, and MSFC wind algorithm 1530 UTC.

temporal changes in the east beam velocities as large as 10 m/s within this period in the 8 km to 12 km region. The temporal averaging procedures employed in the consensus technique smooth the temporal variability present in the data resulting in a consensus east beam component profile with relatively less shear in the 8 km to 12 km zone.

The coherence data in Figure 4.15 indicate both components of the two profiles are highly coherent (i.e., coherency squared values of ~ 0.7 or greater) to wavelengths as short as 1200 meters (i.e., wave number $5 \propto 10^{-3}$ m^{-1}). Again, at shorter wavelengths, the coherence of both components is generally less; this is not surprising in light of the data collection differences between the jimsphere and the DRWP.

Date: 23 January 1992
Jimsphere Time: 1530 UTC
DRWP Time: 1530 UTC
DRWP Configuration #3
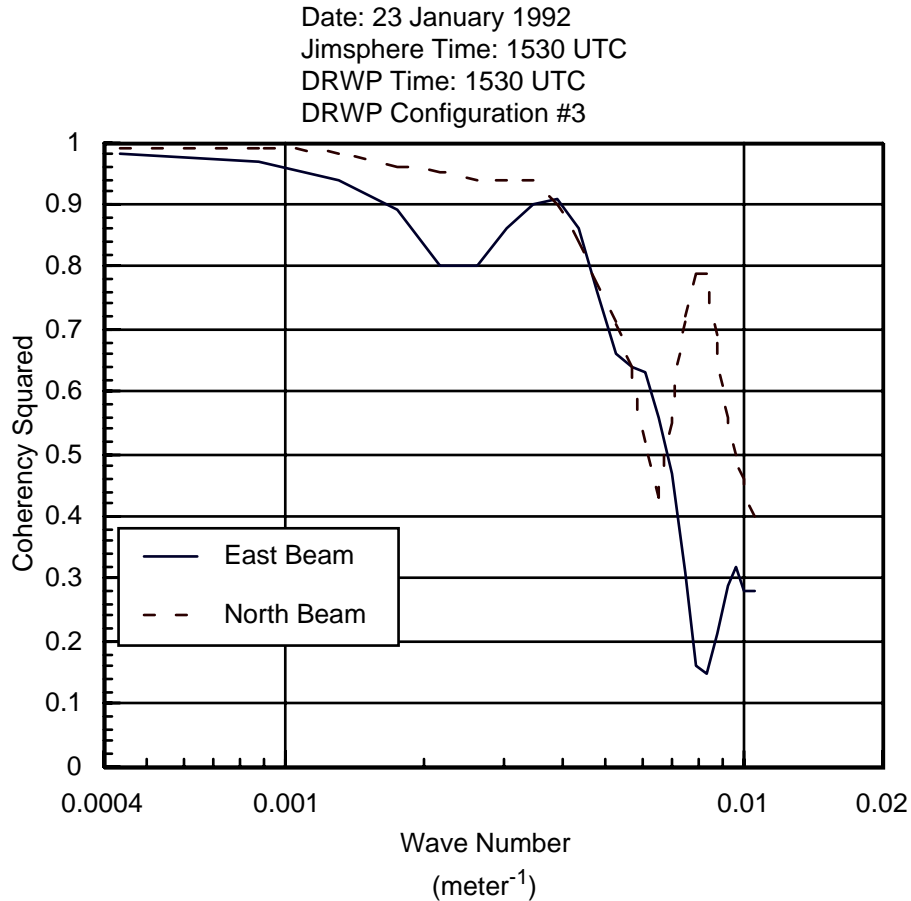
Figure 4.15.   Coherency analysis of jimsphere and MSFC wind algorithm DRWP profiles for 23 January 1992. Profile times are: Jimsphere 1530 UTC and MSFC wind algorithm 1530 UTC.

4.1.8   Third Wind Profile Comparison From 23 January 1992

The third set of time proximate jimsphere, consensus averaged DRWP, and MSFC wind algorithm DRWP profiles from 23 January 1992 is presented in Figures 4.16 and 4.17. The large scale features present in the three profiles are very similar; however, the small scale features represented by the three profiles exhibit notable differences.

In this particular case, all three profiles describe the strong shear zone in the east beam component near 11.5 km quite similarly. In addition, all three profiles describe the
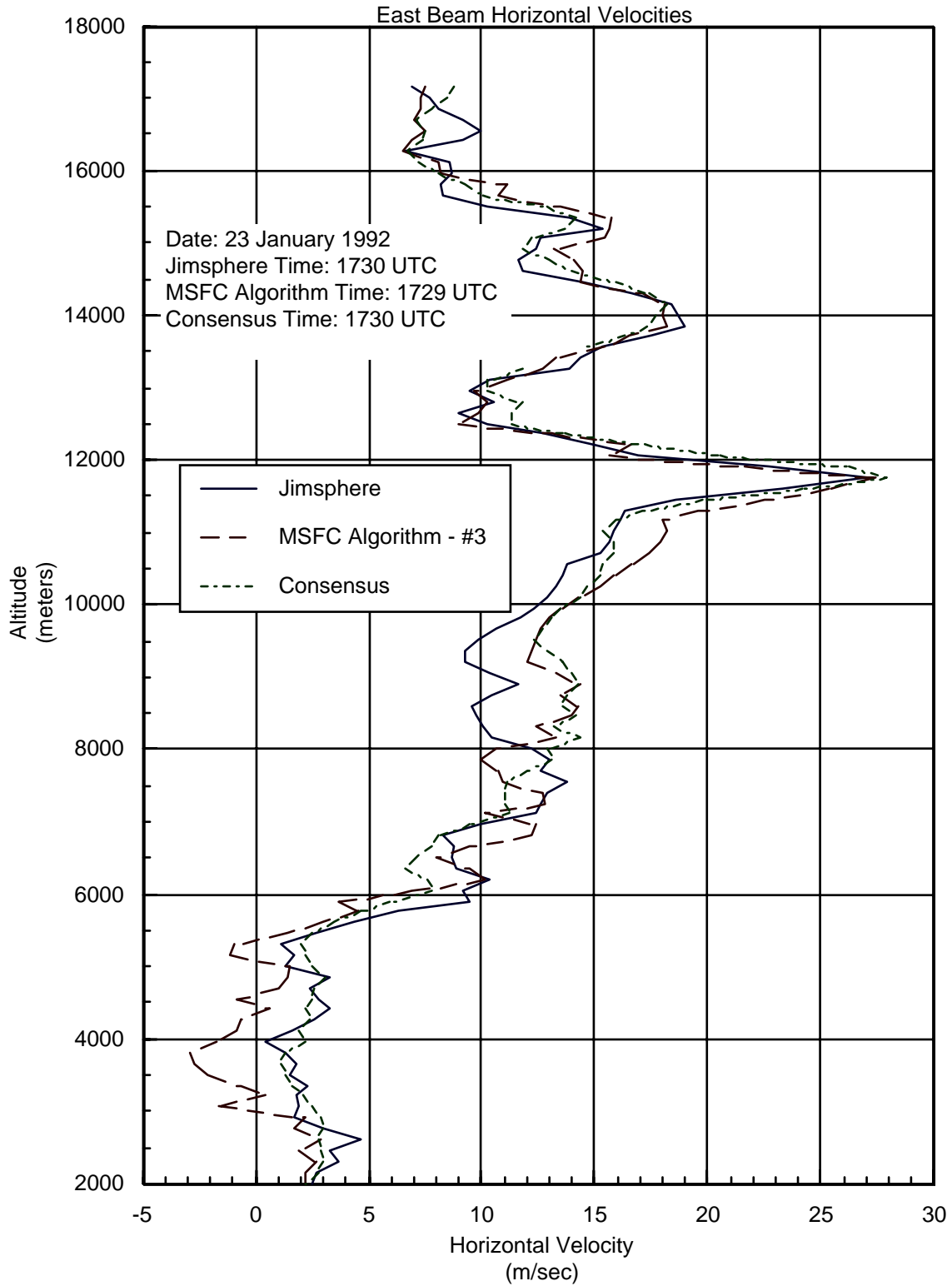
Figure 4.16.   East beam velocities for 23 January 1992.   Profile time stamps are: Jimsphere 1730 UTC, Consensus 1730 UTC, and MSFC wind algorithm 1729 UTC.
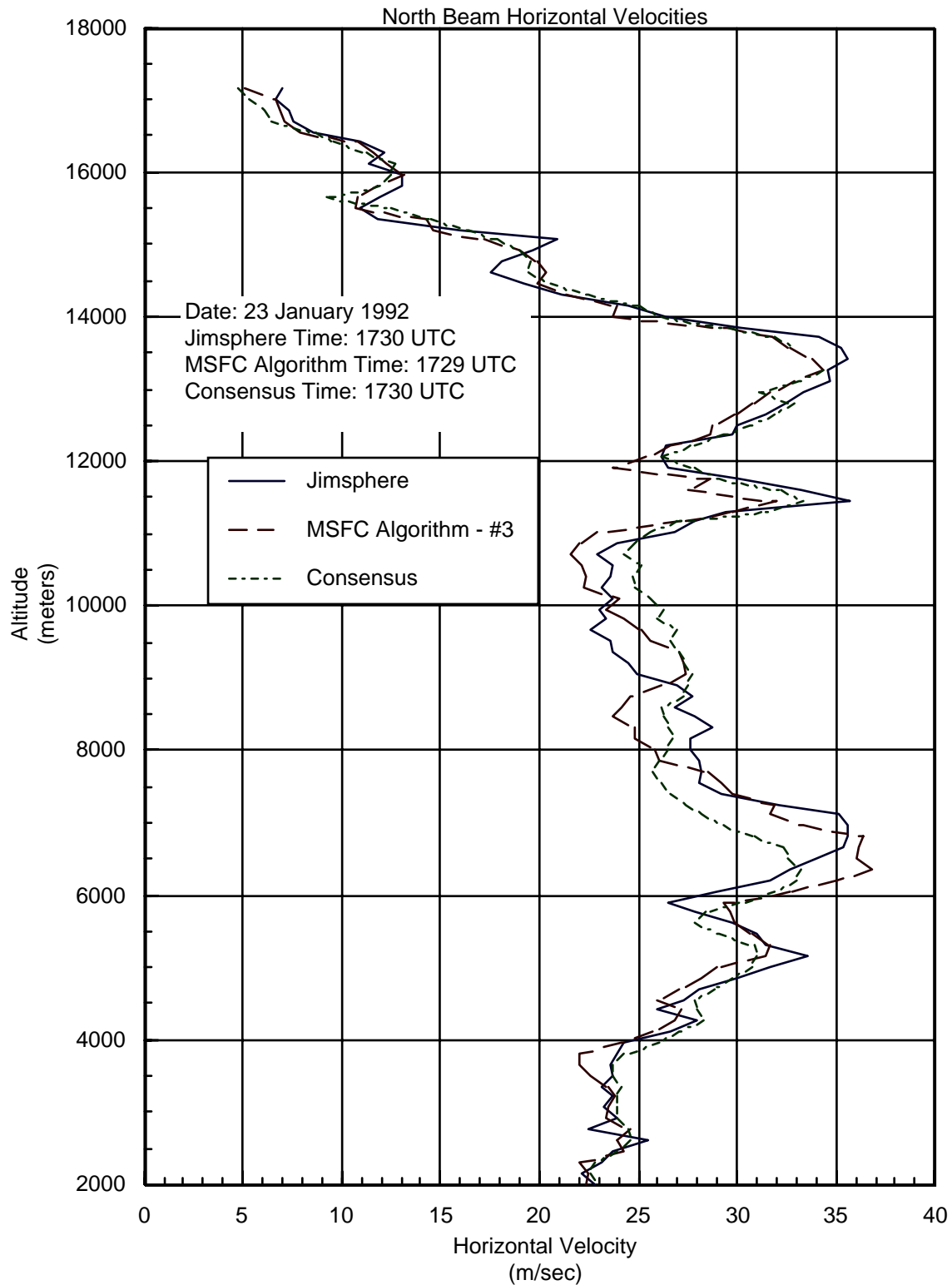
Figure 4.17. North beam velocities for 23 January 1992. Profile time stamps are: Jimsphere 1730 UTC, Consensus 1730 UTC, and MSFC wind algorithm 1729 UTC.

61

shear zone in the east beam component from 12.5 km to 15 km similarly and the same is true of the shear zones in the north beam component from 11 km to 16 km.

The most noticeable differences in the east beam component among the profiles occur in the 3 km to 5 km region and in the 8 km to 10 km region. In the 3 km to 5 km region, configuration #3 of the MSFC wind algorithm appears to have had difficulty estimating the east beam velocity since it is near zero. This problem can be mitigated by using a larger integration window width. Examination of a series of MSFC wind algorithm DRWP profiles from 1632 UTC to 1815 UTC indicates temporal changes in the east beam velocities as large as 10 m/s within this period in the 8 km to 10 km region. Consequently, the east beam component differences between the two DRWP profiles and the jimsphere profile in the 8 km to 10 km region are probably due to temporal and spatial sampling differences between the DRWP and the jimsphere balloon.

The most noticeable differences in the north beam component among the profiles occur in the 6 km to 11 km region. Examination of a series of MSFC wind algorithm DRWP profiles from 1632 UTC to 1815 UTC indicates temporal changes in the north beam component ranging from 5 m/s to 10 m/s within this period in the 6 km to 11 km region. Consequently, the east beam component differences between the MSFC wind algorithm profile and the jimsphere profile in the 6 km to 11 km region are probably due to temporal and spatial sampling differences between the DRWP and the jimsphere balloon. In addition, the east beam component differences between the MSFC wind algorithm profile and the consensus profile in the 6 km to 11 km region are a result of the temporal averaging procedures employed in the consensus technique.

The coherence data in Figure 4.18 indicate both components of the two profiles are highly coherent to wavelengths as short as 900 meters (i.e., wave number $7 \infty 10^{-3}$ m^{-1}). This result is similar to the other two time periods examined on January 23, 1992. However, the enhanced coherence at shorter wavelengths (e.g., ~900 meters) as compared to the other two examples is due to the relatively greater similarity in the short wavelength features between the two profiles above 11 km.

4.1.9 Jimsphere / MSFC Wind Algorithm RMS Velocity Differences From 23 January 1992

The RMS velocity differences between the MSFC wind algorithm DRWP profiles and the jimsphere profiles for 23 January 1992 are contained in Table 4.4. In this case, the RMS velocity differences are slightly larger than the RMS velocity differences for 12 September 1991 (see Table 4.2). Since jimsphere data separated by approximately 50 minutes were not available for this day, RMS velocity differences between temporally separated MSFC wind algorithm DRWP profiles were used to infer the reason for the slightly larger RMS velocity differences between MSFC wind algorithm DRWP profiles and the jimsphere profiles on 23 January 1992 as compared to the differences on 12 September 1991.

The RMS velocity differences between two MSFC wind algorithm DRWP profiles from 12 September 1991 separated by 30 minutes are approximately 1.3 m/s. In contrast, the RMS velocity differences between two MSFC wind algorithm DRWP profiles from 23 January 1992 separated by 30 minutes are approximately 2.2 m/s. This indicates

either increased atmospheric variability or increased temporal changes or a combination of the two. In either case, based on the substantially larger RMS velocity differences in the temporally separated MSFC wind algorithm DRWP profiles on 23 January 1992, the larger RMS velocity differences between the MSFC wind algorithm DRWP profiles and the jimsphere profiles for 23 January 1992 appear reasonable.

Date: 23 January 1992
Jimsphere Time: 1730 UTC
DRWP Time: 1729 UTC
DRWP Configuration #3
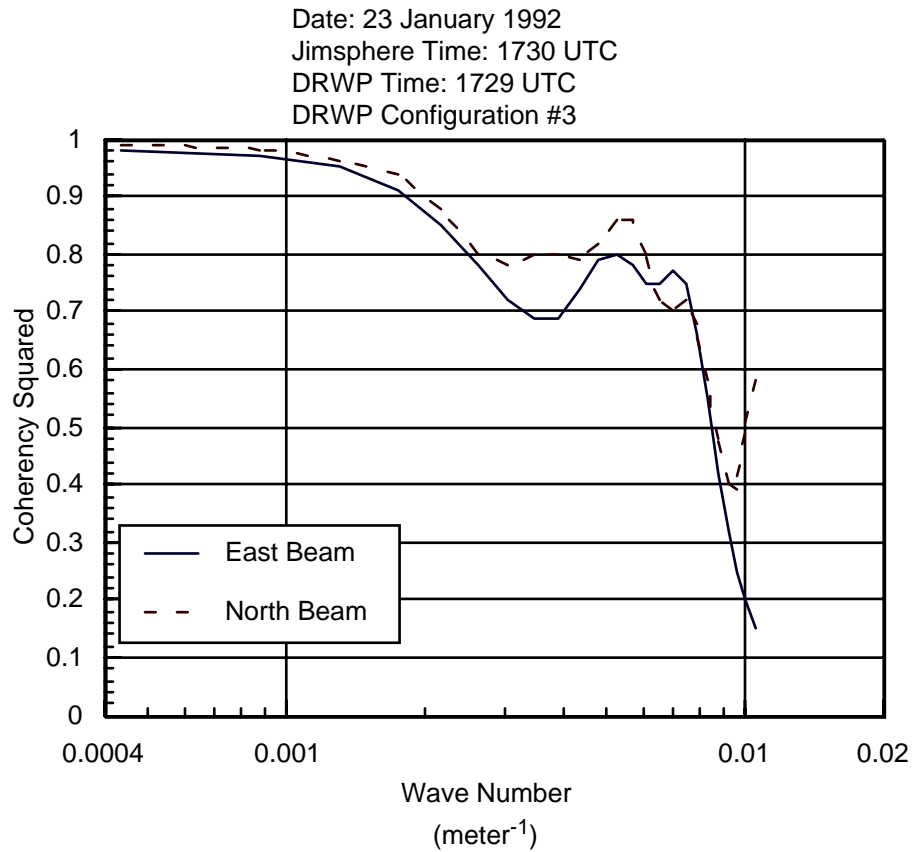
Figure 4.18. Coherency analysis of jimsphere and MSFC wind algorithm DRWP profiles for 23 January 1992. Profile times are: Jimsphere 1730 UTC and MSFC wind algorithm 1729 UTC.

Table 4.4. Jimsphere And MSFC Wind Algorithm DRWP Velocity Comparisons For 23 January 1992			
Jimsphere Profile Time (UTC)	MSFC Algorithm Profile Time* (UTC)	RMS Differences East Beam (m/s)	RMS Differences North Beam (m/s)
1400	1408	1.90	1.52
1530	1530	2.06	1.76
1730	1729	2.21	1.93

* The MSFC wind algorithm DRWP profiles were generated using configuration #3.

4.1.10 Consensus / MSFC Wind Algorithm RMS Velocity Differences From 23 January 1992

The RMS velocity differences between the MSFC wind algorithm DRWP profiles and the consensus averaged DRWP profiles for 23 January 1992 are contained in Table 4.5. The RMS velocity differences in Table 4.5 are generally considerably less than the RMS velocity differences between two MSFC wind algorithm DRWP profiles from 23 January 1992 separated by 30 minutes (i.e., 2.2 m/s). This indicates the profiles produced by the MSFC wind algorithm are generally comparable to the consensus averaged wind profiles. However, there are some notable exceptions. In particular, Figure 4.13 indicates there are regions (e.g., from 8 km to 12 km) where the temporal averaging in the consensus technique produces a "smoother" wind profile than the MSFC wind algorithm. Also, Figure 4.11 presents some examples of erroneous wind estimates produced by the consensus averaging technique. In addition, the RMS velocity differences between the 1800 UTC and 1830 UTC consensus averaged DRWP profiles and the corresponding MSFC wind algorithm DRWP profiles (Table 4.5) are considerably larger than the other RMS velocity differences for 23 January 1992. The larger RMS velocity differences at 1800 UTC can be attributed to contaminated profiler data from 1815 UTC to 1830 UTC due to a thunderstorm near the SLF. Since the contaminated signal regime affected half of the data used to produce the consensus averaged profile, the resulting profile was of poorer quality and, consequently, the RMS differences between the MSFC wind algorithm DRWP profile and the consensus averaged DRWP profile for this period were larger. The relatively large RMS difference between the east beam component of the 1830 UTC consensus averaged DRWP profile and the east beam component of the corresponding MSFC wind algorithm DRWP profile remains unexplained.

Table 4.5. Consensus Averaged And MSFC Wind Algorithm DRWP Velocity Comparisons For 23 January 1992			
Consensus Profile Time (UTC)	MSFC Algorithm Profile Time* (UTC)	RMS Differences East Beam (m/s)	RMS Differences North Beam (m/s)
1300	1314	0.80	0.60
1330	1343	0.96	0.81
1400	1416	0.98	0.84
1430	1445	0.91	0.64
1500	1518	0.93	0.77
1530	1546	0.73	0.93
1600	1615	1.04	0.91
1630	1652	1.18	1.12
1700	1717	1.07	0.75
1730	1746	1.03	0.92
1800	1815	1.85	1.65
1830	1843	1.70	1.10

* The MSFC wind algorithm DRWP profiles were generated using configuration #3.

4.1.11 Example Of Spectral Data Contamination Due to Lightning

Figure 4.19 provides an example of the performance of the DRWP approximately 15 minutes prior to the occurrence of lightning at the SLF. At this time, the DRWP is getting a good atmospheric return and the MSFC wind algorithm is tracking the signal well. At most all levels, the SNR is above the -15 dB minimum. The only region with a noticeable data quality issue is the north beam near 11 km. At this level, there is an increase in the noise power and the velocity trace, although reasonable, is tracking through a relatively weak signal region.

The spectral estimates from the east and north beams at 1831 UTC and 1832 UTC, respectively, are vastly different from their counterparts 15 minutes earlier (Figure 4.20). This time corresponds to the end of the lightning event at the SLF and it is evident the returns from both the east and north beams are contaminated by the discharges. The east beam data appears to be contaminated in the regions from 3 to 5 km, around 10 km, and around 12 km. At these levels, it is generally difficult to discern the atmospheric wind signal and the noise power is significantly elevated. The contamination of the north beam data is worse. The noise power is elevated at most all levels and it is very difficult to discern the atmospheric wind signal at all levels above 10 km. Although the MSFC wind algorithm produced velocity estimates from the contaminated returns, the estimates are of poorer quality than normal and contain some questionable estimates.

Yoe, Larsen, and Zipser (1992) detected similar contamination of DRWP data during periods of lightning with a 50 MHz profiler located in Kansas. Similar spectra were observed by Larsen and Rottger (1987) during periods of lightning with the SOUSY-VHF Doppler radar system in The Federal Republic of Germany.

Although not important to launch and landing operations, lightning contamination of profiler data may impact daily use of the data from the system. Consequently, it is important to be able to recognize lightning contaminated returns. The contamination is easily recognizable within the color coded spectral estimates display; however, this information will not be available to the typical user of the wind data[2]. It appears examining the noise power may be one of the best methods to detect lightning contamination of the 50 MHz DRWP. Lightning events which contaminate profiler returns result in relatively large noise power estimates but not necessarily lower SNR. During these events, the wind velocity estimates from the DRWP may be in error and the data should be compared to measurements from other systems and from DRWP data outside of the lightning event.

Two other sources of environmental noise detected by radars have been noted by Skolnik (1980) and Wilfong et al (1992). The first is the cosmic background noise which produces the minimum noise floor for all range for all data collection periods in the DRWP. The cosmic background noise does fluctuate and reaches a maximum twice daily when the profiler beams sweep through the galactic plane and receive signals from the Milky Way galaxy. Some signal loss may occur in the higher range gates of the oblique beams during the short-lived cosmic noise peaks.

The other source of environmental noise is solar noise which occurs twice a year in the oblique 135□ azimuth beam during May and August. Solar noise can have a significant effect upon data collection because it can raise the noise power sufficiently to obscure atmospheric signals above about 9 km (Wilfong et al, 1992). The elevated noise power due to solar noise lasts for about 25 minutes during the days when the profiler beam passes through the solar radiation.

---

[2] Typical users of the wind data include Spaceflight Meteorology Group forecasters, Range Weather Operations forecasters, Shuttle ascent community personnel, and Expendable Launch vehicle community personnel. Generally, only the quality control operator will have access to the color coded spectral estimates display.
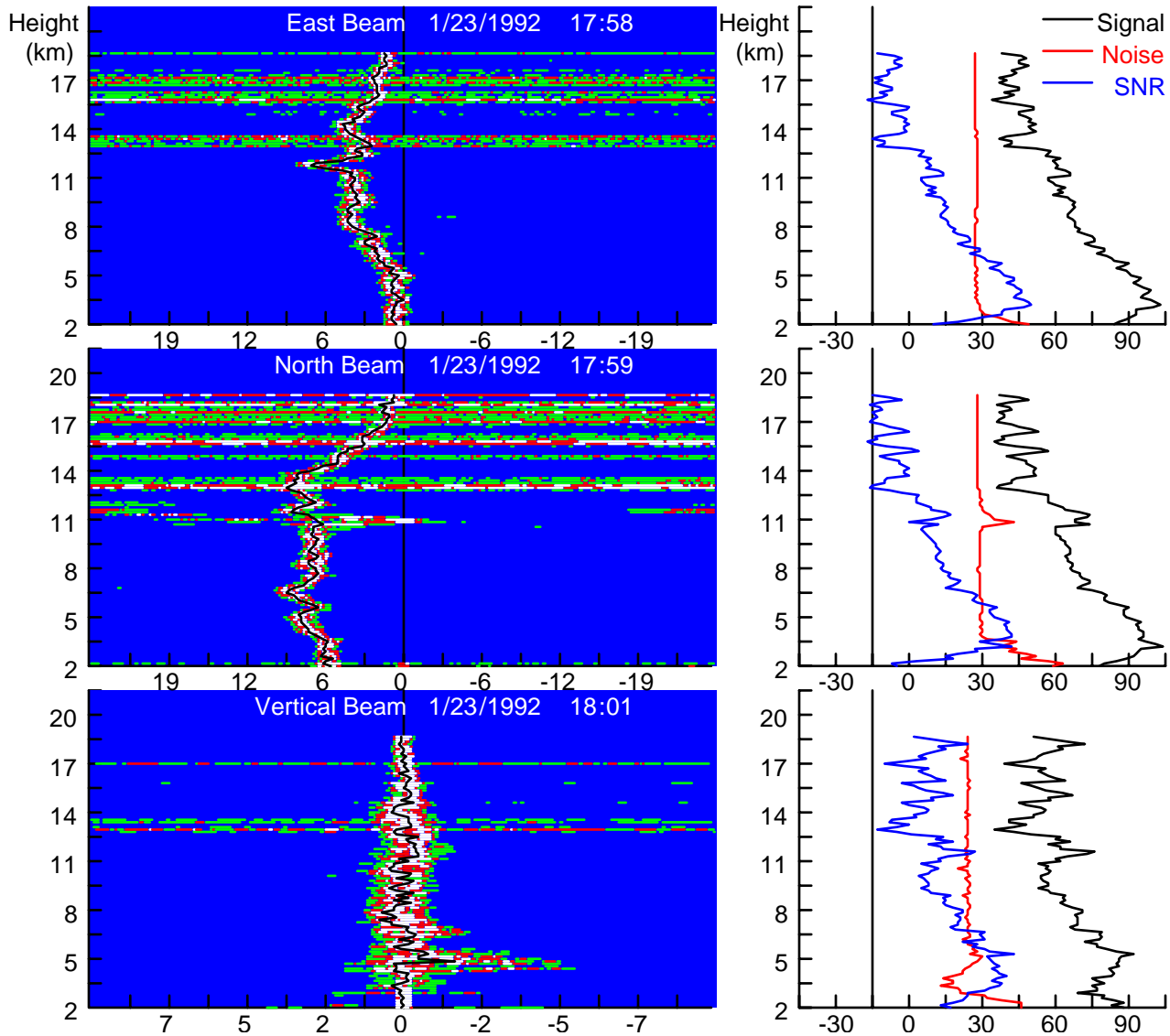
Figure 4.19. Example of spectral data prior to lightning occurrence at the SLF. Spectral estimates for the east, north, and vertical beams are color coded and overlaid with the radial velocity estimates (black trace). Relatively larger spectral estimates are coded white while relatively smaller spectral estimates are coded blue. The units on the horizontal axis of the spectral estimate displays are m/s. The units of the corresponding signal, noise, and SNR profiles are decibels.
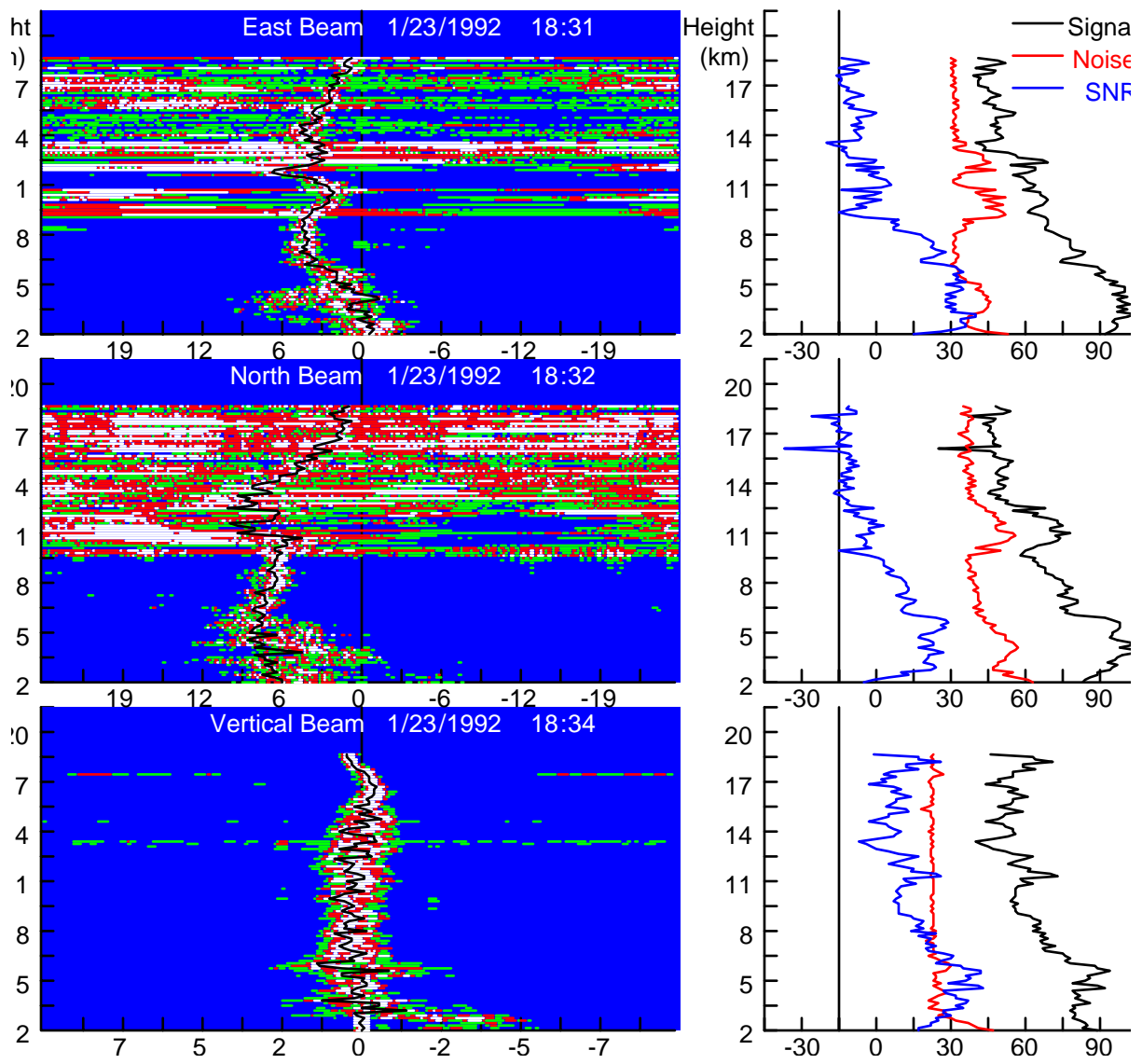
Figure 4.20.   Example of spectral data contaminated by lightning.   Spectral estimates for the east, north, and vertical beams are color coded and overlaid with the radial velocity estimates (black trace).   Relatively larger spectral estimates are coded white while relatively smaller spectral estimates are coded blue.   The units on the horizontal axis of the spectral estimate displays are m/s.   The units of the corresponding signal, noise, and SNR profiles are decibels.

4.1.12 First Wind Profile Comparison From 20 February 1992

The first set of time proximate jimsphere, consensus averaged DRWP, and MSFC wind algorithm DRWP profiles from 20 February 1992 is presented in Figures 4.21 and 4.22. As with the other two days examined, the large scale features present in the three profiles are very similar; however, the small scale features represented by the three profiles exhibit some differences.

The east beam profiles are very similar from 8 km to 15 km. Both above and below that region, the differences among the three profiles are more pronounced. The differences among the profiles in the lower altitudes are generally associated with the amplitude rather than the phase of the waves. In particular, the amplitudes of the small wavelength features in the consensus averaged profile between 4 km and 8 km are generally smaller than the corresponding features in the MSFC wind algorithm profile. Examination of a series of MSFC wind algorithm DRWP profiles from 1419 UTC to 1602 UTC indicates temporal changes in the east beam component ranging from 5 m/s to 7 m/s within this period in the 4 km to 8 km region. The temporal averaging procedures employed in the consensus technique smooth the temporal variability present in the data. This smoothing accounts for the east component differences in the 4 km to 8 km region between the consensus profile and the MSFC wind algorithm profile.

The most noticeable differences in the north beam profiles is in the region from 5 km to 10 km. In this region, the magnitude of the jimsphere velocities are typically 2 to 3 m/s less than the corresponding MSFC wind algorithm velocities.

The coherence data in Figure 4.23 indicate the north beam components of the two profiles are highly coherent to wavelengths as short as 1000 meters (i.e., wave number equal to $6 \infty 10^{-3}$ m^{-1}) and the east beam components of the two profiles are highly coherent to wavelengths as short as 1200 meters (i.e., wave number equal to $5 \infty 10^{-3}$ m^{-1}). Again, at shorter wavelengths, the coherence of both components is generally less; this is expected in light of the data collection differences between the jimsphere and the DRWP.

4.1.13 Second Wind Profile Comparison From 20 February 1992

The second set of time proximate jimsphere, consensus averaged DRWP, and MSFC wind algorithm DRWP profiles from 20 February 1992 is presented in Figures 4.24 and 4.25. As with the other examples presented, the large scale features present in the three profiles are very similar; however, the small scale features represented by the three profiles exhibit some differences.

The east beam profiles exhibit notable differences in small scale features at many levels. The differences in small scale features among the profiles are most pronounced near the east beam component maximum at 15 km, between 5 km and 8 km, and in the lowest 2 km.

The north beam profiles are very similar in the lowest 8 km. Above that level, the differences among the three profiles are more pronounced. In particular, there are

differences in the north beam component short wavelength features among the three profiles between 8 km and 10 km. In addition, although the profile shapes are similar, the magnitude of the two north beam velocities from the DRWP from 10 km to 12 km are larger than the corresponding jimsphere velocities. Finally, the MSFC wind algorithm DRWP profile and the jimsphere profile indicate a small jet feature in the north beam
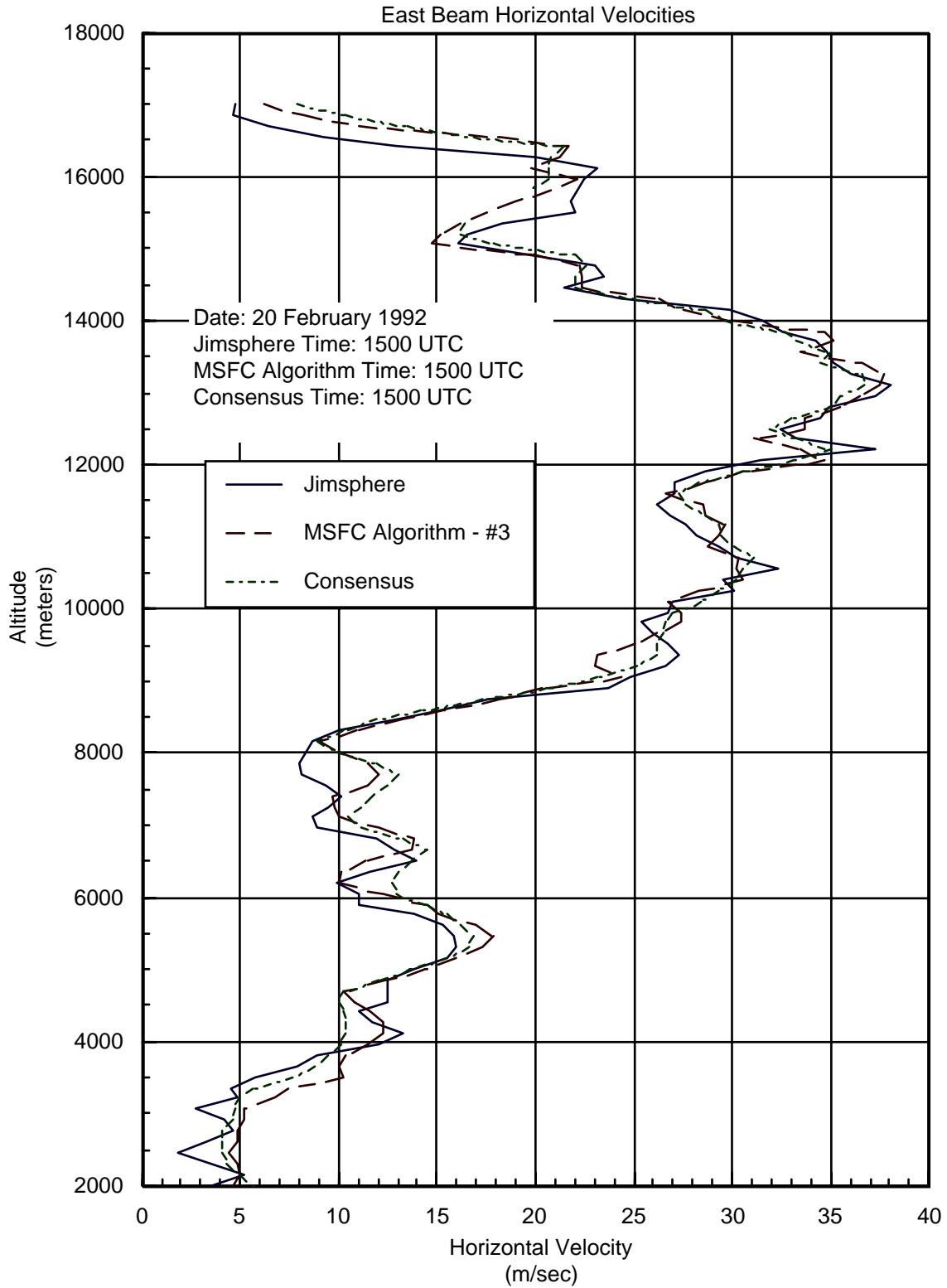
Figure 4.21.   East beam velocities for 20 February 1992. Profile time stamps are: Jimsphere 1500 UTC, Consensus 1500 UTC, and MSFC wind algorithm 1500 UTC.
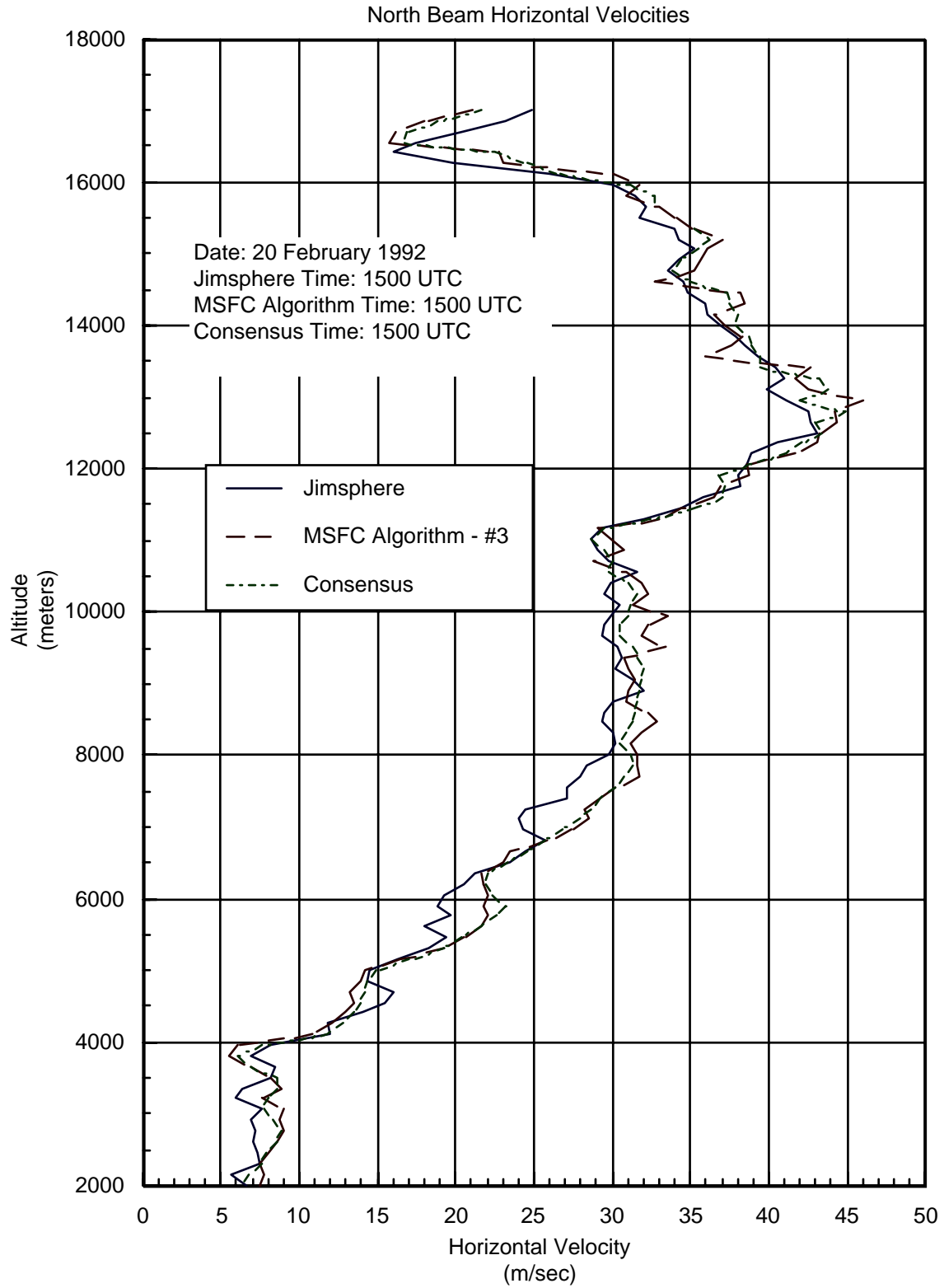
Figure 4.22. North beam velocities for 20 February 1992. Profile time stamps are: Jimsphere 1500 UTC, Consensus 1500 UTC, and MSFC wind algorithm 1500 UTC.

Date: 20 February 1992
Jimsphere Time: 1500 UTC
DRWP Time: 1500 UTC
DRWP Configuration #3
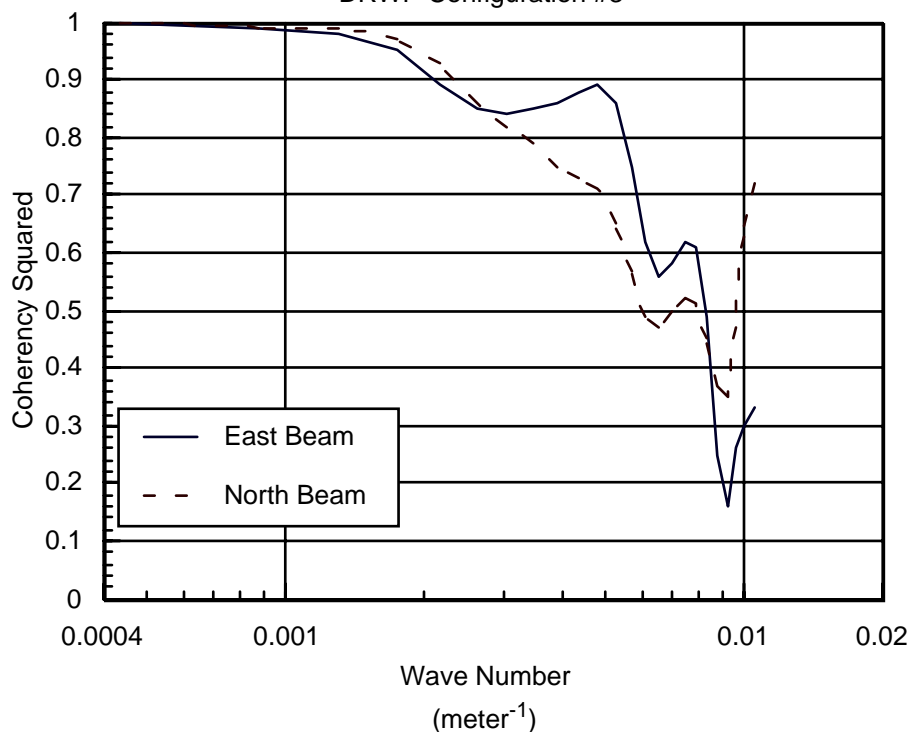
Figure 4.23.   Coherency analysis of jimsphere and MSFC wind algorithm DRWP
profiles for 20 February 1992. Profile times are: Jimsphere 1500 UTC
and MSFC wind algorithm 1500 UTC.

component at approximately 15.5 km. This feature is not present in the corresponding
consensus averaged profile. Examination of a series of MSFC wind algorithm DRWP
profiles from 1533 UTC to 1728 UTC indicates the north beam component jet feature at
15.5 km was not present during much of the consensus averaging period (i.e., 1630 UTC
to 1700 UTC). Consequently, the temporal averaging procedures employed in the
consensus technique eliminate this feature from the consensus profile.

The coherence data in Figure 4.26 indicate the north beam components of the two
profiles are highly coherent to wavelengths as short as 600 meters (i.e., wave number
equal to $1 \infty 10^{-2}$ m^{-1}). This is in contrast to most of the other examples where the
coherence between the north beam components is generally lower for the shorter
wavelengths. The higher degree of coherence at short wavelengths for this case is
associated with the high degree of similarity between the north beam components of the
MSFC wind algorithm DRWP profile and the jimsphere profile in the lowest 8 km
(Figure 4.25). The east beam components are highly coherent to wavelengths as short as
1000 meters (i.e., wave number equal to $6 \infty 10^{-3}$ m^{-1}). At shorter wavelengths, the
coherence of the east beam components decreases which is similar to the other examples
presented.

73
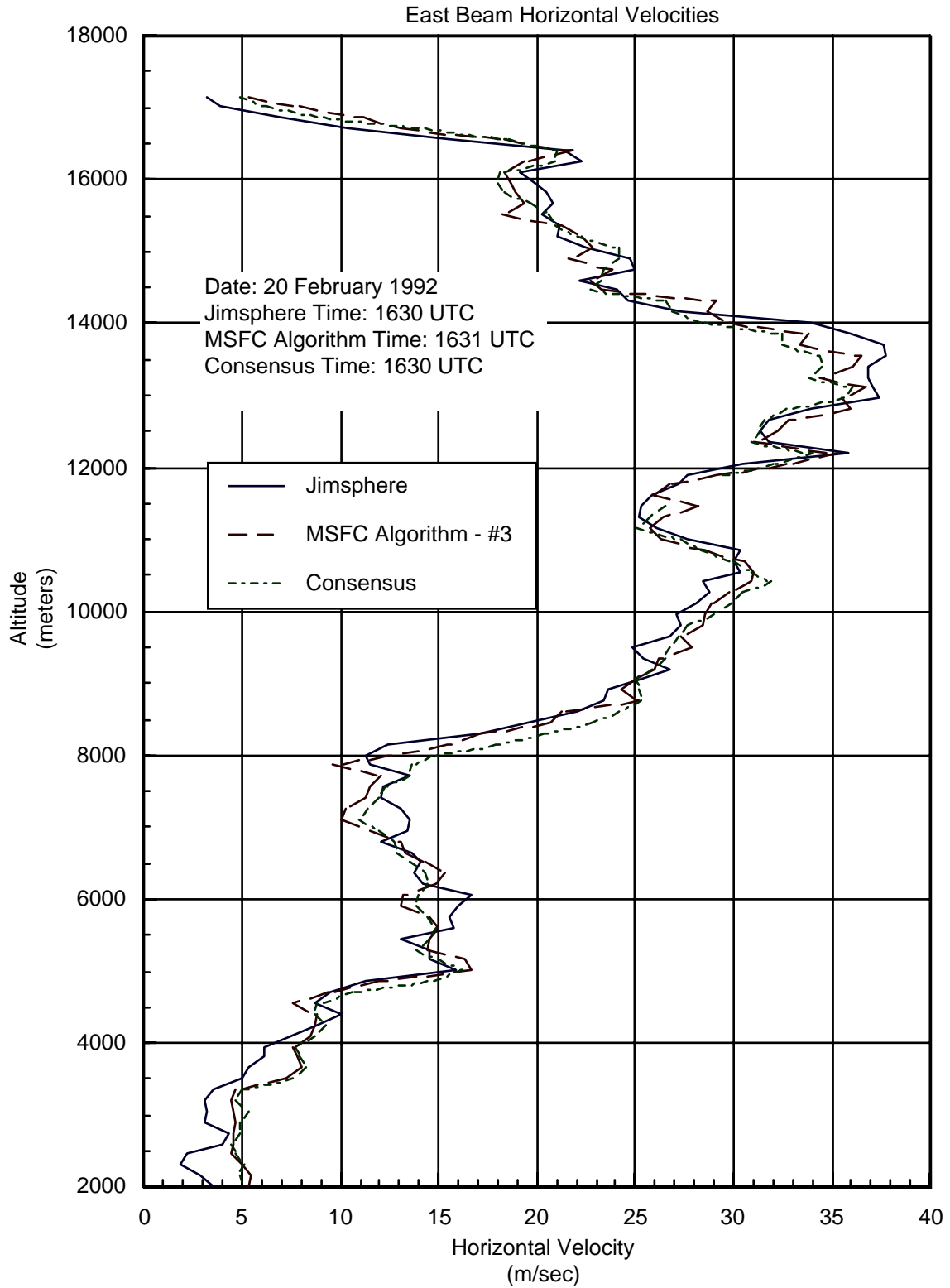
Figure 4.24. East beam velocities for 20 February 1992. Profile time stamps are: Jimsphere 1630 UTC, Consensus 1630 UTC, and MSFC wind algorithm 1631 UTC.
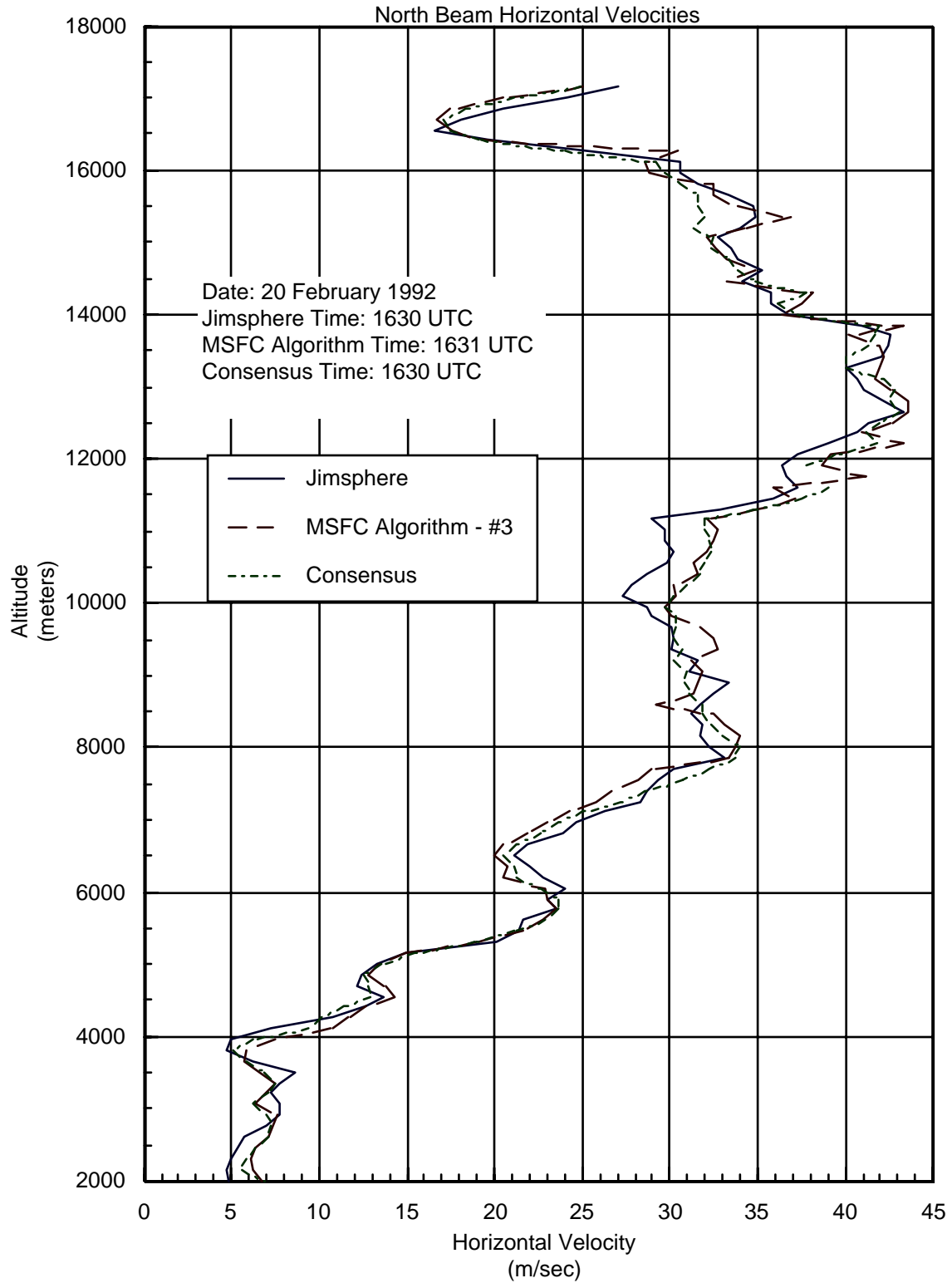
Figure 4.25. North beam velocities for 20 February 1992. Profile time stamps are: Jimsphere 1630 UTC, Consensus 1630 UTC, and MSFC wind algorithm 1631 UTC.

Date: 20 February 1992
Jimsphere Time: 1630 UTC
DRWP Time: 1631 UTC
DRWP Configuration #3
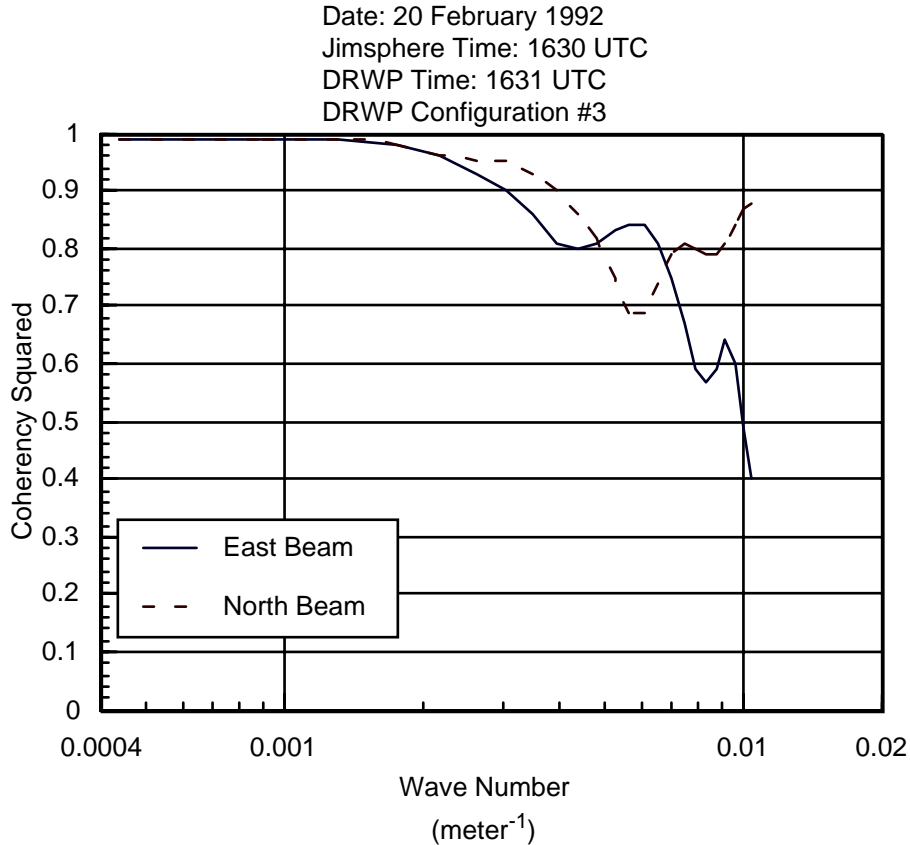
Figure 4.26.   Coherency analysis of jimsphere and MSFC wind algorithm DRWP
profiles for 20 February 1992. Profile times are: Jimsphere 1630 UTC
and MSFC wind algorithm 1631 UTC.

4.1.14 Third Wind Profile Comparison From 20 February 1992

The third set of time proximate jimsphere, consensus averaged DRWP, and MSFC
wind algorithm DRWP profiles from 20 February 1992 is presented in Figures 4.27 and
4.28. As with the other examples presented, the large scale features present in the three
profiles are similar; however, the small scale features represented by the three profiles
exhibit some differences.

The shear zones in the east beam velocity from 6 km to 8 km and from 16.5 km to
17.5 km are represented similarly by all three profiles. The largest difference in the east
beam profiles occurs between 9 km and 11 km. In this region of relatively large
velocities, the east beam velocity differences between the jimsphere profile and the
MSFC wind algorithm profile approach 5 m/s. Examination of a series of MSFC wind
algorithm DRWP profiles from 1728 UTC to 1928 UTC indicates temporal changes in
the east beam velocities of the order of 5 m/s within this 2 hour in the 9 km to 11 km
region. Consequently, the east beam component differences in the 9 km to 11 km range
between the jimsphere and DRWP profiles are probably due to the sampling differences
between the two systems.

76

As with the 1630 UTC example (Figure 4.25), the north beam profiles are very similar in the lowest 8 km. Above that level, the differences among the three profiles are more pronounced. In particular, there are differences in the north beam component short
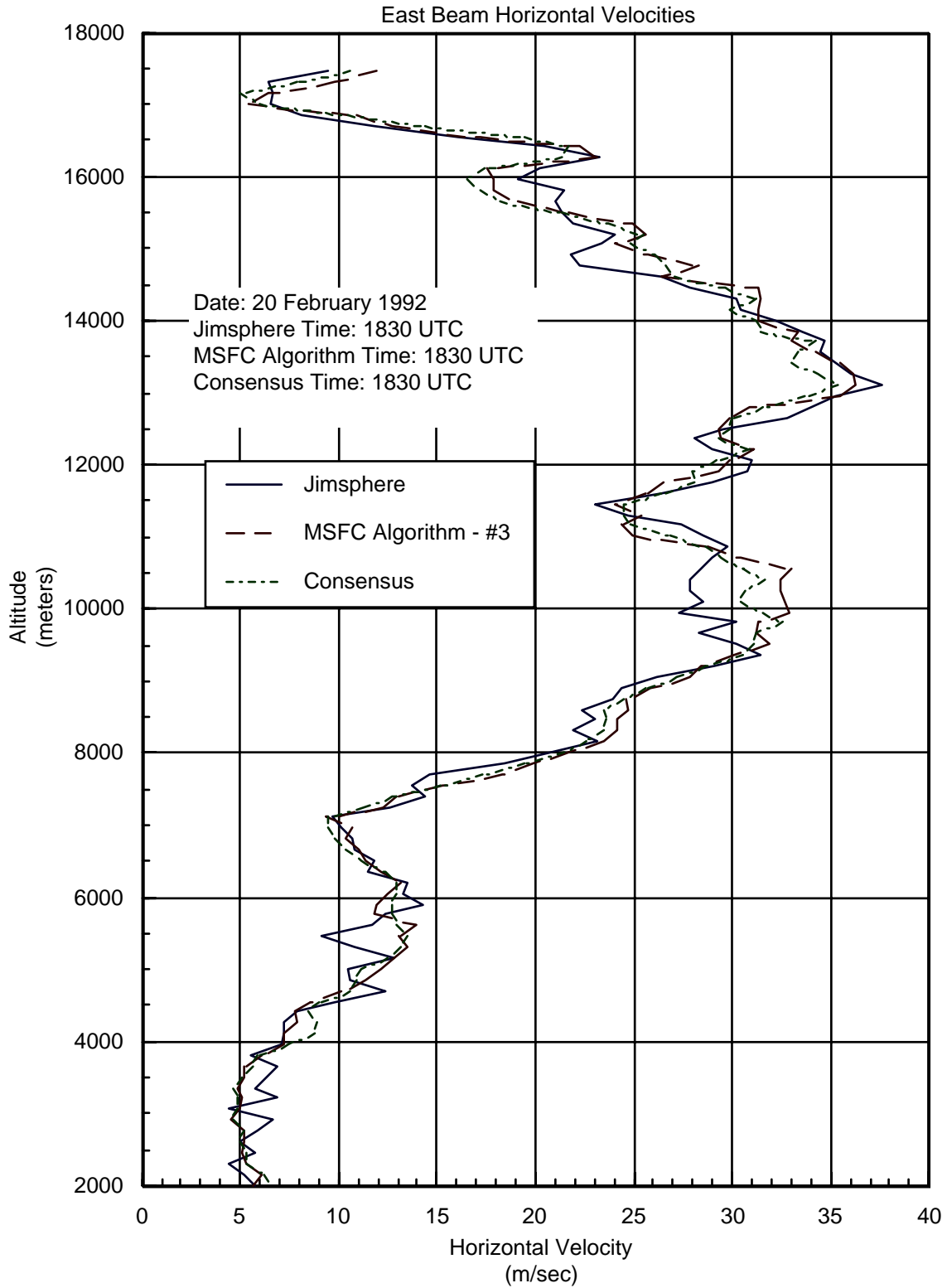
Figure 4.27.   East beam velocities for 20 February 1992. Profile time stamps are: Jimsphere 1830 UTC, Consensus 1830 UTC, and MSFC wind algorithm 1830 UTC.

78

North Beam Horizontal Velocities

Date: 20 February 1992
Jimsphere Time: 1830 UTC
MSFC Algorithm Time: 1830 UTC
Consensus Time: 1830 UTC

Jimsphere
MSFC Algorithm - #3
Consensus
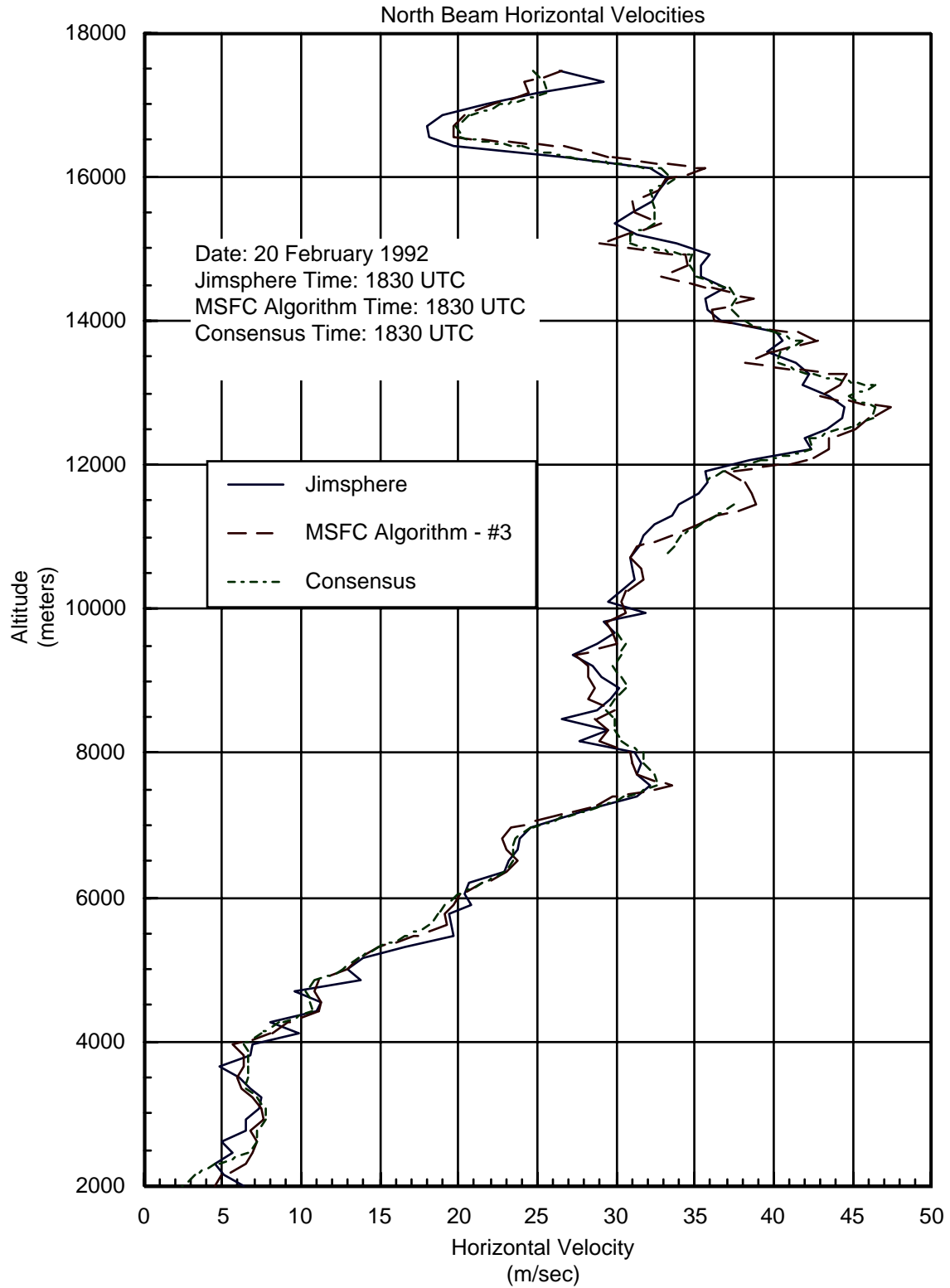
Figure 4.28.   North beam velocities for 20 February 1992. Profile time stamps are:
Jimsphere 1830 UTC, Consensus 1830 UTC, and MSFC wind
algorithm 1830 UTC.

79

wavelength features among the three profiles between 8 km and 10 km. In addition, although the profile shapes are similar, the magnitude of the two north beam velocities from the DRWP from 10 km to 12 km are larger than the corresponding jimsphere velocities.

The coherence data in Figure 4.29 indicate the north beam components of the two profiles are highly coherent to wavelengths as short as 900 meters (i.e., wave number equal to $7 \infty 10^{-3}$ m^{-1}). At shorter wavelengths, the north beam components are still moderately coherent with coherence values ranging between 0.6 and 0.7. The east beam components are highly coherent to wavelengths as short as 1000 meters (i.e., wave number equal to $6 \infty 10^{-3}$ m^{-1}). At shorter wavelengths, the coherence of the east beam components decreases which is similar to the other examples presented.

Date: 20 February 1992
Jimsphere Time: 1830 UTC
DRWP Time: 1830 UTC
DRWP Configuration #3
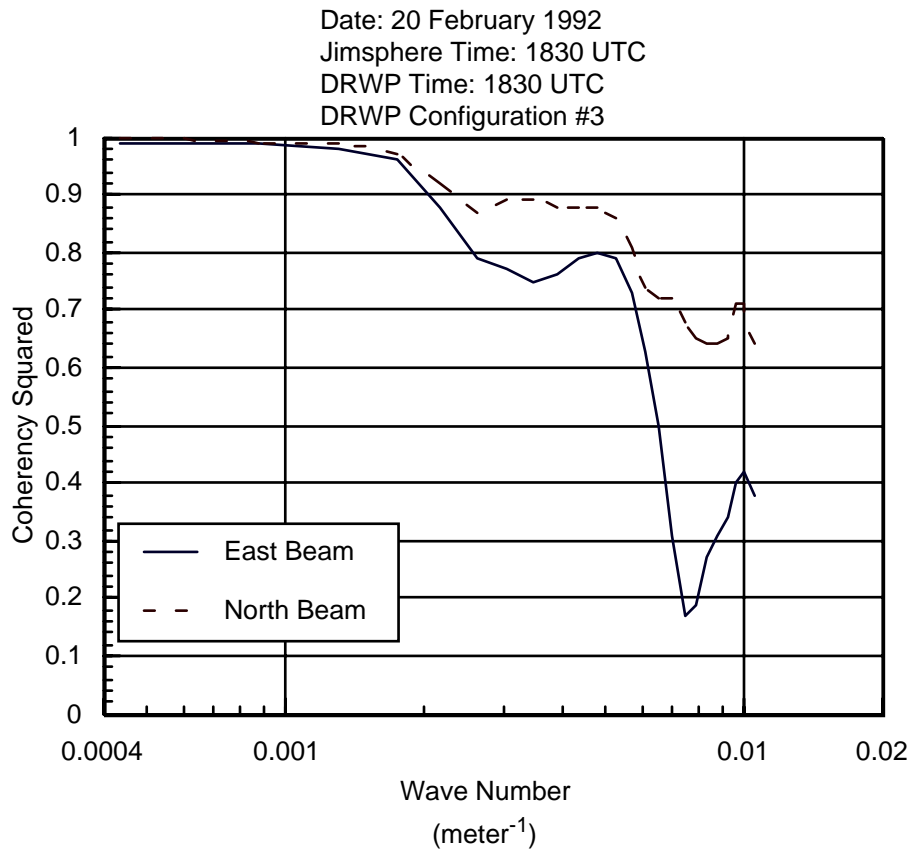
Figure 4.29. Coherency analysis of jimsphere and MSFC wind algorithm DRWP profiles for 20 February 1992. Profile times are: Jimsphere 1830 UTC and MSFC wind algorithm 1830 UTC.

4.1.15 Jimsphere / MSFC Wind Algorithm RMS Velocity Differences From 20 February 1992

The RMS velocity differences between the MSFC wind algorithm DRWP profiles and the jimsphere profiles for 20 February 1992 are contained in Table 4.6. In this case, the RMS velocity differences are very similar to the RMS velocity differences for 23 January 1992 (Table 4.4). As with the 23 January 1992 data, RMS velocity differences between temporally separated MSFC wind algorithm profiles were used to infer the reason for the slightly larger RMS velocity differences between MSFC wind algorithm DRWP profiles and the jimsphere profiles on 20 February 1992 as compared to the differences on 12 September 1991.

Table 4.6. Jimsphere And MSFC Wind Algorithm DRWP Velocity Comparisons For 20 February 1992			
Jimsphere Profile Time (UTC)	MSFC Algorithm Profile Time* (UTC)	RMS Differences East Beam (m/s)	RMS Differences North Beam (m/s)
1500	1500	2.30	2.25
1630	1631	1.84	1.82
1830	1830	2.04	1.85

* The MSFC wind algorithm DRWP profiles were generated using configuration #3.

The RMS velocity differences between two MSFC wind algorithm DRWP profiles from 12 September 1991 separated by 30 minutes are approximately 1.3 m/s. In contrast, the RMS velocity differences between two MSFC wind algorithm DRWP profiles from 20 February 1992 separated by 30 minutes are approximately 2 m/s. As with the 23 January 1992 data, this indicates either increased atmospheric variability or larger temporal changes or a combination of the two. In any event, based on the substantially larger RMS velocity differences in the temporally separated MSFC wind algorithm DRWP profiles on 20 February 1992, the larger RMS velocity differences between the MSFC wind algorithm DRWP profiles and the jimsphere profiles for 20 February 1992 appear reasonable.

4.1.16 Consensus / MSFC Wind Algorithm RMS Velocity Differences From 20 February 1992

The RMS velocity differences between the MSFC wind algorithm DRWP profiles and the consensus averaged DRWP profiles for 20 February 1992 are contained in Table 4.7. The RMS velocity differences in Table 4.7 are considerably less than the RMS velocity differences between two MSFC wind algorithm DRWP profiles from 20

February 1992 separated by 30 minutes. This indicates the profiles produced by the MSFC wind algorithm are comparable to the consensus averaged wind profiles.

Table 4.7. Consensus Averaged And MSFC Wind Algorithm DRWP Velocity Comparisons For 20 February 1992			
Consensus Profile Time (UTC)	MSFC Algorithm Profile Time* (UTC)	RMS Differences East Beam (m/s)	RMS Differences North Beam (m/s)
1400	1419	0.87	0.71
1430	1444	0.80	0.99
1500	1517	0.92	0.74
1530	1546	0.91	0.88
1600	1614	1.04	0.96
1630	1643	0.93	0.80
1700	1716	0.85	0.87
1730	1745	0.80	0.74
1800	1814	0.84	0.70
1830	1843	0.80	0.82
1900	1916	0.79	0.82
1930	1944	0.88	0.70

* The MSFC wind algorithm DRWP profiles were generated using configuration #3.

4.1.17 Consensus / MSFC Wind Algorithm Profile Comparisons

In addition to the velocity comparisons between the MSFC wind algorithm DRWP profiles and the consensus averaged DRWP profiles, the number of levels where the velocity extraction techniques are either unable to produce a velocity estimate or produce an erroneous velocity have been catalogued and analyzed. These data are important in evaluating the relative performance of the two techniques and are also an important measure of the data quality.

Table 4.8 contains the number of levels where the consensus averaging technique was unable to produce a velocity estimate or produced an erroneous velocity (i.e., a velocity estimate which is clearly unrealistic) for the data from 12 September 1991. The table also contains the number of levels where the first guess velocity has been propagated more than two times consecutively by the MSFC wind algorithm. The critical value for the number of first guess propagations has been selected in relation to the proposed use of the DRWP in support of shuttle operations. At this time, proposed use of the DRWP calls for a wind profile to be distributed to the customer at least every fifteen minutes.

With a cycle time of five minutes, this means every third profile would be transmitted to the customer. Therefore, if the first guess velocity is propagated three or more times consecutively, the customer is not provided with a new estimate of the wind at that particular level. Hence, the critical value for the number of first guess propagations was set at two.

The data in Table 4.8 indicate both velocity extraction techniques were able to produce reasonable velocity estimates at most all levels throughout the five hour period on 12 September 1991. In addition, the data do not suggest one procedure is performing better than the other since the number of levels where the first guess velocity was propagated more than two times consecutively by the MSFC wind algorithm is similar to the number of levels reporting missing or erroneous data by the consensus technique.

Table 4.8. Consensus Averaged And MSFC Wind Algorithm DRWP Profile Comparisons For 12 September 1991			
Consensus Profiles		MSFC Algorithm Profiles*	
Time (UTC)	Number of Levels**	Time (UTC)	Number of Levels***
1900	0	1915	0
1930	0	1946	1
2000	0	2015	1
2030	0	2044	1
2100	0	2116	1
2130	0	2145	2
2200	1	2214	0
2230	0	2246	1
2300	2	2314	1
2300	3	2346	3

* The MSFC wind algorithm DRWP profiles were generated using configuration #3.
** The number of levels with either erroneous data or missing data.
*** The number of levels with the number of first guess velocity propagations for the east beam and/or the north beam greater than two (2).

The results from 23 January 1992 data, however, are not quite as good (Table 4.9). In this case, the signal returns from the profiler were generally weaker above 13 km than the signal returns from 12 September 1991. Consequently, the number of levels where the consensus averaging technique was unable to produce a velocity estimate or produced an erroneous velocity and the number of levels where the first guess velocity has been propagated more than two times consecutively by the MSFC wind algorithm is greater

for the 20 January 1992 data than for the 12 September 1991 data. The data in Table 4.9 do not suggest one velocity extraction technique is performing better overall than the other. However, one significant difference affecting the time resolution of the profiles produced by the two techniques is illustrated by the January data.

Table 4.9. Consensus Averaged And MSFC Wind Algorithm DRWP Profile Comparisons For 23 January 1992			
Consensus Profiles		MSFC Algorithm Profiles*	
Time (UTC)	Number of Levels**	Time (UTC)	Number of Levels***
1330	0	1343	1
1400	5	1416	1
1430	3	1445	4
1500	2	1518	4
1530	5	1546	3
1600	7	1615	5
1630	0	1652	1
1700	2	1717	4
1730	1	1746	2
1800	25	1815	3
1830	1	1843	0

*   The MSFC wind algorithm DRWP profiles were generated using configuration #3.
**   The number of levels with either erroneous data or missing data.
***   The number of levels with the number of first guess velocity propagations for the east beam and/or the north beam greater than two (2).

At 1800 UTC the consensus averaging procedure was unable to produce a velocity estimate or produced an erroneous velocity at 25 of the 112 levels. This is a result of the lightning contamination during the period from 1815 to 1830 UTC. Conversely, the first guess velocity was propagated more than two times consecutively by the MSFC wind algorithm at only 3 levels on the 1815 UTC wind profile. Strictly speaking, this is not a truly fair comparison since the lightning contamination was from the period 1815 UTC to 1830 UTC or just after the 1815 UTC MSFC wind algorithm profile. However, it does highlight an important difference between the two velocity extraction techniques. Poor signal returns for as brief a period as 15 minutes may result in a one hour time span between two consecutive high quality wind profiles from the consensus averaging algorithm. In contrast, poor signal returns for a 15 minute period would result in only a

20 minute time span between two consecutive high quality wind profiles from the MSFC wind algorithm.

The results from the data quality profile comparison for 20 February 1992 (Table 4.10) are different from the results from the other two days. Except for the time period associated with the lightning contamination (i.e., 1800 UTC on 23 January 1992), the results of the data quality profile comparisons for 12 September 1991 and for 23 January 1992 do not indicate one of the two algorithms generally performs better than the other. However, this is not true for the 20 February 1992 case. In this case, the MSFC wind algorithm performs as well as or better than the consensus technique for most time periods between 1600 UTC through 1930 UTC because the number of levels where the first guess velocity was propagated more than two times consecutively by the MSFC wind algorithm is generally less than the number of levels reporting missing or erroneous data by the consensus technique.

Table 4.10. Consensus Averaged And MSFC Wind Algorithm DRWP Profile Comparisons For 20 February 1992			
Consensus Profiles		MSFC Algorithm Profiles*	
Time (UTC)	Number of Levels**	Time (UTC)	Number of Levels***
1430	3	1444	6
1500	3	1517	4
1530	1	1546	3
1600	3	1614	0
1630	3	1643	0
1700	0	1716	1
1730	0	1745	1
1800	3	1814	0
1830	6	1843	0
1900	6	1916	0
1930	4	1944	0

*   The MSFC wind algorithm DRWP profiles were generated using configuration #3.

**   The number of levels with either erroneous data or missing data.

***   The number of levels with the number of first guess velocity propagations for the east beam and/or the north beam greater than two (2).

4.1.18 MSFC Wind Algorithm First Guess Velocity Propagation Analysis

The number of times the first guess velocity was propagated by the MSFC wind algorithm for each range gate for the three days are presented in Figures 4.30, 4.31, and 4.32. Not surprisingly, the data indicate first guess velocity propagations are rare below 10 km. Above that level, the number of first guess velocity propagations is highly dependent upon atmospheric conditions and can be quite high. For example, the first guess velocity for the east beam at the 18.4 km level on 12 September 1991 was propagated in 44 of the 109 profiles (~40%). Similarly, the first guess velocity for the north beam at the 15.7 km level on 20 February 1992 was propagated in 38 of the 76 profiles (50%).

Also of interest, is the large number of first guess velocity propagations for both beams at around 13 km on 23 January 1992. The 13 km level corresponds to the jet stream level and, in this case, is a region of relatively weak signal returns resulting in a large number of first guess velocity propagations. For example, the first guess velocity for the east beam at the 13.1 km level was propagated in 31 of the 71 profiles (~45%). The majority of these east beam first guess velocity propagations occurred during the period 1400 UTC to 1520 UTC. The east beam first guess velocity was propagated at the 13.1 km level throughout this entire 80 minute period. However, since the MSFC wind
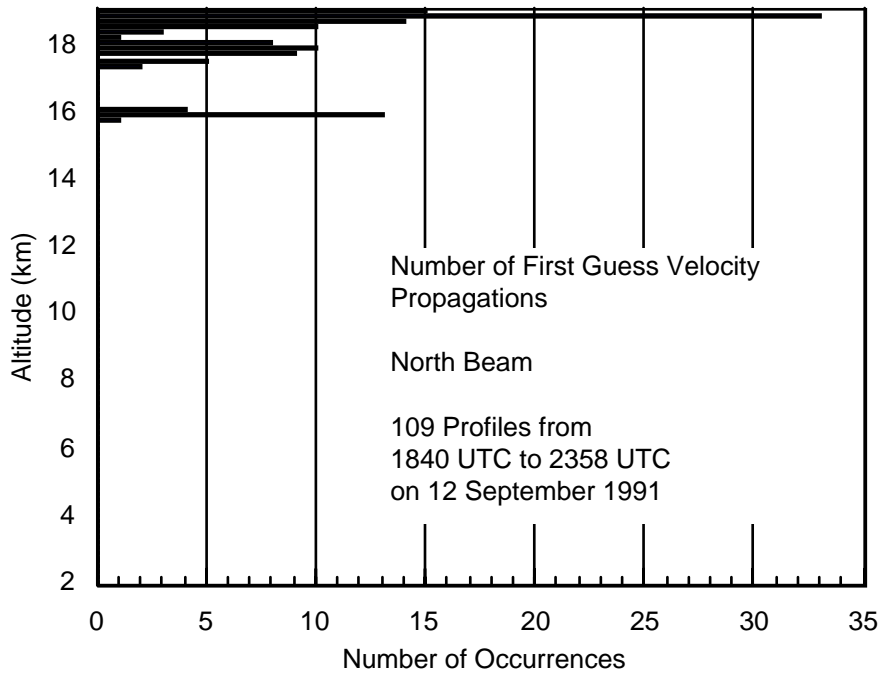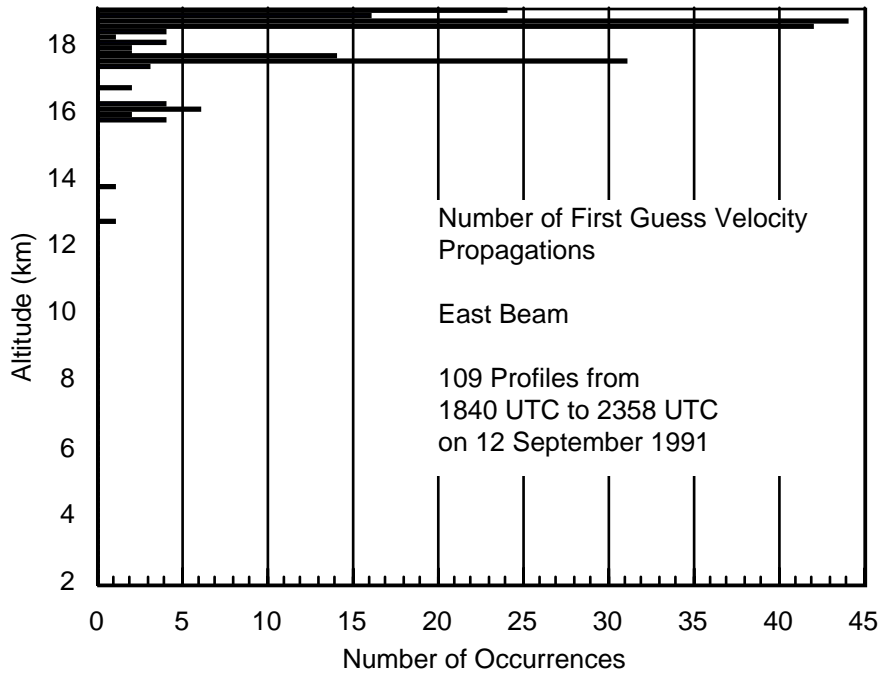
Figure 4.30.   Number of first guess velocity propagations for the 109 MSFC wind algorithm DRWP profiles developed using configuration #3 from 12 September 1991.
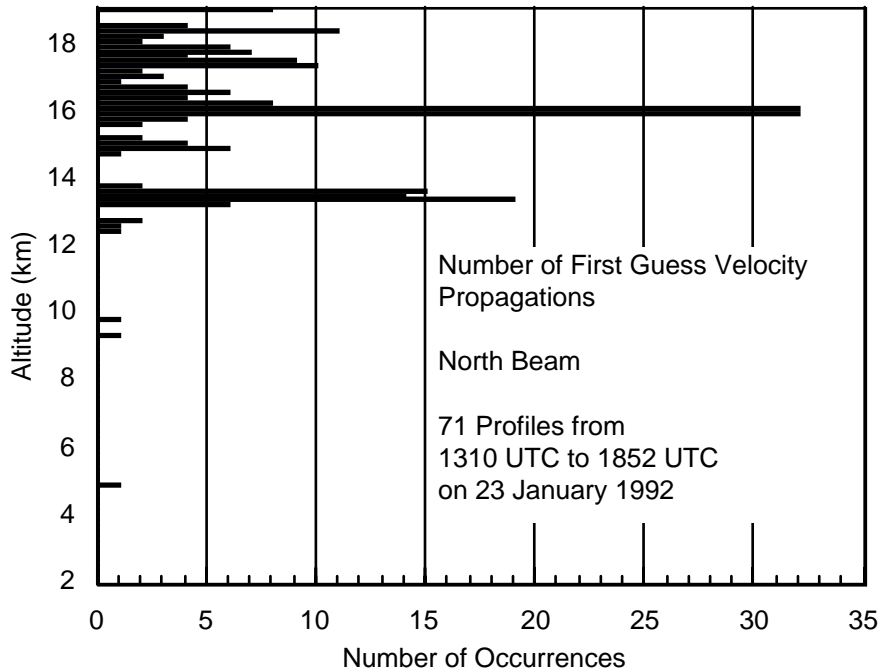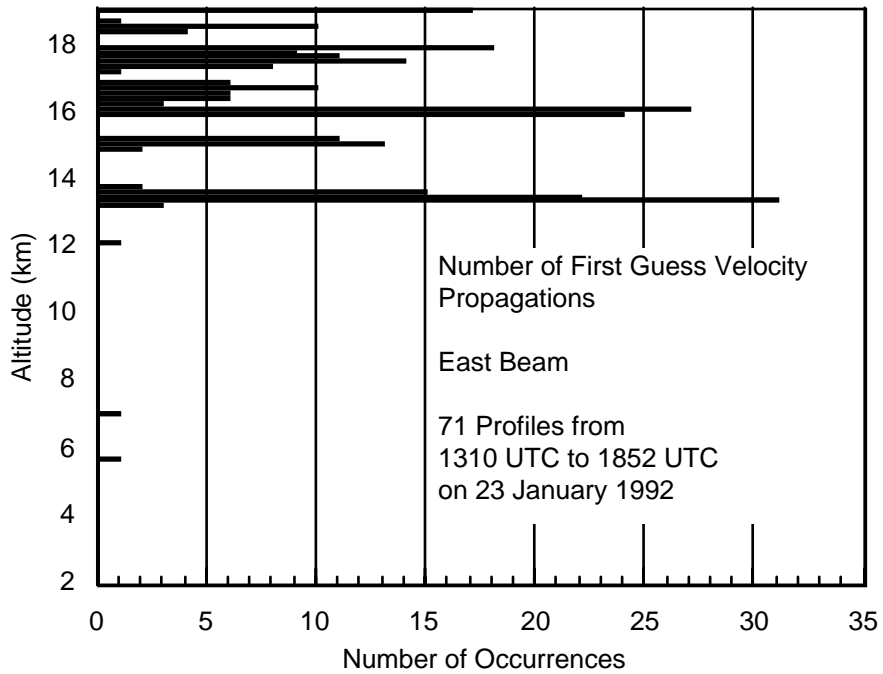
Figure 4.31. Number of first guess velocity propagations for the 71 MSFC wind algorithm DRWP profiles developed using configuration #3 from 23 January 1992.
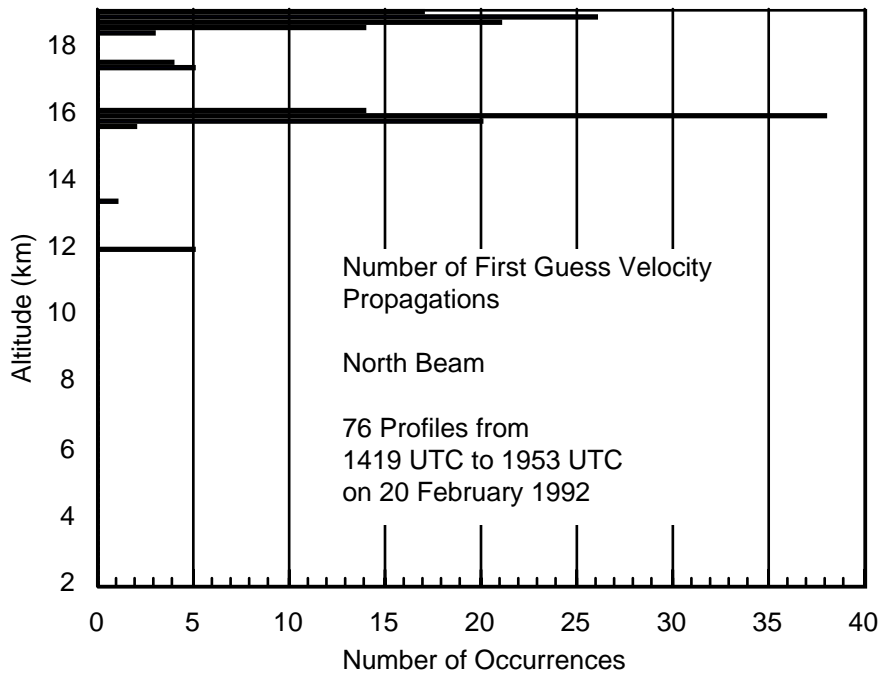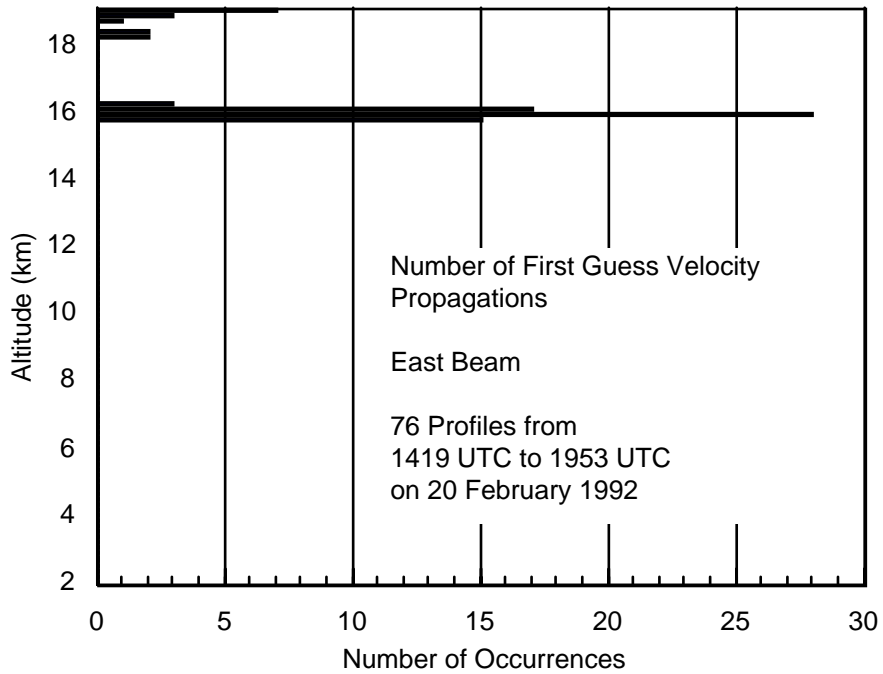
Figure 4.32.   Number of first guess velocity propagations for the 76 MSFC wind algorithm DRWP profiles developed using configuration #3 from 20 February 1992.

algorithm was frequently able to estimate east beam component velocities just above and below 13.1 km level during this period and since the MSFC wind algorithm replaces the first guess velocity with a smoothed wind estimate based on data above and below the given level after five consecutive first guess velocity propagations (Section 3.1.3), the east beam component velocity at the 13.1 km level may have been reflected by the DRWP fairly well (e.g., Figure 4.10). Unfortunately, an absolute measure of the "correct" east beam component velocity at the 13.1 km level around 1500 UTC does not exist. Therefore, the error in the east beam component velocity resulting from the extended period of first guess velocity propagations at the 13.1 km level is unknown. The number of first guess velocity propagations in the jet stream is particularly significant since the jet stream boundary is a region of relatively strong shear which is of importance to the shuttle program.

4.2   Performance Evaluation of Five Different Configurations of the MSFC Wind Algorithm

This section of the report contains the results of the performance evaluation of different configurations of the MSFC wind algorithm. The evaluation has focused on optimizing the first guess window width, the integration window width, and the minimum acceptable signal-to-noise ratio within the algorithm. The five configurations of the MSFC wind algorithm that were evaluated are presented in Table 4.1.

The MSFC wind algorithm uses the first guess window width in conjunction with the first guess velocity to constrain the range of frequency bins that are searched for the maximum signal (Figure 3.2). This first guess approach has the advantage of increasing the probability of the selected maximum signal being related to the wind velocity and decreasing the probability of the selected maximum signal being related to a side lobe or transient signal not of interest. Since the width of the first guess window affects the performance of the first guess technique, this evaluation has examined the impact of using different first guess window widths.

After the maximum signal has been selected, the MSFC algorithm computes the average Doppler shift based on the maximum signal strength and the integration window width (Figure 3.2). As with the first guess window, the width of the integration window affects the resulting average Doppler shift. If the window is too narrow, the peak of the wind velocity signal may not be included in the average Doppler shift integration. In contrast, if the window is too wide, side lobe and/or transient signal data may be included in the average Doppler shift computations. Since the width of the integration window affects the performance of the new wind algorithm, this evaluation has examined the impact of using different integration window widths.

The third and final parameter examined in this evaluation is the minimum acceptable SNR. After the average Doppler shift has been calculated, the SNR is computed. If the SNR does not exceed the minimum acceptable value, the average Doppler shift and the other moments are recomputed using alternative approaches (e.g., using a different first guess velocity and/or smoothing the spectral estimates). If the new SNR still does not

exceed the minimum acceptable value, the first guess velocity is propagated. Thus, the minimum acceptable SNR impacts the results under weak signal conditions.

4.2.1 Spectral Data Analysis From 12 September 1991

Examination of the profiler data from 12 September 1991 indicates all five configurations generally produced very similar velocity estimates in strong signal regimes, and configurations #1, #2, and #3 produced very similar velocity estimates in all signal regimes. In particular, examination of five time coincident profiles produced by DRWP configurations #1, #2, and #3 indicates that 99% of the differences in velocity estimates between configurations #1 and #2 and between configurations #1 and #3 are less than 2 m/s and 98% of the differences in velocity estimates are less than 1 m/s. Consequently, the estimation of the average Doppler shift is substantially affected by changing the first guess velocity window width and/or the integration window width for only a few cases within the September 1991 profiler data. Six such examples are illustrated in Figures 4.33 - 4.38.

The spectral estimates plotted in Figure 4.33 illustrate a weak signal regime. In this example, none of the average Doppler shifts computed by the five DRWP configurations are close to the signal peak near frequency bin -2; however, the solution returned by configuration #1 is not too distant from the signal peak and is the best solution of the five. Configurations #4 and #5 which have a higher minimum acceptable SNR reject the solution and propagate the first guess velocity. In this case, the solution returned by configuration #3 is the worst of the five.
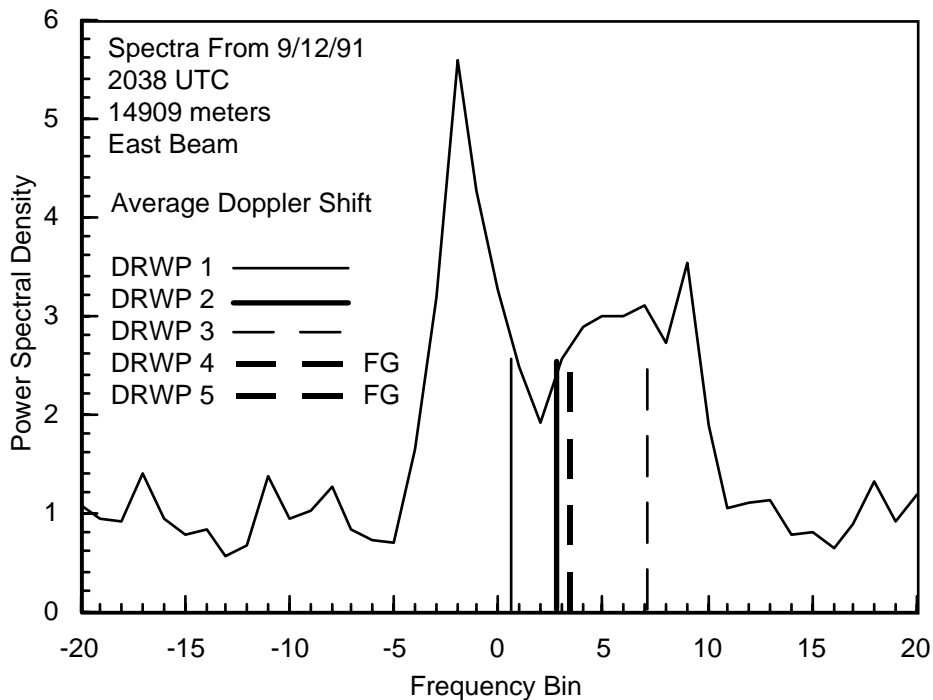

Figure 4.33. East beam spectral estimates from the 14909 meter level at 2038 UTC on 12 September 1991. FG indicates the first guess velocity was

propagated. Identical line types are used for identical or nearly identical average Doppler shifts.

Figures 4.34 and 4.35 present two examples of how persistent interference signals near the atmospheric signal affect the performance of the five different MSFC wind algorithm configurations. In the example from the 4259 meter level (Figure 4.34), the atmospheric signal is centered on frequency bin -2 and the relatively weaker interference signals are centered on frequency bins ± 6. In this case, all of the configurations, except #2 which uses a narrow first guess velocity window width and a wide integration window width, produce good estimates of the average Doppler shift.
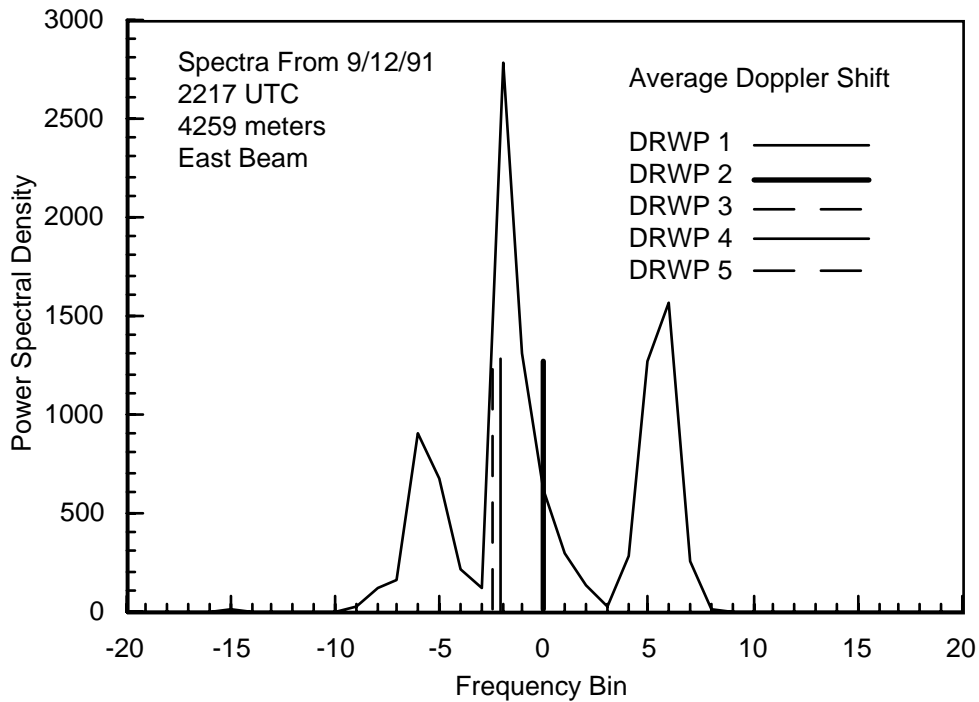
Figure 4.34. East beam spectral estimates from the 4259 meter level at 2217 UTC on 12 September 1991. Identical line types are used for identical or nearly identical average Doppler shifts.

The results from the second example (Figure 4.35) are somewhat different. In this case, the interference signal located at frequency bin +6 is stronger than the atmospheric signal at frequency bin +2. Consequently, the average Doppler shifts produced by the configurations which use the wider first guess velocity window width (configurations #3 and #5) are shifted toward the stronger interference signal. The other configurations are less affected by the interference signal and produce better average Doppler shifts.

The spectral estimates in Figure 4.36 illustrate an example of a relatively broad spectrum width atmospheric signal which is indicative of a large degree of variability and/or turbulence within the sample domain. In this case, the MSFC wind algorithm configurations with large integration window widths (configurations #2 and #5) produce an average Doppler shift which is near the center of the broad atmospheric signal. The average Doppler shift produced by configuration #3 which has the large first guess

velocity window width and the small integration window width is shifted toward the peak signal within the broad atmospheric return. The average Doppler shift produced by configurations #1 and #4, which are of poorer quality, are shifted toward the weaker side of the atmospheric signal.

The spectral estimates from the 14009 meter level at 2217 UTC also contain a broad atmospheric signal (Figure 4.37). However, in this example the peak signal is near the center of the atmospheric signal and is large relative to the other spectral estimates. Consequently, the configurations with a large first guess velocity window width and/or a large integration window width (configurations #2, #3, and #5) return an average Doppler
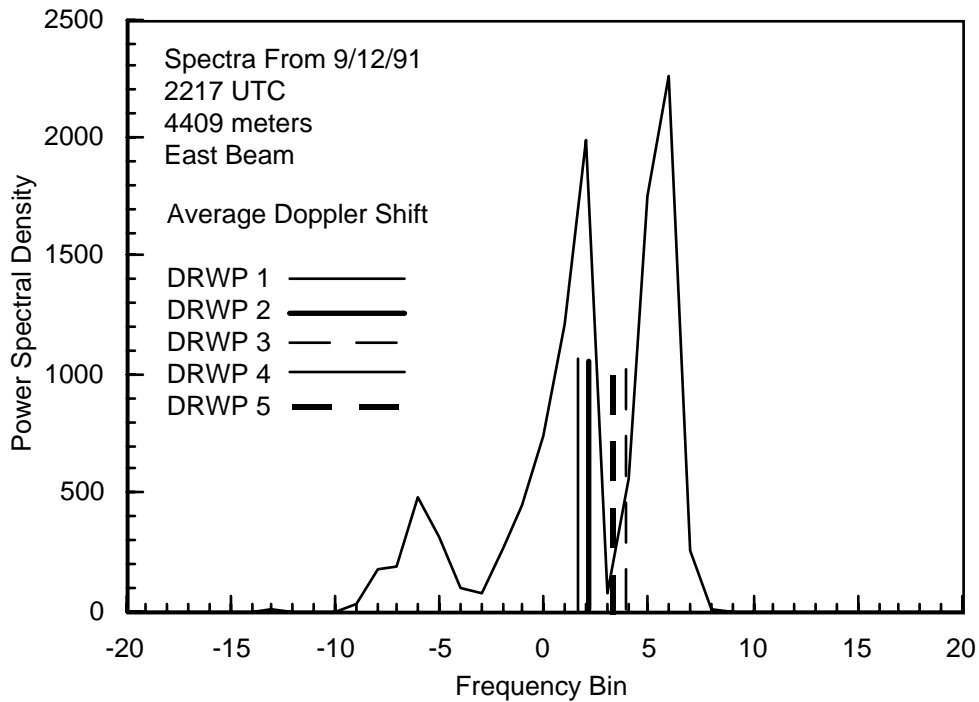

Figure 4.35.   East beam spectral estimates from the 4409 meter level at 2217 UTC on 12 September 1991. Identical line types are used for identical or nearly identical average Doppler shifts.
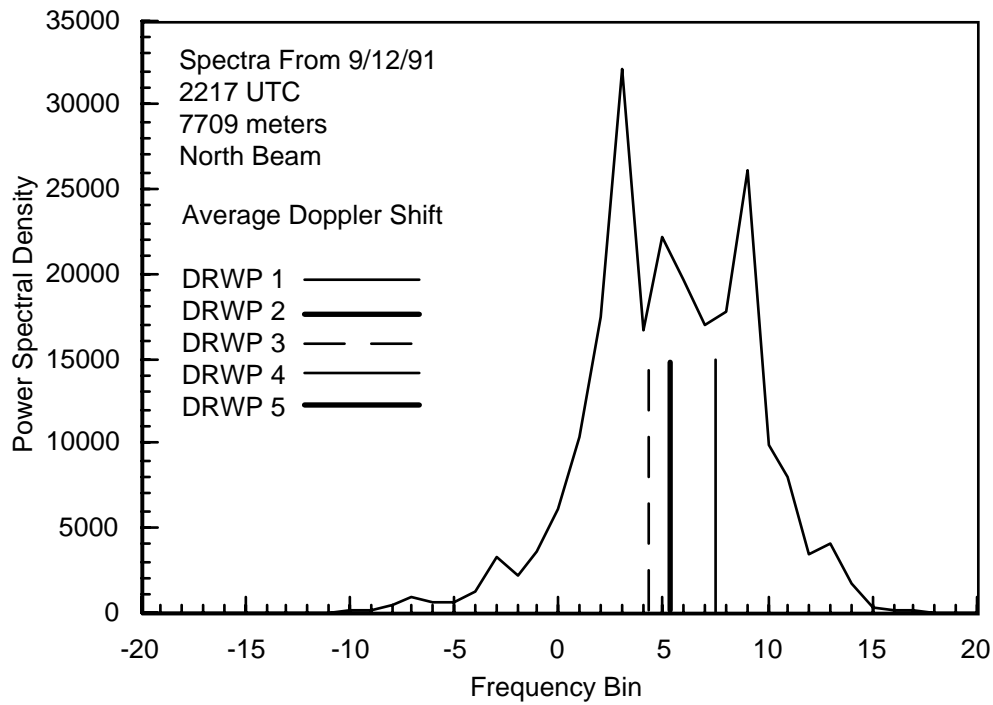
Figure 4.36.   North beam spectral estimates from the 7709 meter level at 2217 UTC on 12 September 1991. Identical line types are used for identical or nearly identical average Doppler shifts.
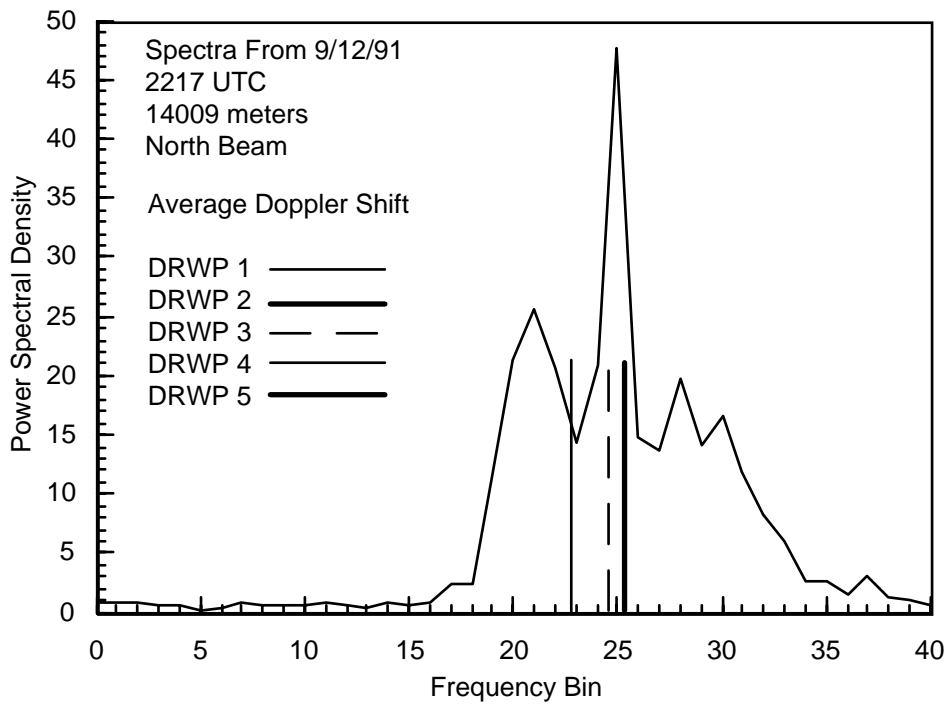

Figure 4.37.   North beam spectral estimates from the 14009 meter level at 2217 UTC on 12 September 1991. Identical line types are used for identical or nearly identical average Doppler shifts.

94

shift near the peak signal. The configurations with the small first guess velocity window width and the small integration window width (configurations #1 and #4) do not locate the signal peak and, consequently, do not return an average Doppler shift near the signal peak.

The last case from 12 September 1991 is a second example of a weak signal regime (Figure 4.38). In this example, there is an obvious, albeit weak, atmospheric signal at frequency bin -3. All of the configurations with low minimum acceptable SNR accurately locate the atmospheric signal and return a reasonable average Doppler shift. However, the SNR in this example is too low for the configurations with the higher minimum acceptable SNR and those configurations propagate the first guess velocity which is clearly an inferior result.

4.2.2   Spectral Data Analysis From 23 January 1992

Examination of the profiler data from 23 January 1992 indicates all five configurations generally produced very similar velocity estimates in strong signal regimes, and configurations #1, #2, and #3 produced very similar velocity estimates in all signal regimes. In particular, examination of four time coincident profiles produced by DRWP configurations #1, #2, and #3 indicates that 99% of the differences in velocity estimates between configurations #1 and #2 and between configurations #1 and #3 are less than 2 m/s and 94% of the differences in velocity estimates are less than 1 m/s. Consequently, the estimation of the average Doppler shift is substantially affected by changing the first guess velocity window width and/or the integration window width for only a few cases within the January 1992 profiler data. Seven such examples are illustrated in Figures 4.39 - 4.45.
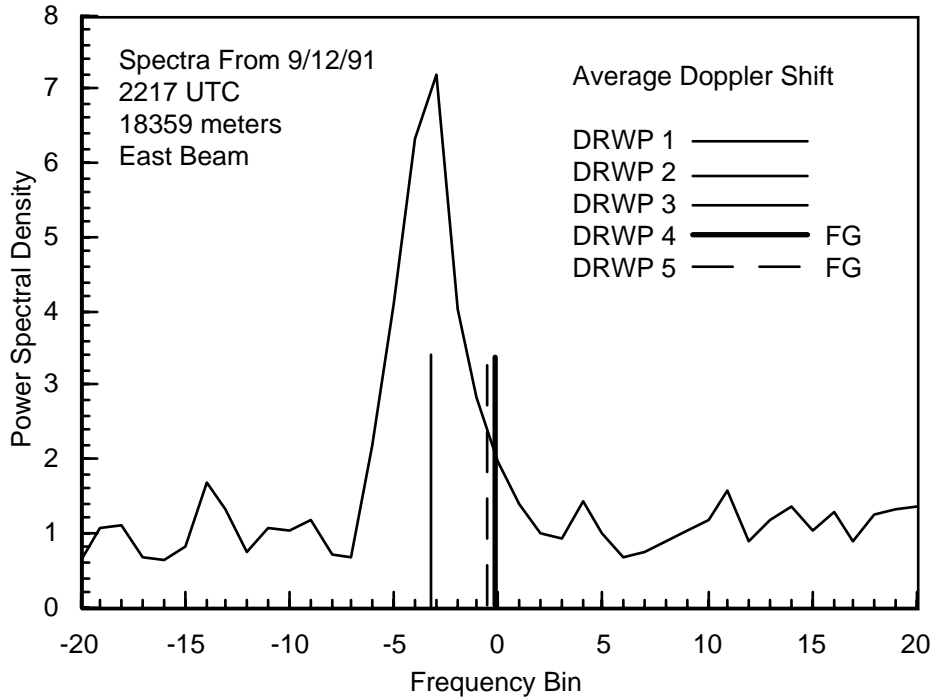
Figure 4.38.   East beam spectral estimates from the 18359 meter level at 2217 UTC on 12 September 1991. FG indicates the first guess velocity was propagated.   Identical line types are used for identical or nearly identical average Doppler shifts.

The spectral estimates in Figures 4.39 and 4.40 illustrate two examples of a relatively broad spectrum width atmospheric signal which is indicative of a large degree of variability and/or turbulence within the sample domain. In the first case (Figure 4.39), the MSFC wind algorithm configurations with large integration window widths (configurations #2 and #5) produce an average Doppler shift which is near the center of the broad atmospheric signal.   The average Doppler shift produced by the other configurations are shifted more towards the signal peak. In the second case (Figure 4.40), all of the configurations except #3 produce an average Doppler shift near the center of the atmospheric signal. The average Doppler shift returned by configuration #3 is shifted towards the signal peak. In both of these cases, it is difficult to say that one solution is better than any other.

Figure 4.41 contains the spectral estimates from the 7259 meter level at 1530 UTC on 23 January 1992. This particular level is in the middle of a moderate shear zone in the north beam component and examination of the data above and below this level suggest the atmospheric signal of interest is centered around frequency bin - 31. As evidenced by the chart (Figure 4.41), none of the configurations return an average Doppler shift particularly close to the signal peak; however, configurations #2 and #5 produce the best results of the five configurations.

The spectral estimates presented in Figure 4.42 are another illustration of a weak signal regime.   In this case, all configurations with low minimum acceptable SNR (configurations #1, #2, and #3) produce reasonable average Doppler shifts. However, the

96

configurations with the higher minimum acceptable SNR (configurations #4 and #5) reject the solution and propagate the first guess velocity.
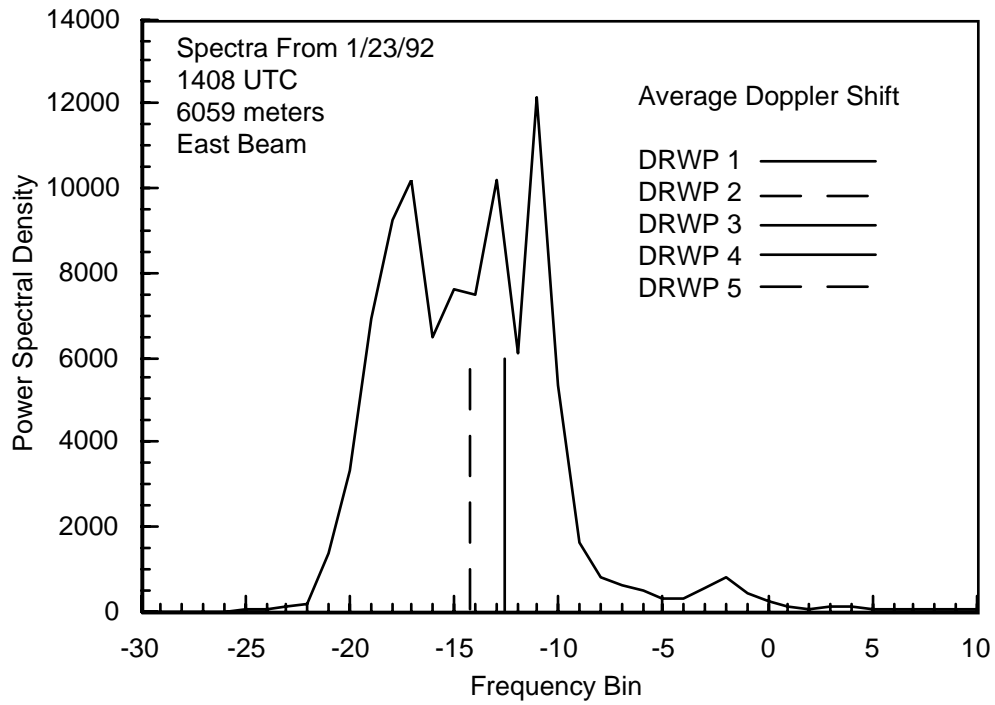
Figure 4.39.   East beam spectral estimates from the 6059 meter level at 1408 UTC on 23 January 1992. Identical line types are used for identical or nearly identical average Doppler shifts
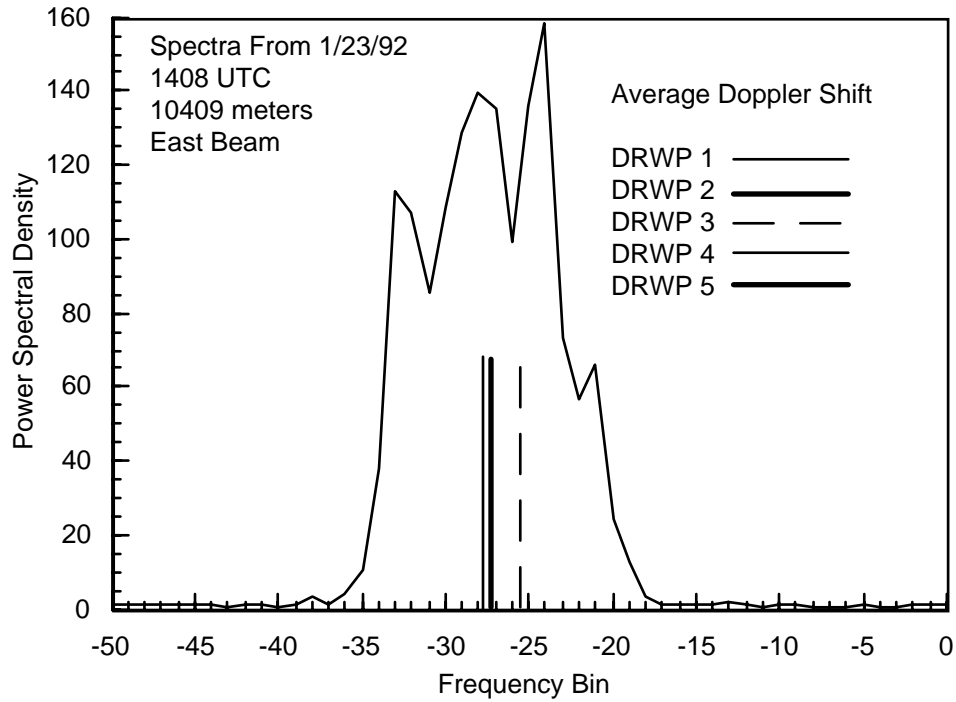
Figure 4.40.   East beam spectral estimates from the 10409 meter level at 1408 UTC on 23 January 1992. Identical line types are used for identical or nearly identical average Doppler shifts.
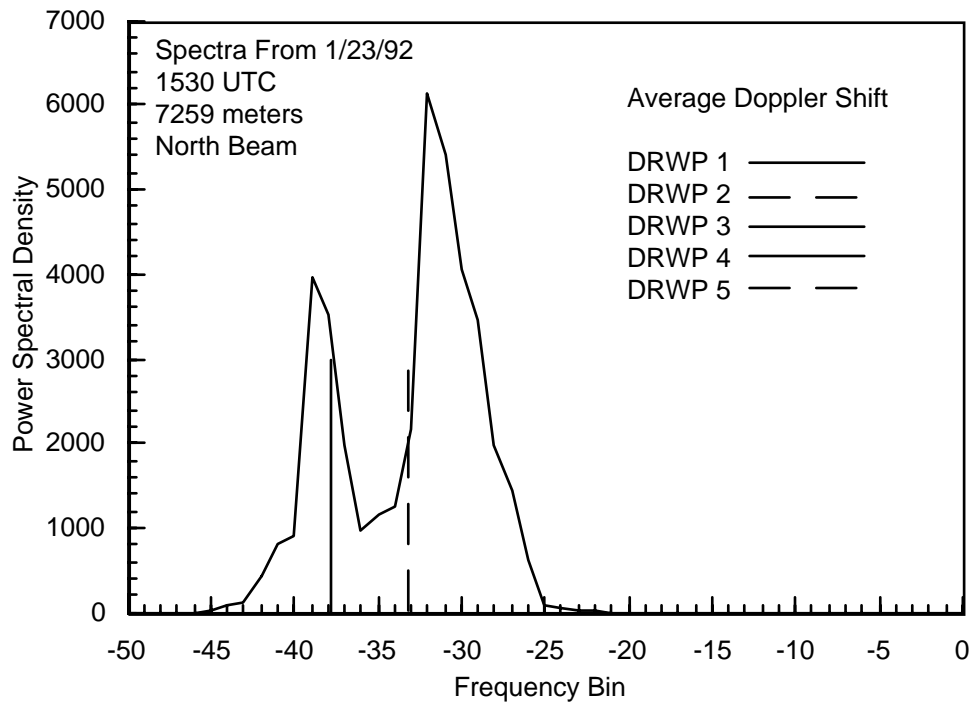
Figure 4.41.   North beam spectral estimates from the 7259 meter level at 1530 UTC on 23 January 1992. Identical line types are used for identical or nearly identical average Doppler shifts.
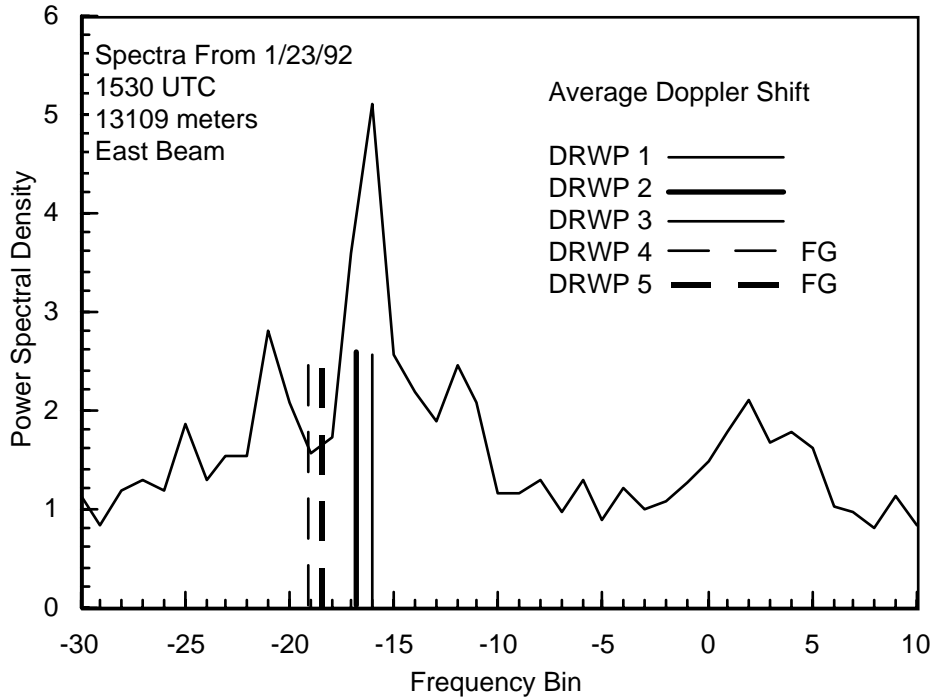
Figure 4.42.   East beam spectral estimates from the 13109 meter level at 1530 UTC on 23 January 1992.   FG indicates the first guess velocity was propagated.   Identical line types are used for identical or nearly identical average Doppler shifts.

An example of the problems encountered when the atmospheric signal is near 0 is illustrated in Figure 4.43. In this case, examination of all available data including DRWP data from above and below the 3059 meter level and jimsphere information suggest the true north beam wind component is near 0 m/s. However, there is not a strong return near frequency bin 0 because the ground clutter removal process has smoothed the spectral estimates around the zero Doppler shift.   In spite of that, all of the configurations, except configuration #3, produce an average Doppler shift near frequency bin 0. Because of the large first guess velocity window width and the small integration window width, the average Doppler shift returned by configuration #3 is shifted toward the maximum signal at frequency bin 4. In these situations, a configuration with a wider integration window width is most likely to produce reasonable results.
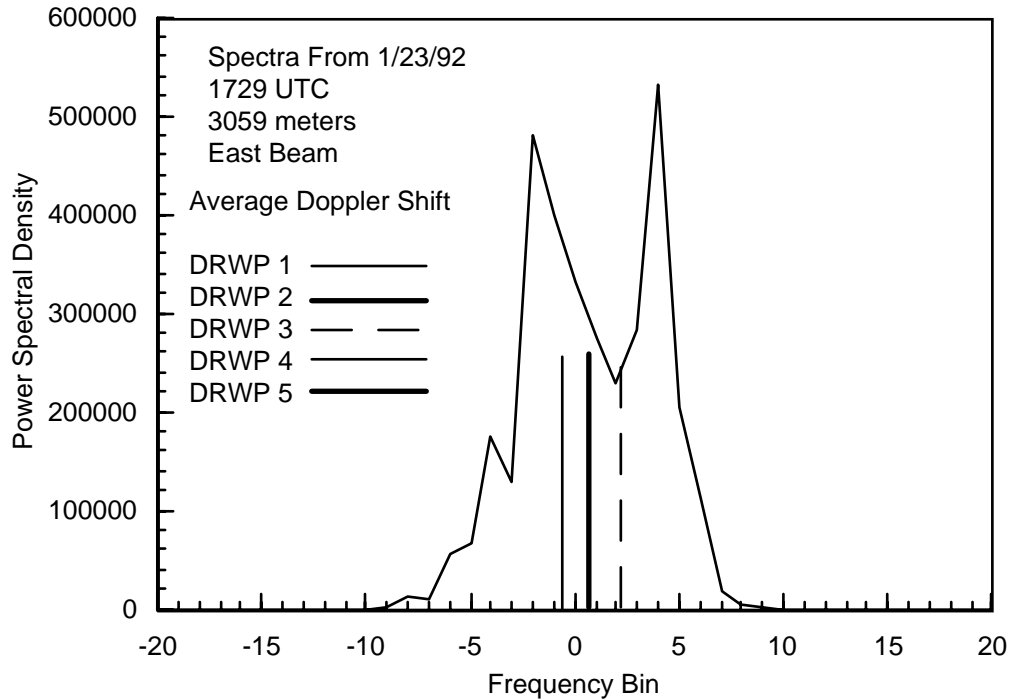
Figure 4.43. East beam spectral estimates from the 3059 meter level at 1729 UTC on 23 January 1992. Identical line types are used for identical or nearly identical average Doppler shifts.

The spectral estimates presented in Figures 4.44 and 4.45 illustrate two examples where MSFC wind algorithm configurations based on small first guess velocity window widths and small integration window widths (i.e., configurations #1 and #4) do not perform as well as other configurations. For the case from the 7109 meter level Figure 4.44), all of the configurations based on large first guess velocity window widths and/or large integration window widths produce good average Doppler shifts. For the case from the 16559 meter level (Figure 4.45), configuration #3, with the large first guess velocity window width, returns the best average Doppler shift. In this case, the SNR did not exceed the minimum acceptable SNR for the two configurations with the higher SNR threshold (configurations #4 and #5) so the first guess velocity was propagated.
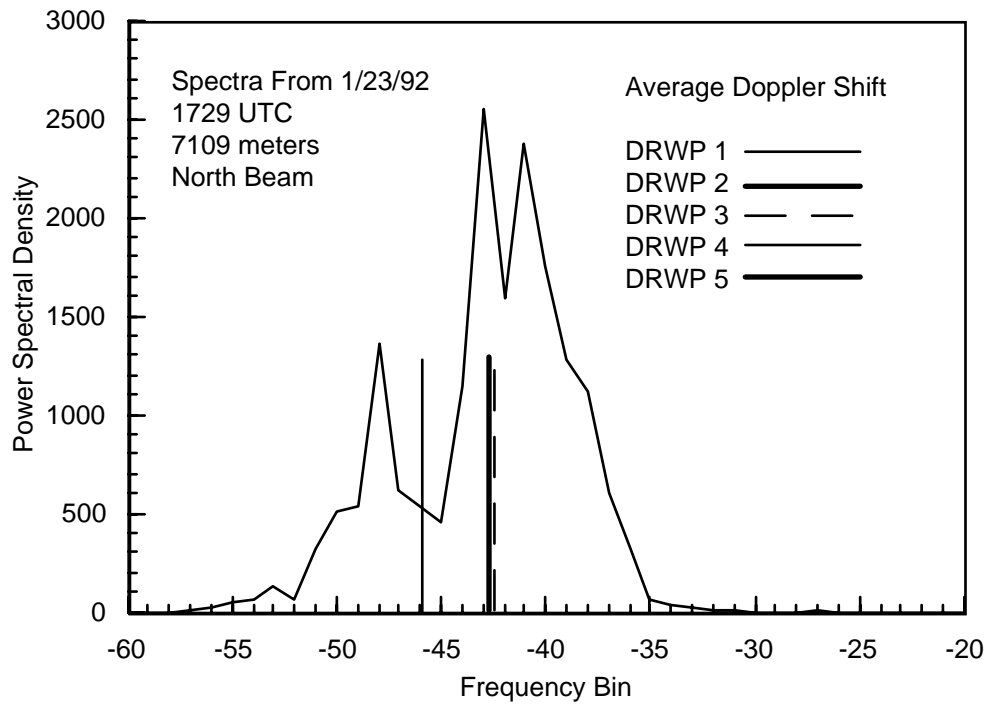
Figure 4.44.   North beam spectral estimates from the 7109 meter level at 1729 UTC
on 23 January 1992. Identical line types are used for identical or
nearly identical average Doppler shifts.
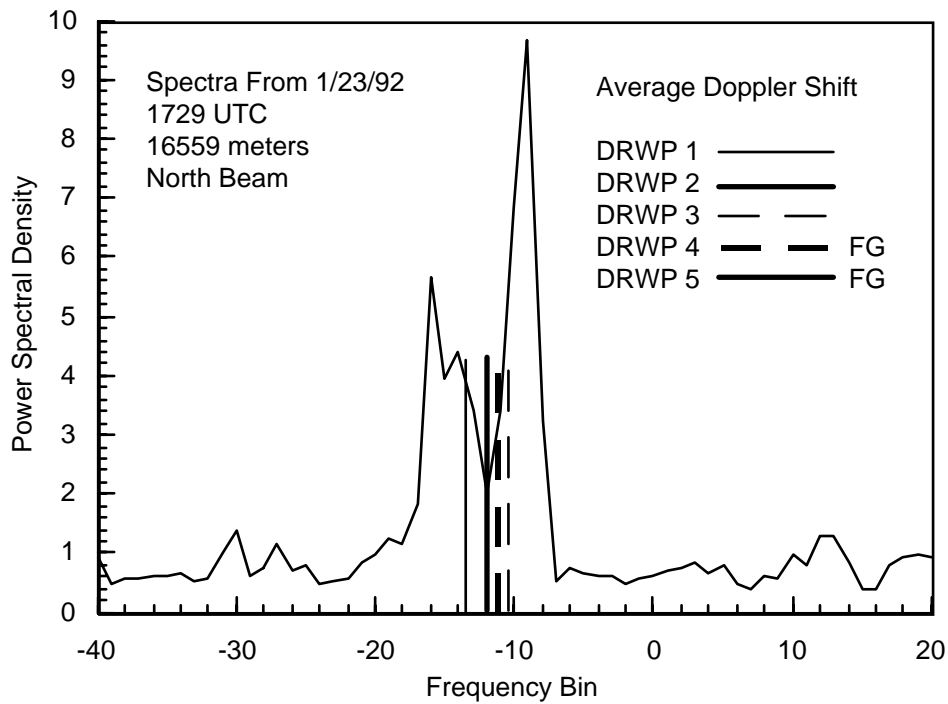
Figure 4.45.   North beam spectral estimates from the 16559 meter level at 1729
UTC on 23 January 1992. FG indicates the first guess velocity was

propagated. Identical line types are used for identical or nearly identical average Doppler shifts.

4.2.3 Spectral Data Analysis From 20 February 1992

Examination of the profiler data from 20 February 1992 indicates all five configurations generally produced very similar velocity estimates in strong signal regimes, and configurations #1, #2, and #3 produced very similar velocity estimates in all signal regimes. In particular, examination of three time coincident profiles produced by DRWP configurations #1, #2, and #3 indicates that 98% of the differences in velocity estimates between configurations #1 and #2 and between configurations #1 and #3 are less than 2 m/s and 91% of the differences in velocity estimates are less than 1 m/s. Consequently, the estimation of the average Doppler shift is substantially affected by changing the first guess velocity window width and/or the integration window width for only a few cases within the February 1992 profiler data. Five such examples are illustrated in Figures 4.46 - 4.50.

The spectral estimates presented in Figures 4.46 and 4.47 are two examples of broad spectrum width atmospheric signals resulting from strong vertical wind shear. In both cases, the average Doppler shifts returned by the five MSFC wind algorithm configurations vary considerably because of the broad atmospheric signal. Although the average Doppler shifts returned by configuration #3 are closest to the signal maximum, examination of other data sources suggest the average Doppler shifts produced by configurations #2 and #5 may be the best. Clearly, the average Doppler shifts returned by configurations #1 and #4 using the small first guess velocity window width and the small integration window width are the poorest.
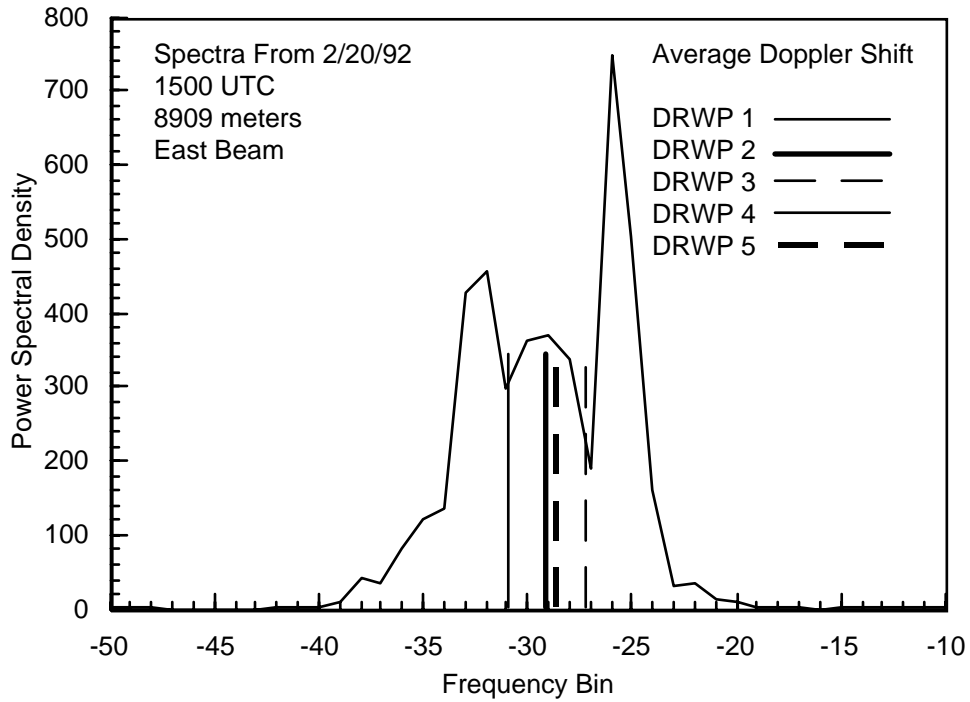
Figure 4.46. East beam spectral estimates from the 8909 meter level at 1500 UTC on 20 February 1992. Identical line types are used for identical or nearly identical average Doppler shifts.
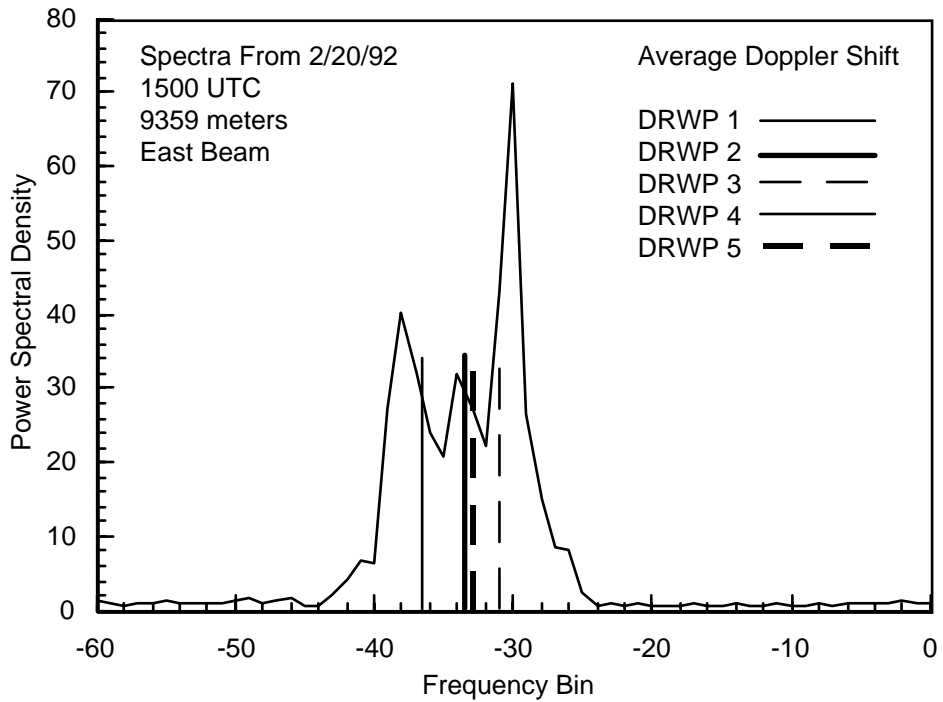

Figure 4.47. East beam spectral estimates from the 9359 meter level at 1500 UTC on 20 February 1992. Identical line types are used for identical or nearly identical average Doppler shifts.

103

The spectral estimates presented in Figure 4.48 illustrate another example of a fairly broad atmospheric signal with clearly defined maximum signal. Similar to the other two cases, the average Doppler shift returned by configuration #3 is closest to the signal maximum and the average Doppler shifts returned by the configurations with larger integration window widths are shifted more towards the center of the atmospheric signal. Again, the average Doppler shifts returned by configurations #1 and #4 which use the small first guess velocity window width and the small integration window width are the poorest.

The spectral estimates presented in Figure 4.49 are another example of a broad spectrum width atmospheric signal resulting from strong vertical wind shear. The average Doppler shifts returned by the five MSFC wind algorithm configurations vary considerably because of the broad atmospheric signal. The average Doppler shift returned by configuration #3 is closest to the signal maximum and the average Doppler shifts returned by the configurations with larger integration window widths are shifted more towards the center of the atmospheric signal. Again, the average Doppler shifts returned by configurations #1 and #4 which use small first guess velocity window width and the small integration window width are the poorest.

The final set of spectral estimates from the 20 February 1992 (Figures 4.50) data set is another example of a broad spectrum width atmospheric signal resulting from strong vertical wind shear. In this case, the average Doppler shifts returned by the five MSFC wind algorithm configurations vary considerably because of the broad signal. Although the average Doppler shift returned by configuration #3 is closest to the signal maximum, examination of other data sources suggest the average Doppler shifts produced by configurations #2 and #5 may be the best. The average Doppler shifts returned by configurations #1 and #4 are the poorest estimates.
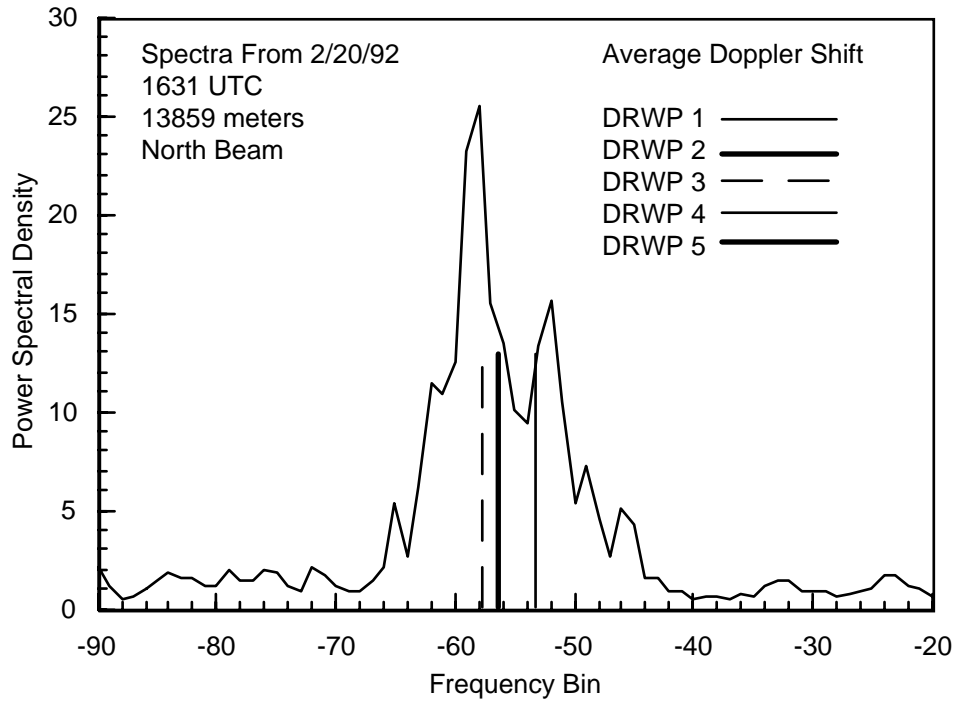
Figure 4.48.   North beam spectral estimates from the 13859 meter level at 1631 UTC on 20 February 1992. Identical line types are used for identical or nearly identical average Doppler shifts.
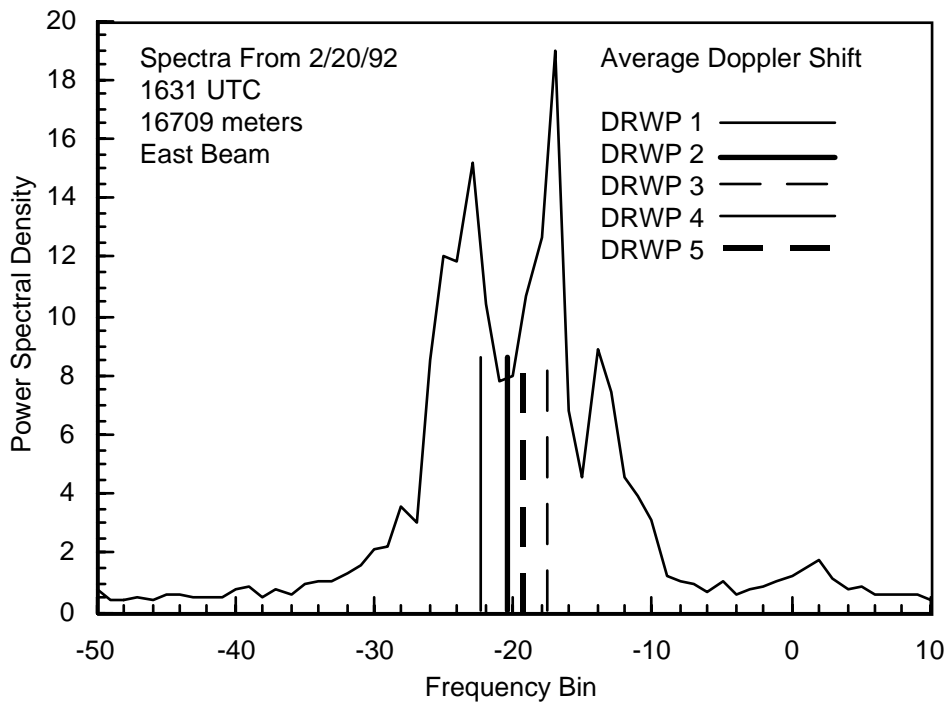
Figure 4.49.   East beam spectral estimates from the 16709 meter level at 1631 UTC on 20 February 1992. Identical line types are used for identical or nearly identical average Doppler shifts.
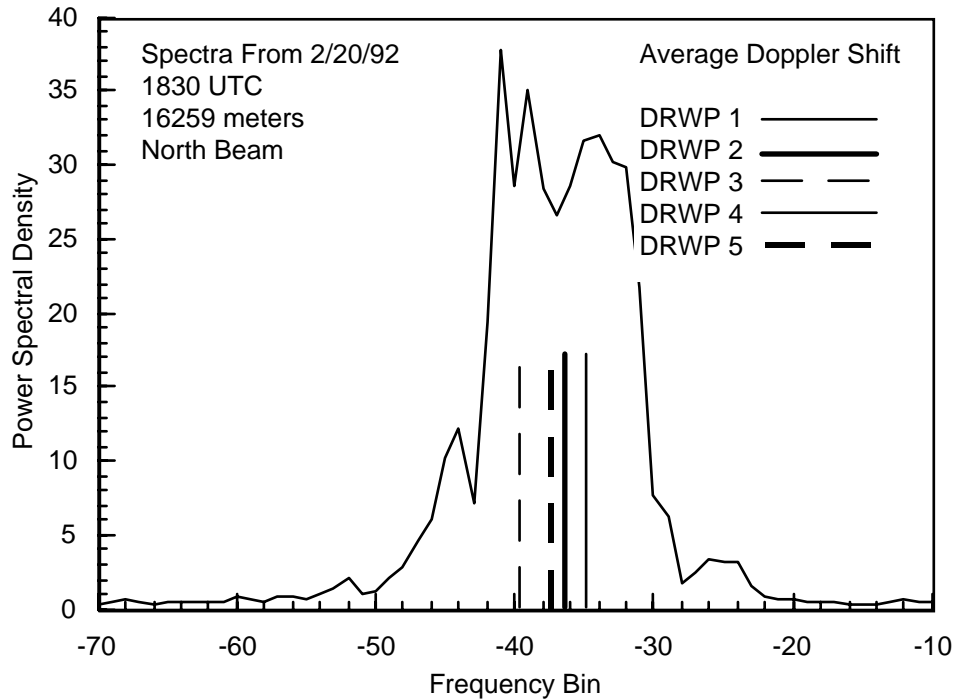
Figure 4.50.   North beam spectral estimates from the 16259 meter level at 1830 UTC on 20 February 1992. Identical line types are used for identical or nearly identical average Doppler shifts.

4.2.4   Spectrum Width Analysis

In addition to the effect upon the average Doppler shift calculations, the width of the integration window also affects spectrum width estimates. Obviously, a small integration window width will limit the size of the spectrum width estimate and possibly mask important information about the turbulence and/or shear within a layer. The spectrum width profiles presented in Figures 4.51 and 4.52 illustrate this point. The profiles suggest for layers with relatively little shear and/or turbulence (e.g., spectrum width values near 0.6 m/s), the width of the integration window had little impact upon the estimated spectrum width. However, for layers with significant shear and/or turbulence (e.g., the east beam jet core near 12 km (Figure 4.16)), the width of the integration window has a significant impact upon the estimated spectrum width. In the case of the east beam jet core near 12 km, the spectrum width calculated using the larger integration window width (configuration #2) is twice as large as the spectrum width calculated using the smaller integration window width (configuration #3). There are also large differences in the estimated spectrum widths between the two different configurations in the 5 km to 7 km region, a region of significant vertical wind shear (Figures 4.16 and 4.17), for both the east and north beam profiles.

Conclusions and a summarization of the meteorological evaluation are contained in Section 5.0, Summary and Recommendations.
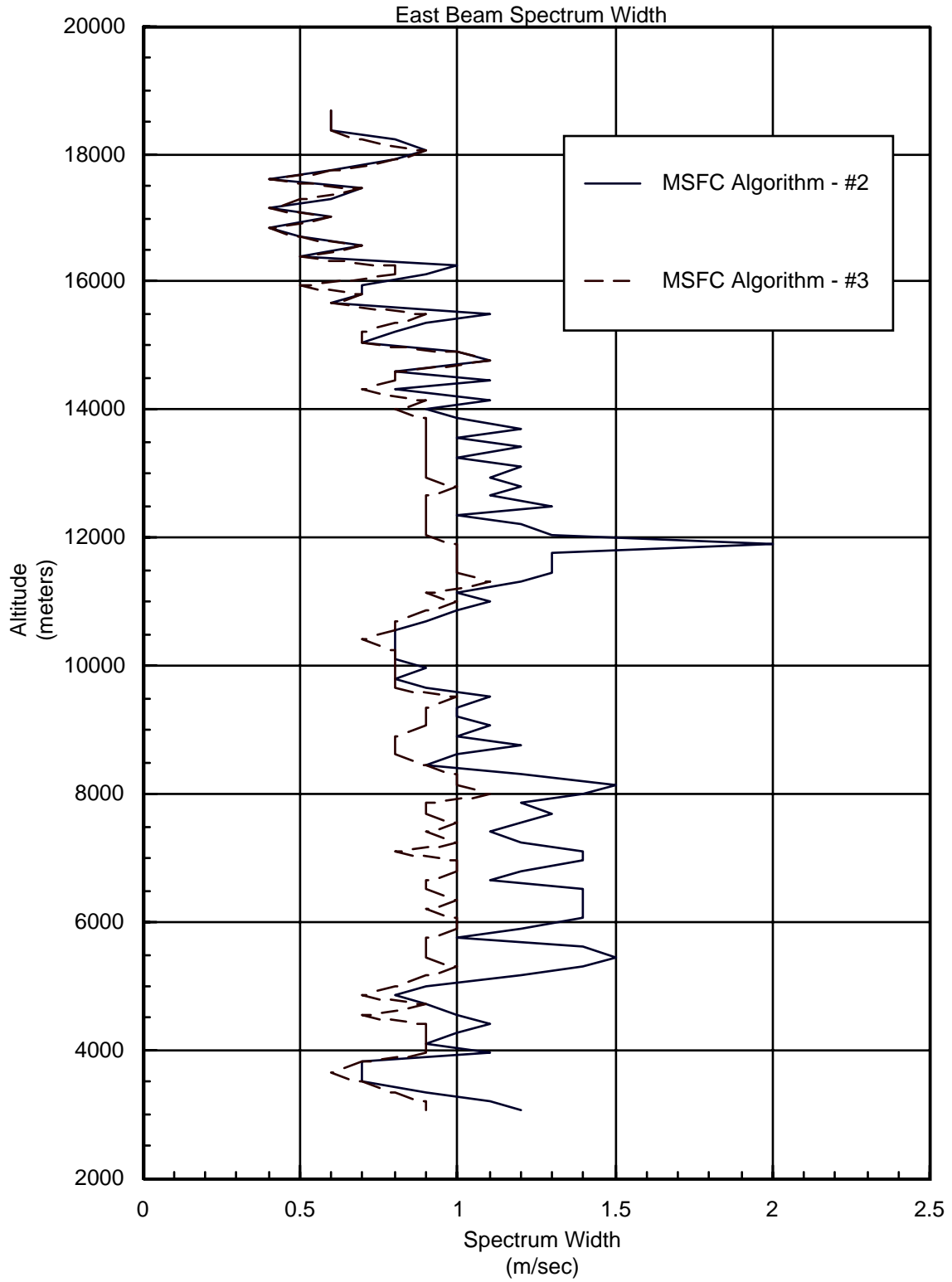
Figure 4.51. East beam spectrum width profiles at 1729 UTC on 23 January 1992 for MSFC wind algorithm configurations #2 and #3.
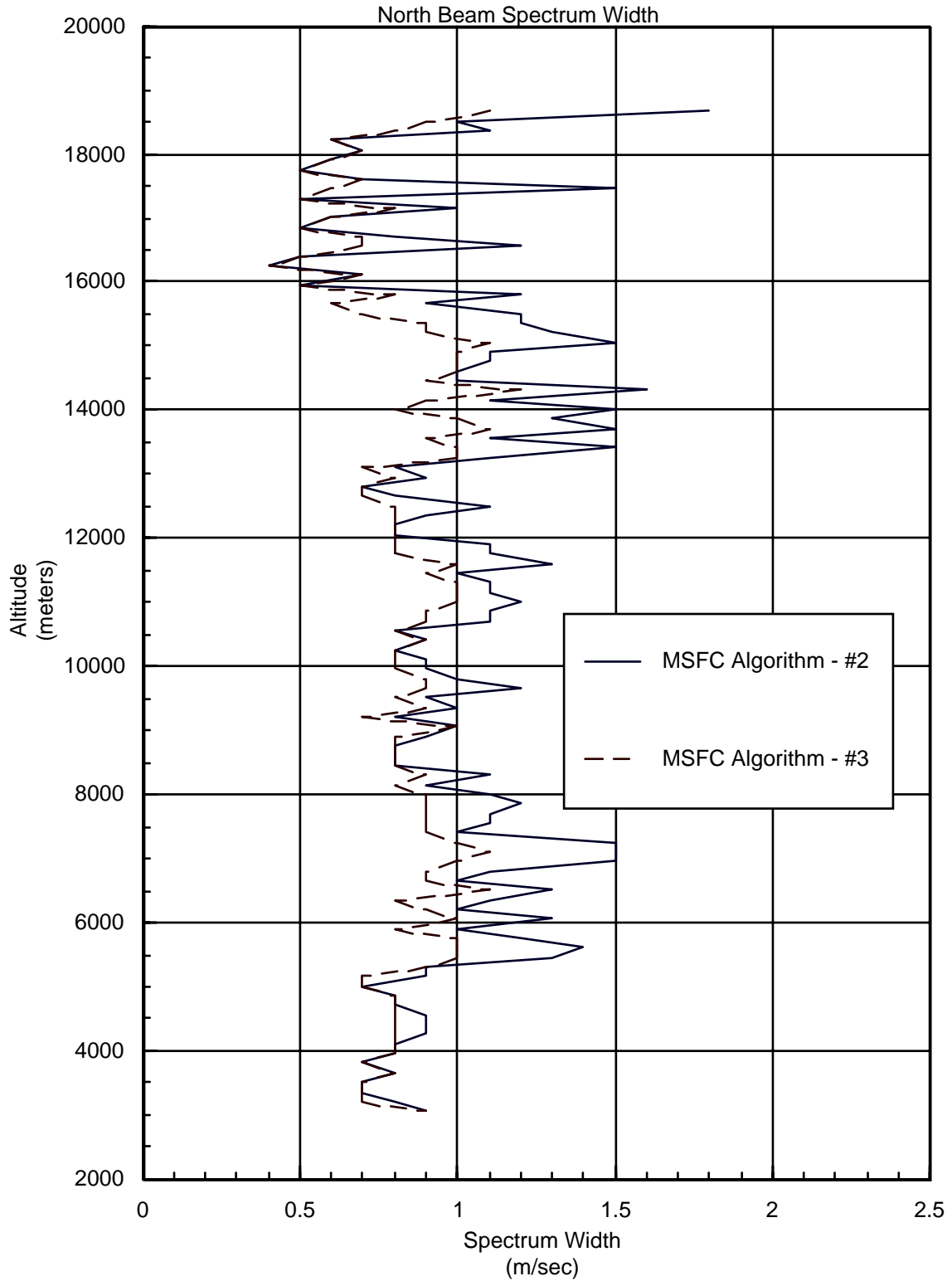
Figure 4.52. North beam spectrum width profiles at 1729 UTC on 23 January 1992 for MSFC wind algorithm configurations #2 and #3.

5.0 Summary and Recommendations

The first part of this section contains a summary of the meteorological evaluation of the MSFC wind algorithm including recommended values for the minimum acceptable SNR, the first guess velocity window width, and the integration window width. This is followed by discussion of the capabilities and limitations of the 50 MHz DRWP with the current implementation of the MSFC wind algorithm. The final component of this section contains recommendations for enhancements to the 50 MHz DRWP and suggestions for an enhanced operational wind profiling capability.

5.1   Meteorological Evaluation Summary

Analysis of jimsphere wind profiles and time proximate DRWP profiles from the MSFC wind algorithm indicate:

- The RMS velocity differences between the jimsphere profiles and the DRWP profiles ranged from 1.5 m/s to 2.3 m/s. The larger RMS differences are associated with the stronger wind speed cases where the spatial separation between the jimsphere balloon and the DRWP is greater. This result is similar to the RMS velocity differences reported by MSFC (Creasey, 1992).

- The small scale features (wavelengths less than 1000 meters) present in the DRWP profiles and the jimsphere profiles frequently exhibit considerable differences. These differences are not surprising in light of the spatial and temporal differences in data collection between the jimsphere and the DRWP and do not indicate a data quality issue with either system.

- The DRWP profiles and the jimsphere profiles are generally coherent to wavelengths as short as 1200 meters. This result is similar to the coherence between nearly simultaneous profiles from jimsphere and windsonde releases (Smith, 1988). In some instances, the profiles are coherent to wavelengths as short as 600 meters.

DRWP advantages include:

- Frequent update cycle (new wind profiles can be produced every three to five minutes) of the DRWP facilitates detection of rapidly changing wind velocity.

- The DRWP wind profile includes more information than just wind speed and direction. Spectrum width estimates produced by the DRWP provide a measure of the turbulence and/or vertical shear within each range gate (150 meter layer).

DRWP disadvantages include:

- The DRWP cannot produce independent wind velocity estimates in regions of weak signal returns. If the environmental conditions producing the weak returns in a particular region persist for a period of many hours, the DRWP will only be able to produce interpolated wind estimates for that region.

- The DRWP has difficulty accurately estimating the component wind speed when the component speed is near zero. This is because the atmospheric signal will be smoothed by the ground clutter removal process.

Analysis of DRWP profiles from the MSFC wind algorithm and time proximate DRWP consensus averaged profiles indicate:

- The RMS velocity differences between the MSFC wind algorithm profiles and the consensus averaged profiles ranged from 0.4 m/s to 1.2 m/s (excluding the lightning contaminated data). The larger RMS differences are associated with the stronger wind speed cases where the temporal variability was greater.

- The MSFC wind algorithm is able to resolve some small scale features that are heavily smoothed by the consensus averaging technique.

- The MSFC wind algorithm generally returns the same (or more) number of levels with high quality data.

MSFC wind algorithm advantages include:

- The MSFC wind algorithm provides more frequent profile updates. The MSFC wind algorithm can provide updates as frequently as every five minutes (hardware limited) while the consensus procedure can provide updates only as frequently as every 30 minutes.

- With the proper configuration of the key parameters, the MSFC wind algorithm is able to reject persistent interference signals.

MSFC wind algorithm disadvantages include:

- The MSFC requires interactive quality control to ensure the first guess velocity and the algorithm parameters are appropriate.

Based on the analysis of the spectral estimates and the average Doppler shifts and spectrum widths produced by the five different configurations of the MSFC wind algorithm, some conclusions can be drawn regarding the preferred configuration of the algorithm for operational use. First, it is apparent the lower minimum acceptable SNR is the preferred choice. The configurations with the higher minimum acceptable SNR rejected solutions and propagated the first guess velocity in situations when the atmospheric signal is clearly detectable. Selecting a preferred configuration for the first guess velocity window width and the integration window width is not as straightforward.

110

First, it is important to recall changing the first guess velocity window width and/or the integration window width changed the resulting velocity estimates by less than 1 m/s in more than 90% of the cases examined. Consequently, reasonable adjustments of these two parameters is not likely to produce substantial changes in the estimated average Doppler shift in most cases.

For the limited number of situations where the configuration of these two parameters does affect the solution, examination of the spectral estimates suggests three principle reasons for the differing results. The primary reason is the presence of a broad atmospheric signal indicative of significant vertical shear and/or turbulence within the sample volume. A second reason is the inherent difficulty associated with estimating the wind velocity when the atmospheric signal is within the ground clutter. The final reason is the presence of persistence interference signals, often DRWP hardware related, near the atmospheric signal.

For the "problem integrations", analysis of the data indicates using a larger first guess velocity window width and a larger integration window width will generally produce the best results when the spectral estimates are characterized by either a broad atmospheric signal or an atmospheric signal within the ground clutter. This configuration will also tend to produce the best spectrum width estimates. However, when the "problem integration" is characterized by persistence interference signals that are near the atmospheric signal, a small first guess velocity window width and a small integration window width will generally produce the best results. The recommended configuration of the key parameters within the MSFC are contained in Table 5.1.

Table 5.1. Recommended DRWP Configurations			
Characteristics of Spectral Estimates	First Guess Window Width (Frequency Bin #)	Integration Window Width (Frequency Bin #)	Minimum SNR (dB)
Absence of Persistent Interference Signals Near the Atmospheric Signal	12	20	-15
Presence of Persistent Interference Signals Near the Atmospheric Signal	6	10	-15

5.2   Operational Considerations

Many of the advantages and disadvantages of the implementation of the MSFC within the 50 MHz DRWP relative to the consensus averaging technique and to the jimsphere system were described in Section 5.1. However, there are some limitations to the new configuration of the DRWP which were not described yet deserve comment.

The MSFC wind algorithm has been implemented on the Data Analysis Processor (DAP) of the DRWP. This is a MicroVAX II computer which, by today's standards, is a very slow processor. Although the system is sufficiently fast to meet profile update requirements, system response to user input when performing quality control functions is slower than desired. A faster processor would facilitate interactive quality control.

The other hardware limitation examined as part of the implementation of the MSFC wind algorithm is the parallel interface between the Real-Time Processor (RTP) and the DAP of the DRWP. This interface is used to transfer the spectral estimates from the RTP to the DAP. Since the MSFC wind algorithm requires the spectral estimates, the robustness of this interface will have significant impact upon the performance of the new configuration of the DRWP.

To test the performance of the parallel interface, the new configuration of the system was run for a period of 45 hours consecutively. During this time period, the parallel interface failed three times for a period of nine minutes each time. Based on a DRWP cycle time of five minutes coupled with the temporal median filter processing, each of these parallel interface failures resulted in a time lapse of 20 minutes between profile updates (the nominal update period was 5 minutes). Additional testing of the parallel interface will be required to determine if this small sample is representative of the typical performance of the interface.

5.3   Recommendations

The recommendations contained in this section address the disadvantages and limitations of the new configuration of the DRWP described in Sections 5.1 and 5.2. The first three recommendations are all related to the processing of the data from the profiler. The fourth recommendation involves a modification to the profiler.

As noted in Section 5.2, the MicroVAX II computer used for the MSFC wind algorithm is slow, and consequently, the system response to user prompts in the interactive quality control is considerably slower than desired. A potential remedy to this deficiency is to rehost the MSFC wind algorithm software on a high-end personal computer (e.g., a 486 class computer) or a low-end workstation. This solution would greatly facilitate interactive quality control. If the interactive quality control is to be performed at a location other than the profiler site, this solution would require communication lines of sufficient bandwidth to transfer the raw spectral estimates from the profiler site to the quality control location. It is important to note that rehosting the MSFC wind algorithm software on a low-end VMS workstation would minimize the amount of software requiring modification.

112

The second recommendation eliminates the requirement for interactive quality control in the MSFC wind algorithm. Since the quality control issue is basically one of pattern recognition, artificial neural network technology, which has proven capability in this arena, in conjunction with techniques being examined by the NOAA ERL Wave Propagation Laboratory (Wuertz and Weber, 1989; van de Kamp, 1993, personal communication) may be able to eliminate the need for interactive quality control in the MSFC wind algorithm. Consequently, because of the potential benefits, research in this arena is warranted.

The third recommendation is based on a proposal made by Mr. Wilfong (Wilfong, 1993) at the NASA Environmental Sensitivities Workshop Group Meeting held at the Kennedy Space Center in June 1993. The key component of the proposal is an objective analysis procedure which would utilize data from all wind sensor systems (e.g., tower, balloon, rocketsonde, LIDAR, DRWP) to produce a "best estimate" wind profile. This synergistic technique would take into account the known error characteristics of the sensors as well as the spatial and temporal sampling differences among the sensors. The technique would make maximum use of the strengths of each sensor system and minimize the impacts of each sensor system's deficiencies. Before significant resources are expended, the customers should be queried to determine their requirements, if any, for this product.

The fourth recommendation is to determine the need for, advantages of, and cost of converting the 50 MHz DRWP into a five beam system. A five beam system will certainly have some advantages in terms of data quality. However, depending upon the data requirements and the cost, it may or may not be advisable to convert the DRWP into a five beam system.

6.0 References

Creasey, Robert L., 1992: Summary of Preliminary Radar Profiler Assessment. *Presentation To NASA Management.*

Gage, K.S., 1979: Evidence For A K$^{-5/3}$ Law Inertial Range In Mesoscale Two Dimensional Turbulence. *Journal of Atmospheric Sciences*, 13, 1950-1954.

Hildebrand, P.H. and R.S. Sekhon, 1974: Objective Determination Of The Noise Level In Doppler Spectra. *Journal of Applied Meteorology*, 13, 808-811.

Jenkins, G.M. and D. G. Watts, 1968: *Spectral Analysis and its Applications.* Holden-Day, Inc., 525 pp.

Larsen, M.F. and J. Rottger, 1987: Observations of thunderstorm reflectivities and Doppler velocities measured at VHF and UHF. *Journal of Atmospheric and Oceanic Technology,* 4, 151-159.

Schumann, R.S., M.K. Atchison, G.E. Taylor, J.D. Warburton, M.M. Wheeler, and A.M. Yersavich, 1993: *Software Requirements Specification for the New Wind Algorithm in NASA's 50 MHz Doppler Radar Wind Profiler.* Prepared for NASA Kennedy Space Center Under Contract NAS10-11844, 31 pp.

Skolnik, M.I., 1980: *Introduction to Radar Systems.* McGraw-Hill Publishing Company, 461-464.

Smith, S.A., 1988: Resolution and Accuracy of Balloon Wind Sounding Systems Used in Support of STS Ascent Performance Assessments. *Memorandum To Claude Green, Chief, Atmospheric Effects Branch, Earth Sciences and Applications Division, MSFC.*

Tycho Technologies, Inc., 1990: *Program Maintenance Manual for the NASA 50 MHz Wind Profiler System.* Prepared for NASA Marshall Space Flight Center Under Contract NAS8-36995.

Tycho Technologies, Inc., 1990: *Software User's Manual for the NASA 50 MHz Wind Profiler System.* Prepared for NASA Marshall Space Flight Center Under Contract NAS8-36995.

Wuertz, D.B. and B.L. Weber, 1989: Editing Wind Profiler Measurements. *NOAA Technical Report ERL 438--WPL 62,* 78 pp.

Wilfong, T.L., S.A. Smith and R.L. Creasey, 1992: High Temporal Resolution Velocity Estimates From The NASA 50 MHz Wind Profiler. *Thirtieth Aerospace Sciences Meeting*, Reno, Nevada, January 1992, 8 pp.

Wilfong, T.L., 1993: Integrated Operational Concept for Upper Air Measurements. *Presentation at the Environmental Sensitivities Workshop Group Meeting,* Kennedy Space Center, FL.

Yoe, J.G., M.F. Larsen, and E.J. Zipser, 1992: VHF Wind-Profiler Data Quality and Comparison of Methods for Deducing Horizontal and Vertical Air Motions in a Mesoscale Convective Storm. *Journal of Atmospheric and Oceanic Technology,* 9, 713-727.

Appendix A

Signal-to-Noise Ratio Profiles

This appendix contains the SNR profiles for the configuration #3 DRWP profiles from 12 September 1991, 23 January 1992, and 20 February 1992.

MSFC Algorithm Profile
Configuration #3
Date: 12 September 1991
Time: 1912 UTC

East Beam
North Beam

Altitude (meters)

Signal-to-Noise Ratio
(db)

A-2

MSFC Algorithm Profile
Configuration #3
Date: 12 September 1991
Time: 2128 UTC

East Beam
North Beam

Altitude (meters)

Signal-to-Noise Ratio
(db)

MSFC Algorithm Profile
Configuration #3
Date: 12 September 1991
Time: 2358 UTC

Altitude (meters)

Signal-to-Noise Ratio (db)

East Beam

North Beam

MSFC Algorithm Profile
Configuration #3
Date: 23 January 1992
Time: 1408 UTC

MSFC Algorithm Profile
Configuration #3
Date: 23 January 1992
Time: 1530 UTC

East Beam

North Beam

Altitude
(meters)

Signal-to-Noise Ratio
(db)

MSFC Algorithm Profile
Configuration #3
Date: 23 January 1992
Time: 1729 UTC

East Beam

North Beam

Altitude (meters)

Signal-to-Noise Ratio
(db)

MSFC Algorithm Profile
Configuration #3
Date: 20 February 1992
Time: 1500 UTC

East Beam
North Beam

Altitude (meters)

Signal-to-Noise Ratio
(db)

MSFC Algorithm Profile
Configuration #3
Date: 20 February 1992
Time: 1830 UTC

East Beam
North Beam